SERVICEABILITY LIMIT STATE DESIGN OF DEEP FOUNDATIONS

by

Farzaneh Naghibi

Submitted in partial fulfillment of the requirements
for the degree of Doctor of Philosophy

at

Dalhousie University
Halifax, Nova Scotia
November 2014

TABLE OF CONTENTS

LIST OF TABLES

LIST OF FIGURES

ABSTRACT

Although the settlement of deep foundations (piles, hereafter) is not generally a concern if the piles are driven to refusal, settlement can become a design issue if no stiff substratum is encountered. The settlement of individual and pairs of floating piles founded in a three-dimensional spatially random soil model are studied using finite element methods. A probabilistic model for total and differential settlement is developed and validated by Monte Carlo simulation. Moreover, this study investigates the reliability-based design factors required for the serviceability limit state design of deep foundations and recommends the geotechnical resistance and consequence factors required to achieve specified target reliability indices against excessive settlement of deep foundations. The effect of pile redundancy on geotechnical system design is also investigated.

LIST OF ABBREVIATIONS AND SYMBOLS USED

ASD   Allowable Stress Design

CPT   Cone penetration test for in-situ soil testing

LAS   Local Average Subdivision

FFT   Fast Fourier Transform

LRFD   Load and Resistance Factor Design

LSD   Limit States Design

RBD   Reliability-Based Design

SLS   Serviceability Limit State

SPT   Standard penetration test for in-situ soil testing

TBM   Turning Bands Method

ULS   Ultimate Limit State

WSD   Working Stress Design

a_i settlement prediction parameter

b_i interval boundry

B_p width of soil volume used in the geometric average around the pile

B_s width of soil sample volume used in the sample geometric average

c cohesion

$\bar{c}$ arithmetic average of cohesion field along pile surface

$\hat{c}$ arithmetic average of observed (sampled) cohesion values

$\hat{c}_i$ observed (sampled) cohesion value

C	depth of soil volume used in the geometric average around the pile
$\text{Cov}[X, Y]$	covariance between random variables X and Y
d	pile diameter = 0.3 m
D	depth of soil sample
E	soil's elastic modulus (random)
$\hat{E}$	estimate of effective elastic modulus, derived from soil samples (random)
E_{eff}	effective uniform soil elastic modulus that, if surrounding the pile, would yield the same settlement as actually observed (random)
E_g	elastic modulus geometric mean
E_j^o	one of m elastic modulus soil samples actually observed
E_p	pile's elastic modulus
E_s	soil's elastic modulus used in deterministic analysis (non-random)
$E(\underset{\sim}{x}_i)$	elastic modulus at the spatial location $\underset{\sim}{x}_i$
$E(z)$	elastic modulus at the spatial location z
$\text{E}[\cdot]$	expectation operator
F	pile system failure event
F_D	true dead load (random)
$\hat{F}_D$	characteristic dead load = $k_D \mu_D$
F_i	individual pile failure event
$\hat{F}_i$	i'th characteristic load effect
F_L	true live load (random)
$\hat{F}_L$	characteristic live load = $k_L \mu_L$
F_s	Factor of safety

F_T	true total load (random)
$\hat{F}_T$	characteristic or applied total load (non-random)
$G(z)$	standard normal (Gaussian) random field
H	designed pile length
H_{max}	Maximum desired pile length
I_i	importance factor corresponding to i'th characteristic load effect
I_p	settlement influence factor
$I_{p,max}$	maximum value of I_p required to satisfy eq. (CAP)
k	pile to soil stiffness ratio $= E_p/\hat{E}$
k_D	dead load bias factor
k_L	live load bias factor
l_x	pile location measured from the left edge of the soil mass ($x = 0$)
m	number of soil observations
M	safety margin $= R - L$ or R/L
n	design lifetime (years)
n_p	number of piles in a pile system
n_{sim}	number of simulations
p	pile perimeter length
p_{ann}	annual maximum acceptable failure probability
p_f	probability of failure ($\mathrm{P}\left[\delta > \delta_{max}\right]$)
p_{max}	lifetime maximum acceptable failue probability
$\mathrm{P}\left[.\right]$	probability operator
$\mathrm{P}\left[F\right]$	probability of system failure $= p_f = \mathrm{P}\left[F_T > R\right]$

r	distance between soil sample and pile centerline
r_x	plan $x-$ direction distance between common corners of geometric averaging volumes at sample and pile
r_y	plan $y-$ direction distance between common corners of geometric averaging volumes at sample and pile
R	pile resistance
R_s	true design geotechnical resistance (random)
$\hat{R}_s$	serviceability characteristic resistance (based on characteristic soil properties)
s	center-to-center pile spacing
v_c	coefficient of variation of cohesion
v_E	elastic modulus coefficient of variation (σ_E/μ_E)
v_R	resistance coefficient of variation (σ_R/μ_R)
v_T	total load coefficient of variation (σ_T/μ_T)
V_p	volume of geometric average around the pile ($= B_p \times B_p \times C$)
V_s	volume of sample geometric average ($= B_s \times B_s \times D$)
W	true load times ratio of characteristic to equivalent elastic modulus in soils under total stress conditions ($F\hat{E}/E_{eff}$)
$\underset{\sim}{x}$	spatial coordinate, (x, y, z) in 3-D
$\underset{\sim}{x}_i^o$	spatial coordinate of the center of the i'th soil sample
X_i	ratio of load to elastic modulus geometric average ($X = F_{T_i}/E_{g_i}$)
z	spatial coordinate in 1-D
Z_i	$(n_p - i + 1)R/F_T$
Z_i^j	parameters used in LAS
α	total load factor
α_D	dead load factor

α_i	load factor corresponding to the i'th load effect
α_L	live load factor
β	reliability index $= -\Phi^{-1}(p_f)$
β_i	reliability index of an individual pile
β_{sys}	reliability index of a pile system
γ	variance reduction function (due to local averaging)
$\gamma(V_p)$	variance function giving variance reduction due to averaging over the soil volume surrounding the pile
$\gamma(V_s)$	variance function giving variance reduction due to averaging over the sample volume
$\gamma_{V_p V_p}$	average correlation coefficient between elastic modulus along two piles over the volume V_p
$\gamma_{V_p V_s}$	average correlation coefficient between elastic modulus samples over the volume V_s and elastic modulus values over the volume V_p
δ	pile settlement, positive downwards
$\hat{\delta}$	predicted pile settlement
δ_{det}	pile settlement when $E = \mu_E$ everywhere
δ_{max}	maximum acceptable settlement for an individual pile
Δ	differential settlement between two piles
Δ_{max}	maximum acceptable differential settlement
ζ	variable in Randolph's prediction for I_p
η	mechanical interaction factor
$\theta_{\ln E}$	isotropic correlation length of the random log-elastic modulus field
λ	variable in Randolph's prediction for I_p
μ_c	cohesion mean
μ_D	mean dead load

μ_E	mean elastic modulus
μ_L	mean live load
$\mu_{\ln E}$	mean of log-elastic modulus
$\mu_{\ln \hat{E}}$	mean of the logarithm of the estimated effective elastic modulus (based on a geometric average of elastic modulus observations)
$\mu_{\ln E_{eff}}$	mean of the logarithm of the effective elastic modulus (based on a geometric average of elastic modulus over pile length H)
$\mu_{\ln F_T}$	mean total log-load on pile
$\mu_{\ln W}$	mean of $\ln W$
$\mu_{\ln X_i}$	mean of $\ln X_i$
$\mu_{\ln Z_i}$	mean of $\ln Z_i$
μ_R	mean resistance
μ_T	mean total load
μ_{X_i}	mean of X_i
μ_{Z_i}	mean of Z_i
μ_Δ	mean differential settlement
$\mu_{|\Delta|}$	mean absolute differential settlement
ν	Soil poisson's ratio
ρ_{F_T}	correlation coefficient between F_T at two points
$\rho_{\ln E}$	correlation coefficient between $\ln E$ at two points
$\rho_{\ln F}$	correlation coefficient between $\ln F$ at two points
ρ_X	correlation coefficient between X at two points, $X = F_T/E_g$
σ_D	dead load standard deviation
σ_E	standard deviation of elastic modulus

σ_F	total load standard deviation
σ_L	live load standard deviation
$\sigma_{\ln E}$	standard deviation of log-elastic modulus
$\sigma_{\ln \hat{E}}$	standard deviation of the logarithm of the estimated effective elastic modulus
$\sigma_{\ln E_{eff}}$	standard deviation of the logarithm of the effective elastic modulus
$\sigma_{\ln F_T}$	standard deviation of the log-pile load
$\sigma_{\ln W}$	standard deviation of $\ln W$
$\sigma_{\ln X_i}$	standard deviation of $\ln X_i$
$\sigma_{\ln Z_i}$	standard deviation of $\ln Z_i$
σ_R	standard deviation of resistance
σ_T	standard deviation of total load
σ_{X_i}	standard deviation of X_i
σ_{Z_i}	standard deviation of Z_i
σ_Δ	standard deviation of differential settlement
τ	lag distance
φ_{gu}	geotechnical resistance factor at ULS
φ_{gs}	geotechnical resistance factor at SLS
ϕ	soil friction angle
Φ	standard normal cumulative distribution function
Ψ_u	consequence factor at ULS
Ψ_s	consequence factor at SLS

ACKNOWLEDGEMENTS

CHAPTER 1

INTRODUCTION

1.1 GENERAL

Deep foundations, or piles, are structural members made of steel, concrete, and/or timber which transmit some or all of the applied load to the ground below the surface. Piles can sometimes be costly, yet may be necessary to confirm structural safety in situations where the upper soil layer is highly compressible and/or too weak to support the applied load. The ground usually increases in strength with depth and piles are used to transfer the load to underlying bedrock or a stronger soil layer. Piles resting on a stiffer stratum are called end-bearing. If not end-bearing, they are often called floating piles where most of the resistance is derived from skin friction and/or adhesion. To simplify the random soil model, only floating piles are considered in this research.

As load is applied to the pile, the pile settles due to both deformation of the pile itself and deformation of the surrounding soil. Assuming that the surrounding soil is perfectly bonded to the pile shaft through friction and/or adhesion, any displacement of the pile is associated with an equivalent displacement of the adjacent soil. Following the classic work of authors such as Poulos and Davis (1980), Randolph and Wroth (1978) and Vesic (1977), the soil is assumed to be linearly elastic, so that this displacement is resisted by a force which is proportional to the soil's elastic modulus and the magnitude of the displacement. Thus, the support provided by the soil to the pile depends on the elastic properties of the surrounding soil. As stated by Vesic (1977), the pile settlement is a constant (dependent on Poisson's

ratio and pile geometry) times F_T/E_s, where F_T is the total applied load and E_s is the soil's elastic modulus.

The overall goal of the thesis is to develop design provisions for individual floating piles against serviceability limit state failure corresponding to excessive pile settlement, considering uncertainty in the load and resistance, and considering the degree of site understanding as well as the consequences of failure. The "Limit States" are those conditions in which the system ceases to fulfill the functions for which it was designed. Those states concerning safety are called ultimate limit states (ULS), which include exceeding the load carrying capacity (e.g., bearing failure), overturning, sliding, and loss of stability. Those states which restrict the intended use of the system are called serviceability limit states (SLS), which include deflection, permanent deformation, and cracking.

As illustrated in Figure 1.1, the pile is assumed to be founded in a three-dimensional spatially random soil, underlain by bedrock (located at the bottom of the soil model), supporting a vertical load F_T.
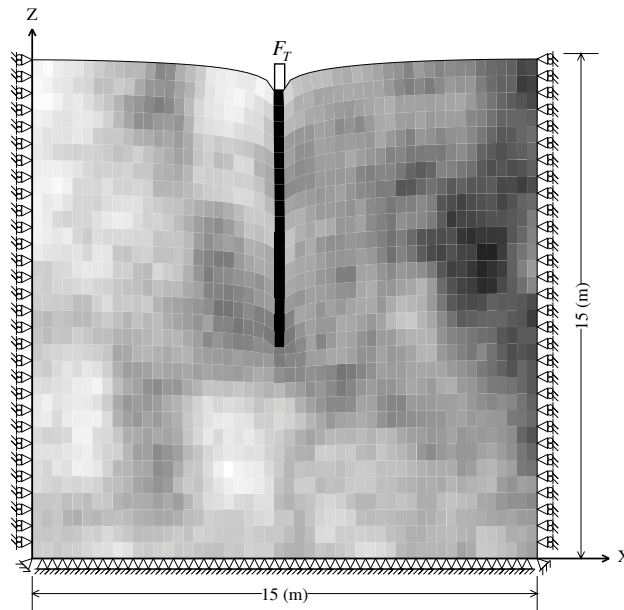
Figure 1.1   Slice through a random field/finite element method mesh supporting a single pile

Piles are often utilized in groups, and differential settlement becomes a major concern when the foundations settle unevenly. This research also investigates the differential settlement between two piles, as shown in Figure 1.2, and establishes a probabilistic model to represent differential settlement.
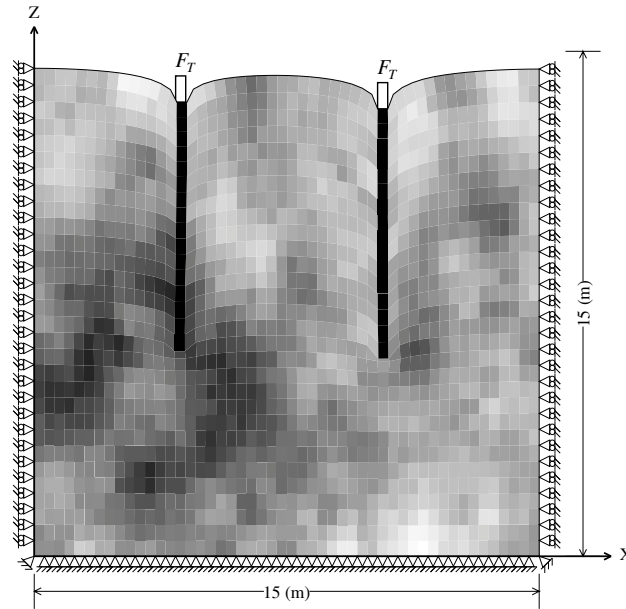
Figure 1.2   Slice through a random field/finite element method mesh supporting two piles

Finally, the reliability of a system of piles is studied based on the reliability of individual piles and the relationship between the number of piles and system reliability for various resistance statistics and various levels of pile dependencies is estimated.

1.2   PILE DESIGN METHODOLOGIES

Working stress design (WSD), also called allowable stress design(ASD), has been widely used for decades by engineers, and is still in use in geotechnical engineering. In this approach the uncertainties in loads, soil strength, and model accuracy are accounted for through a single "factor of safety", F_s, which is sometimes defined as the ratio of the characteristic resistance, $\hat{R}$, to the characteristic load, $\hat{F}_T$,

$$F_s = \frac{\hat{R}}{\hat{F}_T} \tag{1.1}$$

If $F_s > 1$ then the characteristic resistance is larger than the load, and, in a WSD, the system is deemed to be safe. However, even if $F_s > 1$, the system still has some probability of failure, which gets smaller as F_s increases.

In general, the characteristic resistance, $\hat{R}$, is computed by geotechnical formulae using conservative estimates of the soil properties while the characteristic load, $\hat{F}_T$, is the sum of conservative (usually unfactored) estimates of characteristic load actions, $\hat{F}_i$, acting on the system. $\hat{F}_T$ is sometimes taken as an upper percentile (i.e. a load only exceeded by a certain small percentage of loads in any one year), as illustrated in Figure 1.3, while $\hat{R}$ is sometimes taken as a cautious estimate of the mean resistance.
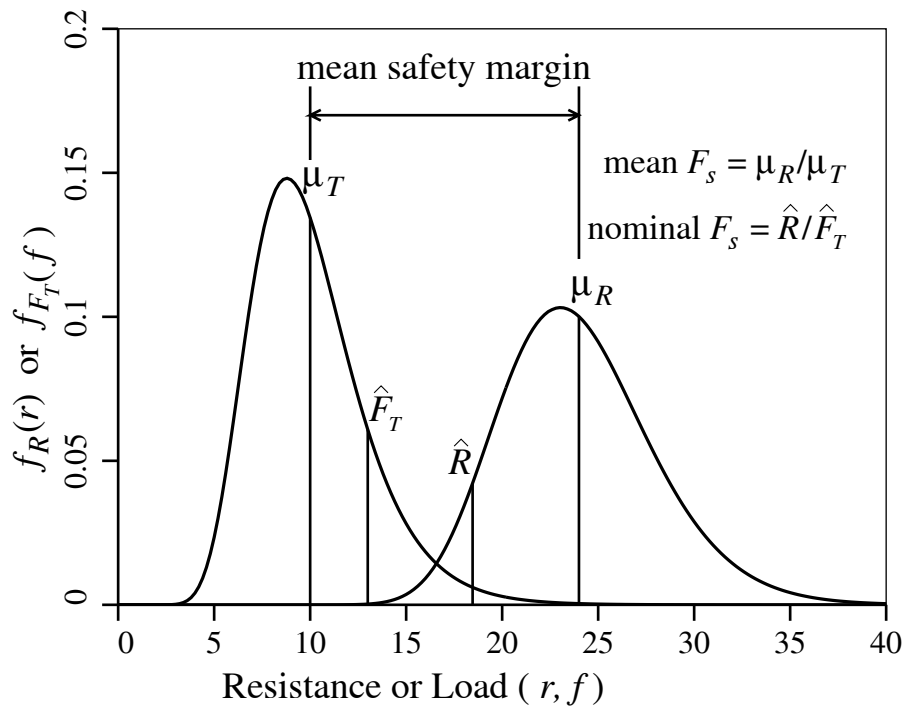
Figure 1.3 Load and resistance distributions

The drawbacks to the WSD approach are:

1) A single factor is used to represent all uncertainties in both load and resistance.

2) Soils with common characteristic resistance and load have the same F_s regardless of the actual variabilities in the load and resistance.

3) The WSD approach cannot be used to determine the probability of failure. For example, if $F_s = 2$ but the variabilities of the resistance and load are very large, then the probability of failure may still be close to 50%. However, if $F_s = 1.1$ but the variabilities are small, then the probability of failure may be very small (see, e.g, Figure 1.4).

While WSD has no doubt been quite successful due to simplicity in implementation, it nevertheless does not adequately reflect the actual design safety, as mentioned previously. Figure 1.4 illustrates how different geotechnical systems can have different probabilities of failure despite having a common mean factor of safety. It is also important to note that WSD does not explicitly differentiate between the behaviour of the structure under ultimate and serviceability limit states. There is, therefore, a desire for a methodology that accomodates both ultimate and serviceability limit states, while maintaining both safety and efficiency of the underlying design. This motivates reliability-based design methodologies discussed next.

An improved approach to WSD uses the "reliability index", β, to characterize the system safety. In this so called "Reliability-based Design" approach, the reliability (probability of success) of a system, which has been designed to have a certain resistance, $\hat{R}$, to the design (or characteristic) load, $\hat{F}_T$, is assessed by calculating the probability that the actual resistance, R, exceeds the actual total load, F_T. For the two random variables R and F_T, this probability is computed as

$$P[R > F_T] = \int_{-\infty}^{\infty} \int_{r>f}^{\infty} f_{RF_T}(r, f) \, dr \, df \tag{1.2}$$

where $f_{RF_T}(r, f)$ is the joint (bivariate) distribution of R and F_T, defined as,

$$f_{RF_T}(r, f) \, dr \, df = P[r < R \leq r + dr \cap f < F_T \leq f + df] \tag{1.3}$$
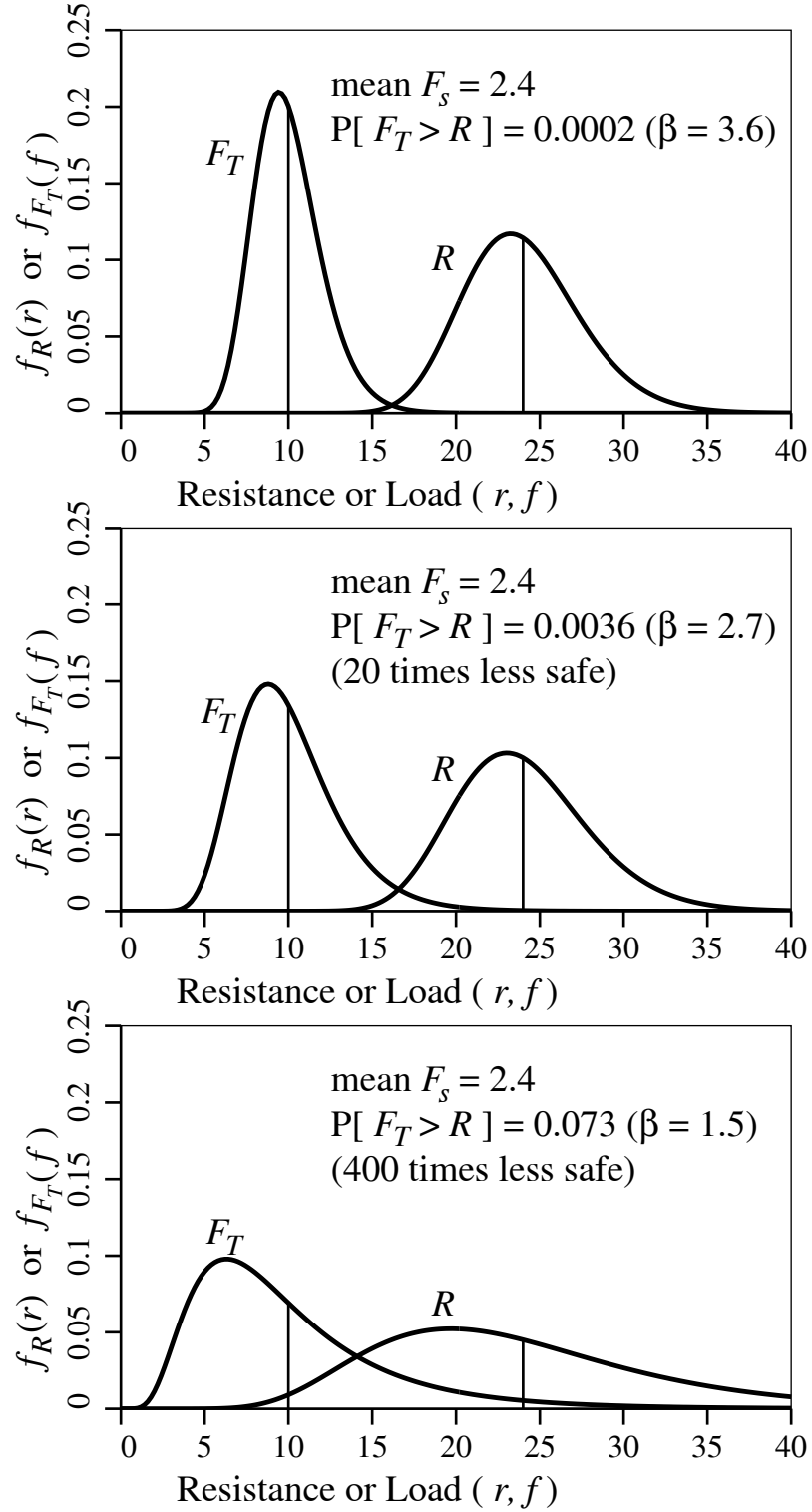
Figure 1.4 Three geotechnical problems with common mean factor of safety and yet different probabilities of failure, $P[F_T > R]$

In general eq. (1.3) is difficult to estimate, in that it requires a large amount of data to accurately fit a bivariate distribution to the bivariate histogram. Accumulating the required amount of data to estimate $f_{RF_T}(r, f)$ is not always a possibility. A common simplification is to assume that R and F_T are independent random variables, so that,

$$f_{RF_T}(r, f) = f_R(f) \cdot f_{F_T}(f) \tag{1.4}$$

which simplifies eq. (1.2) to

$$\mathrm{P}[R > F_T] = \int_{-\infty}^{\infty} \int_{r>f}^{\infty} f_R(r) f_{F_T}(f) \, dr \, df = \int_{-\infty}^{\infty} f_{F_T}(f) \int_{r>f}^{\infty} f_R(r) \, dr \, df \tag{1.5}$$

A further simplification can be made if R and F_T are assumed to be either normal or lognormal. Given that the event $R > F_T$ is equivalent to events $R - F_T > 0$ and $R/F_T > 1$, the so called "safety margin",

$$M = R - F_T \tag{1.6}$$

is normally distributed if R and F_T are normally distributed, with mean and variance,

$$\mu_M = \mu_R - \mu_T \tag{1.7a}$$

$$\sigma_M^2 = \sigma_R^2 + \sigma_T^2 \tag{1.7b}$$

Similarly,

$$M = \frac{R}{F_T} \tag{1.8}$$

is lognormally distributed if R and F_T are lognormally distributed, with mean and variance,

$$\mu_{\ln M} = \mu_{\ln R} - \mu_{\ln FT} \tag{1.9a}$$

$$\sigma_{\ln M}^2 = \sigma_{\ln R}^2 + \sigma_{\ln FT}^2 \tag{1.9b}$$

Finally, eq. (1.6) leads to

$$\mathrm{P}[R > F_T] = \mathrm{P}[R - F_T > 0] = \mathrm{P}[M > 0] = 1 - \Phi\left(-\frac{\mu_M}{\sigma_M}\right) = 1 - \Phi(-\beta) = \Phi(\beta) \tag{1.10}$$

for normal R and F_T, where Φ is the standard normal cumulative distribution function, and $\beta = \mu_M / \sigma_M$ is the reliability index. The reliability index represents the number of standard deviations that $(R - F_T)$ is away from the failure region (i.e. 0). In a similar fashion, if R and F_T are lognormal, then eq. (1.8) leads to

$$\text{P}[R > F_T] = \text{P}\left[R/F_T > 1\right] = \text{P}[M > 1] = \text{P}[\ln M > 0] = 1 - \Phi\left(-\frac{\mu_{\ln M}}{\sigma_{\ln M}}\right) = \Phi(\beta)$$

$$(1.11)$$

where the reliability index is now, $\beta = \mu_{\ln M} / \sigma_{\ln M}$.

The reliability index, β, is inversely related to the probability of failure $p_f = \text{P}[R < F_T]$, and increases with a decrease in p_f. In structural engineering, designs are typically aimed at β values of 3.0 to 3.5.

Most modern design codes are currently implementing geotechnical reliability-based "performance" designs, and the common approach used is the load and resistance factor design (LRFD) methodology, so called Limit State Design(LSD) in Canada. The LRFD approach, for any limit state, specifies that the factored resistance must exceed the sum of the factored load effects. Thus, the LRFD requirement can be generally written as

$$\varphi_g \hat{R} \geq \sum I_i \alpha_i \hat{F}_i \tag{1.12}$$

in which φ_g is the geotechnical resistance factor, and $\hat{R}$ is the characteristic ultimate resistance. The right-hand-side consists of I_i, an importance factor, multiplying the $i^{\,th}$ factored characteristic load effect, $\alpha_i \hat{F}_i$. The load factors, α_i, typically account for uncertainty in loads, and are greater than 1.0 for ultimate limit states but often assumed equal to 1.0 for serviceability limit states. The geotechnical resistance factor, φ_g, is typically less than 1.0 and accounts for uncertainties in geotechnical parameters used to estimate the characteristic geotechnical resistance, $\hat{R}$, while the importance factor, I_i, is employed to adjust the target reliability level for differing importances of the supported structure. The importance factor

is typically added to the load side of eq. (1.12) in order to account for failure consequence and is generally applied to site specific and highly uncertain loads (usually snow, wind, and earthquake). I_i is greater than 1.0 for important structures, such as hospitals, and less than 1.0 for structures whose failure is unlikely to threaten safety (eg. storage sheds). An importance factor of 1.0 is commonly used for most typical structures.

The LRFD approach outperforms the WSD approach in that it replaces a single factor of safety with a set of partial safety factors on individual components of resistance and load, and uses limit states as the checking points for design. In general, LRFD leads to safer and more economic designs than does WSD. Nevertheless, geotechnical designs face major and site specific uncertainties in soil resistance, and current LRFD methodologies do not adequately accommodate the effect of spatial randomness of the soil on the design reliability.

1.2.1   Thesis Objective

By and large, the ground is one of the most highly variable, hence uncertain, engineering materials. Unlike quality controlled materials such as wood, concrete, or steel, whose probability distributions are well known and relatively constant world-wide, geotechnical designers face large resistance uncertainties from site to site, and even within a site. Because of this site specific uncertainy, there is a real desire in the geotechnical community to account for site understanding in order to achieve economical, yet safe designs. To accomplish this, it makes sense to have a resistance factor which is adjusted as a function of site understanding and that allows maintaining overall safety at a common target maximum failure probability as well as demonstrating the direct economic advantage of increased site understanding. Currently, the Canadian design codes specify a single resistance factor for each limit state. In other words, the codes make no allowance for changes in the resistance factor as changes in the level of site understanding and, for that matter, of failure consequences, occur.

The overall safety level of any design should depend on at least three factors: 1) the uncertainty in the loads, 2) the uncertainty in the resistance, and 3) the severity of the failure consequences. In most modern codes, these three items are assumed independent of one another and are thus treated separately. The load factors handle the uncertainties in the loads and, on the load side, failure consequences are handled by applying an importance factor to the more uncertain and site specific loads (e.g. earthquake, snow, and wind). Uncertainties in resistance are handled by resistance factors that are usually specific to the material used in the design (e.g. ϕ_c for concrete, ϕ_s for steel, etc). When dealing with a highly variable and site specific material such as the ground, it makes sense to apply a factor that depends on both the resistance uncertainty and on the consequences of failure. The basic idea is that the overall partial factor applied to the geotechnical resistance should vary with both uncertainty and failure consequence. Increased site investigation should lead to lower uncertainty and a higher resistance factor, and thus a more economical design. Similarly, for geotechnical systems with high failure consequences, e.g. failure of the foundation of a major multi-lane highway bridge in a large city, the overall resistance factor should be decreased to provide a decreased maximum acceptable failure probability. Similar to the multiplicative approach taken in structural engineering, where the overall load factor is a product of a load factor and an importance factor, the overall resistance factor applied to geotechnical resistance is taken here to consist of two parts which are multiplied together;

1) a resistance factor, φ_{gu} or φ_{gs}, which accounts for resistance uncertainty. This factor basically aims to achieve a target maximum acceptable failure probability equal to that used for geotechnical designs for typical failure consequences e.g. lifetime failure probability of approximately $1/5{,}000$ for ultimate limit states or $1/300$ for serviceability limit states. The subscript g refers to "geotechnical"(or "ground"), while the subscripts u and s refer to ultimate and serviceability limit states, respectively.

2) a consequence factor, Ψ, which accounts for failure consequences. Essentially, $\Psi > 1$ if failure consequences are low and $\Psi < 1$ if failure consequence exceed those of typical geotechnical systems. For typical systems, or where system importance is already accounted for adequately by load importance factors, $\Psi = 1$. The basic idea of the consequence factor is to adjust the maximum acceptable failure probability of the design down (e.g. to 1/10,000 at ULS and 1/1,000 at SLS) for high failure consequences, or up (e.g. to 1/1,000 at ULS and 1/100 at SLS) for low failure consequences.

The geotechnical design proceeds by confirming that the factored geotechnical resistance at least equals the effect of factored loads. For example, for ultimate limit states (ULS), this means that the geotechnical design should satisfy an equation of the form

$$\Psi_u \varphi_{gu} \hat{R}_u \geq \sum I_i \alpha_i \hat{F}_i \qquad (1.13)$$

in which Ψ_u is a consequence factor, φ_{gu} is the geotechnical resistance factor at ULS, and $\hat{R}_u$ is the characteristic ultimate resistance. The right-hand-side consists of I_i, an importance factor, multiplying the ith factored load effect, $\alpha_i \hat{F}_i$. A similar equation must be satisfied for serviceability limit states (SLS), with the subscript u replaced by s, i.e.,

$$\Psi_s \varphi_{gs} \hat{R}_s \geq \sum I_i \alpha_i \hat{F}_i \qquad (1.14)$$

As mentioned previously, the load factors, α_i, typically account for uncertainty in loads, and are greater than 1.0 for ultimate limit states but usually assumed equal to 1.0 for serviceability limit states. The geotechnical resistance factor, φ_{gu} or φ_{gs}, is typically less than 1.0 and accounts for uncertainties in geotechnical parameters used to estimate the characteristic geotechnical resistance, $\hat{R}_u$ or $\hat{R}_s$, along with other sources of error (e.g. model error). The consequence factor, Ψ_u or Ψ_s, and the importance factor, I_i, are employed to adjust the target reliability level to account for different magnitudes of failure consequences. As discussed earlier, the importance factor is applied to the load side of

eq's. (1.13) and (1.14) in order to account for failure consequences and is generally based on site specific and highly uncertain load distributions (usually snow, wind, and earthquake). Because the ground is also site specific and highly uncertain, it makes sense to apply a consequence factor to the resistance side of eq's. (1.13) and (1.14) and so adjust the factored resistance to account for failure consequences, particularly in those cases not covered by the load side importance factor. Further research needs to be performed to establish the interaction between the importance and consequence factors and their combined effect on failure probability. To avoid double factoring (prior to such research), the consequence factor should probably be set to 1.0 whenever the importance factor is other than 1.0.

The focus of this work is on calibrating resistance factors and studying consequence factors for serviceability limit states. Thus, the importance factors, I_i, will be assumed to have values 1.0, as they are typically in most design codes for SLS. This simplifies the LRFD eq's. (1.13) and (1.14) to

$$\Psi_u \varphi_{gu} \hat{R}_u \geq \sum \alpha_i \hat{F}_i \qquad (1.15a)$$

$$\Psi_s \varphi_{gs} \hat{R}_s \geq \sum \alpha_i \hat{F}_i \qquad (1.15b)$$

Three target reliabilities will be considered; high, typical, and low, corresponding to important structures where failure has large consequences (e.g. hospitals, schools, and lifeline highway bridges), typical structures, which constitute the majority of civil engineering projects, and low-failure consequence structures (e.g. low use storage facilities, low use bridges, etc.), respectively. Most designs will be aimed at the typical failure consequence level, which in this research will be assumed to have a maximum lifetime failure probability, p_{max}, of about 1/5,000 at ULS and 1/300 at SLS. These correspond to lifetime reliability indices of about $\beta = 3.5$ (e.g. Meyerhof, 1995) and 2.7 at ULS and SLS respectively. Note that these target failure probabilities assume some redundancy (as typically required in structural codes), so that the actual system lifetime failure probability is usually less than

the component maximum lifetime failure probability, p_{max}. The effect of redundancy in geotechnical components on reliability may lead to adjustment of the consequence factor, as investigated in Chapter 5.

The theoretical framework required to estimate the resistance factor at SLS, φ_{gs}, is investigated in Chapter 3. Naghibi and Fenton (2011) give a complete discussion, along with simulation-based validation of the theory to find resistance factor at ULS, φ_{gu}, which is summarized in Chapter 4. The factors are targeted to achieve the "typical" failure probabilities, $p_{max} \simeq 1/5{,}000$ at ULS and $p_{max} \simeq 1/300$ at SLS, for which the consequence factor, Ψ_u, is set to 1.0. Chapter 4 then proceeds to concentrate on the consequence factor, both at ULS and SLS, Ψ_u or Ψ_s, and how they vary with respect to target failure probability and site uncertainty, and ultimately, how the consequence factor at SLS compares to the one at ULS.

1.3 SLS DESIGN OF PILES

Prediction of pile settlement has been studied previously by various authors, and the common models used in practice can be categorized into four groups:

1) "Load-transfer" $(t - z)$ methods, which use measured relationships between the load applied to the top of the pile and the pile displacement at various points along the pile (e.g. Coyle and Reese 1966, Kraft et al. 1981, Randolph 1994a, 1994b).

2) Methods based on the theory of elasticity that employ the equations of Mindlin (1936) for subsurface loading within a semi-infinite mass. (e.g. Butterfield and Banerjee 1971, Banerjee and Davies 1977, Poulos and Davis 1980, Randolph and Wroth 1978, Das 2000, and Coduto 2001)

3) Simplified analysis methods which consider localized shear around the pile and can lead to convenient closed-form solutions (e.g. Randolph and Wroth, 1978, Fleming et al., 2009)

4) Numerical methods; and in particular, the finite element method. (Jardine et al. 1986)

The basis of design used in Chapter 3 has the same form as suggested by Poulos (Poulos and Davis, 1980) and Randolph (Randolph and Wroth, 1978), which falls into category 2 (elasticity theory) mentioned above.

1.4   FINITE ELEMENT MODELING OF PILE SETTLEMENT

Finite element analysis is a powerful methodology to predict how an object reacts to real-world physical effects. FE works by breaking down, or 'discretizing', an object into a number of finite elements. In three-dimensional analysis the elements could be cubes. Mathematical equations predict the behaviour of each element under outside influences, and finally all the individual behaviours are added up to predict the behaviour of the object as a whole.

In this thesis, the finite element method (Smith et al. 2014, Fenton and Griffiths, 2005 and 2007) is employed to predict the settlement of piles founded in a three-dimensional linearly elastic soil mass and supporting a vertical load, F_T. A short review of the method, as presented by Smith et al. (2014), is presented in the remainder of this section.

In the finite element analysis, each element is characterized by a number of attributes, such as dimensionality, nodes, geometry, and degrees of freedom (DOF). Elements can have dimensionality of one, two, or three space dimensions. Each element has a set of points called nodes, which basically define element geometry, and host the DOFs, corresponding to that node. Nodes are usually, but not always, located at the corners of elements. The element geometry is defined by the placement of the nodes. The element DOFs signify the state of the element, with respect to the problem of interest, i.e. displacement. In other words, DOFs are the unknown quantities associated with a node that must be solved for mathematically.

'Boundary conditions' specify how the edges of the mesh are s upported. The nodes that are subject to boundary conditions are either fixed or allowed to move in one, two, or all three directions. In this thesis, the mesh considered is fixed along the base i.e. the $x - y$ plane in Figure 1.5 is restrained in the z-direction. In addition, the $y - z$ and $x - z$ planes are restrained in x- and y-directions, respectively. These assumptions imply that no displacement is to be allowed in the z-direction for the nodes on the $x - y$ plane, and so on. The use of vertical rollers on all four side faces allows displacement in the z-direction for all nodes, except for the ones on the $x - y$ plane.
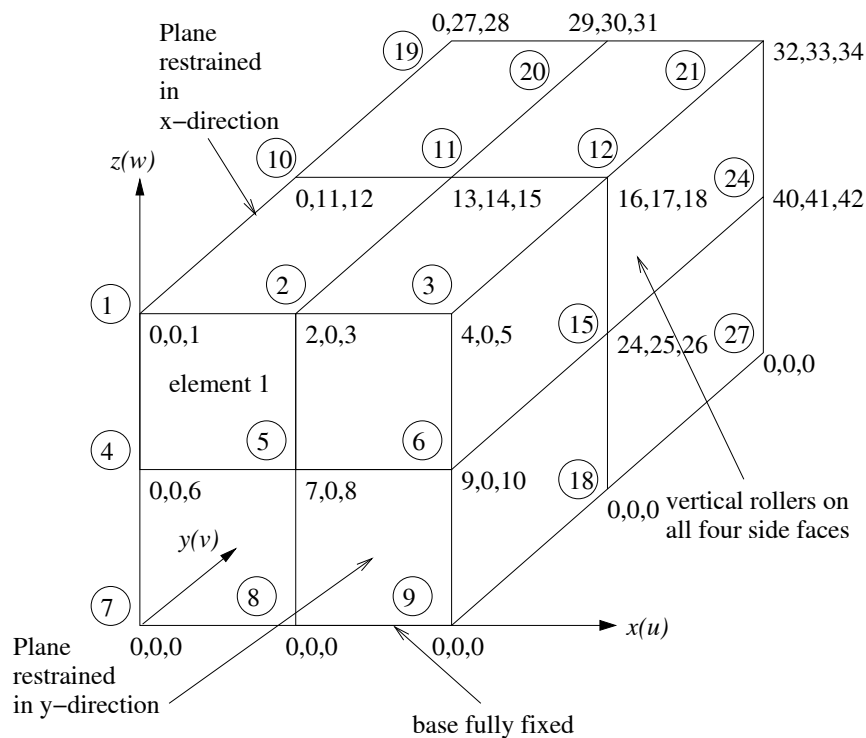
Figure 1.5　8-node brick element with node numbers in circles, and three degrees of freedom per node (not circled)

Nodes are numbered globally with respect to the mesh, and DOFs are numbered in the same order as nodes. Figure 1.5 demonstrates a mesh made up of three-dimensional brick elements with node numbers in circles, and three DOFs per node (not circled). The DOFs at each node represent possible displacements in the x-, y-, and z-directions. For example,

the triplet $(0, 0, 6)$ at node 4 indicates that displacement is only allowed in z-direction. In general, DOFs of the forms $(i, j, 0)$, $(0, j, k)$, and $(i, 0, k)$ are assigned to the nodes on the planes $x - y$, $y - z$, and $x - z$ respectively. For each element, there is a set of nodal forces corresponding to each DOF.

If F is an applied body force (units of force/length^3) with three components F_x, F_y, and F_z, then the differential equation system to be solved for this static equilibrium problem in three-dimensions is,

$$\frac{\partial \sigma_x}{\partial x} + \frac{\partial \tau_{xy}}{\partial y} + \frac{\partial \tau_{zx}}{\partial z} + F_x = 0$$

$$\frac{\partial \sigma_y}{\partial y} + \frac{\partial \tau_{xy}}{\partial x} + \frac{\partial \tau_{yz}}{\partial z} + F_y = 0$$

$$\frac{\partial \sigma_z}{\partial z} + \frac{\partial \tau_{yz}}{\partial y} + \frac{\partial \tau_{zx}}{\partial x} + F_z = 0 \tag{1.16}$$

where σ_x, σ_y, σ_z, τ_{xy}, τ_{yz}, and τ_{zx} are the stress components given by

$$
\begin{bmatrix} \sigma_x \\ \sigma_y \\ \sigma_z \\ \tau_{xy} \\ \tau_{yz} \\ \tau_{zx} \end{bmatrix}
= \frac{E(1-\nu)}{(1+\nu)(1-2\nu)}
\begin{bmatrix}
1 & \frac{\nu}{(1-\nu)} & \frac{\nu}{(1-\nu)} & 0 & 0 & 0 \\
\frac{\nu}{(1-\nu)} & 1 & \frac{\nu}{(1-\nu)} & 0 & 0 & 0 \\
\frac{\nu}{(1-\nu)} & \frac{\nu}{(1-\nu)} & 1 & 0 & 0 & 0 \\
0 & 0 & 0 & \frac{1-2\nu}{2(1-\nu)} & 0 & 0 \\
0 & 0 & 0 & 0 & \frac{1-2\nu}{2(1-\nu)} & 0 \\
0 & 0 & 0 & 0 & 0 & \frac{1-2\nu}{2(1-\nu)}
\end{bmatrix}
\begin{bmatrix} \epsilon_x \\ \epsilon_y \\ \epsilon_z \\ \gamma_{xy} \\ \gamma_{yz} \\ \gamma_{zx} \end{bmatrix}
\tag{1.17}
$$

where E is the soil's elastic modulus, ν is the Poisson's ratio, and ϵ_x, ϵ_y, ϵ_z, γ_{xy}, γ_{yz}, and γ_{zx} are strain components. The full strain-displacement relations are given by (Timoshenko and Goodier, 1982)

$$
\begin{bmatrix} \epsilon_x \\ \epsilon_y \\ \epsilon_z \\ \gamma_{xy} \\ \gamma_{yz} \\ \gamma_{zx} \end{bmatrix}
=
\begin{bmatrix}
\frac{\partial}{\partial x} & 0 & 0 \\
0 & \frac{\partial}{\partial y} & 0 \\
0 & 0 & \frac{\partial}{\partial z} \\
\frac{\partial}{\partial y} & \frac{\partial}{\partial x} & 0 \\
0 & \frac{\partial}{\partial z} & \frac{\partial}{\partial y} \\
\frac{\partial}{\partial z} & 0 & \frac{\partial}{\partial x}
\end{bmatrix}
\begin{bmatrix} u \\ v \\ w \end{bmatrix}
\tag{1.18}
$$

where u, v, and w are the components of displacement at a point in the x-, y-, and z-directions, respectively. Eq. (1.16), (1.17), and (1.18) can be written as

$$[A]^T\{\sigma\} = -\{f\} \tag{1.19}$$

$$\{\sigma\} = [D]\{\epsilon\} \tag{1.20}$$

$$\{\epsilon\} = [A]\{e\} \tag{1.21}$$

where

$$\{\sigma\} = \begin{bmatrix} \sigma_x \\ \sigma_y \\ \sigma_z \\ \tau_{xy} \\ \tau_{yz} \\ \tau_{zx} \end{bmatrix}, \{\epsilon\} = \begin{bmatrix} \epsilon_x \\ \epsilon_y \\ \epsilon_z \\ \gamma_{xy} \\ \gamma_{yz} \\ \gamma_{zx} \end{bmatrix}, \{e\} = \begin{bmatrix} u \\ v \\ w \end{bmatrix}, \{f\} = \begin{bmatrix} F_x \\ F_y \\ F_z \end{bmatrix} \tag{1.22}$$

$$[A] = \begin{bmatrix} \frac{\partial}{\partial x} & 0 & 0 \\ 0 & \frac{\partial}{\partial y} & 0 \\ 0 & 0 & \frac{\partial}{\partial z} \\ \frac{\partial}{\partial y} & \frac{\partial}{\partial x} & 0 \\ 0 & \frac{\partial}{\partial z} & \frac{\partial}{\partial y} \\ \frac{\partial}{\partial z} & 0 & \frac{\partial}{\partial x} \end{bmatrix}, [D] = \frac{E(1-\nu)}{(1+\nu)(1-2\nu)} \begin{bmatrix} 1 & \frac{\nu}{(1-\nu)} & \frac{\nu}{(1-\nu)} & 0 & 0 & 0 \\ \frac{\nu}{(1-\nu)} & 1 & \frac{\nu}{(1-\nu)} & 0 & 0 & 0 \\ \frac{\nu}{(1-\nu)} & \frac{\nu}{(1-\nu)} & 1 & 0 & 0 & 0 \\ 0 & 0 & 0 & \frac{1-2\nu}{2(1-\nu)} & 0 & 0 \\ 0 & 0 & 0 & 0 & \frac{1-2\nu}{2(1-\nu)} & 0 \\ 0 & 0 & 0 & 0 & 0 & \frac{1-2\nu}{2(1-\nu)} \end{bmatrix} \tag{1.23}$$

Substituting eq. (1.20) and (1.21) into (1.19) gives,

$$[A]^T\{\sigma\} = [A]^T[D]\{\epsilon\} = [A]^T[D][A]\{e\} = -\{f\} \tag{1.24}$$

resulting in elimination of $\{\sigma\}$ and $\{\epsilon\}$ from eq. (1.19). Substituting appropriate matrices into eq. (1.24) leads to

$$\frac{E(1-\nu)}{(1+\nu)(1-2\nu)} \begin{bmatrix} \frac{\partial^2 u}{\partial x^2} + \frac{1-2\nu}{2(1-\nu)}(\frac{\partial^2 u}{\partial y^2} + \frac{\partial^2 u}{\partial z^2}) + \frac{3-2\nu}{1-\nu}\frac{\partial^2 v}{\partial x \partial y} + \frac{3-2\nu}{1-\nu}\frac{\partial^2 w}{\partial x \partial z} \\ \frac{3-2\nu}{1-\nu}\frac{\partial^2 u}{\partial x \partial y} + \frac{\partial^2 v}{\partial y^2} + \frac{1-2\nu}{2(1-\nu)}(\frac{\partial^2 v}{\partial x^2} + \frac{\partial^2 v}{\partial z^2}) + \frac{3-2\nu}{1-\nu}\frac{\partial^2 w}{\partial z \partial y} \\ \frac{3-2\nu}{1-\nu}\frac{\partial^2 u}{\partial x \partial z} + \frac{3-2\nu}{1-\nu}\frac{\partial^2 v}{\partial y \partial z} + \frac{\partial^2 w}{\partial z^2} + \frac{1-2\nu}{2(1-\nu)}(\frac{\partial^2 w}{\partial y^2} + \frac{\partial^2 w}{\partial x^2}) \end{bmatrix} = \begin{bmatrix} -F_x \\ -F_y \\ -F_z \end{bmatrix} \tag{1.25}$$

which is a triplet of simultaneous partial differential equations in the continious space variables u, v, and w. The variables u, v, and w are approximated by $\tilde{u}$, $\tilde{v}$, and $\tilde{w}$ in terms of their nodal values, u_i, v_i, and w_i, $i = 1, ..., 8$, through simple functions, so-called 'shape' functions,

$$\tilde{u} = \{N\}^T \{u\}$$

$$\tilde{v} = \{N\}^T \{v\}$$

$$\tilde{w} = \{N\}^T \{w\} \tag{1.26}$$

where $\{N\} = \{N_1 \ N_2 \ ... \ N_8\}^T$, $\{u\} = \{u_1 \ u_2 \ ... \ u_8\}^T$, $v = \{v_1 \ v_2 \ ... \ v_8\}^T$, $w = \{w_1 \ w_2 \ ... \ w_8\}^T$, and (u_i, v_i, w_i) are the displacement components of the ith node. For the 8-node brick elements shown in Figure 1.5, the shape functions, $N_i, i = 1, ..., 8$, are

$$N_1 = (1 - x/a)(1 - y/b)(1 - z/c)$$

$$N_2 = (1 - x/a)(1 - y/b)(z/c)$$

$$N_3 = (x/a)(1 - y/b)(z/c)$$

$$N_4 = (x/a)(1 - y/b)(1 - z/c)$$

$$N_5 = (1 - x/a)(y/b)(1 - z/c)$$

$$N_6 = (1 - x/a)(y/b)(z/c)$$

$$N_7 = (x/a)(y/b)(z/c)$$

$$N_8 = (x/a)(y/b)(1 - z/c) \tag{1.27}$$

where each element is of dimension $a \times b \times c$.

The stiffness matrix for an 8-node brick element is then obtained by discretization. Utilizing Galerkin's method (Szabo and Lee, 1969), and replacing $\frac{d^2u}{dx^2}$ in the differential equation

with $-\int \frac{dN_i}{dx}\frac{dN_j}{dx}dx$ in the matrix equation (and similarly for other derivations) leads to,

$$\frac{E(1-\nu)}{(1+\nu)(1-2\nu)}\int_0^a\int_0^b\int_0^c \begin{bmatrix} \frac{\partial N_i}{\partial x}\frac{\partial N_j}{\partial x}+\frac{1-2\nu}{2(1-\nu)}\left(\frac{\partial N_i}{\partial y}\frac{\partial N_j}{\partial y}+\frac{\partial N_i}{\partial z}\frac{\partial N_j}{\partial z}\right) \\ \times\frac{3-2\nu}{1-\nu}\frac{\partial N_i}{\partial x}\frac{\partial N_j}{\partial y} \\ \times\frac{3-2\nu}{1-\nu}\frac{\partial N_i}{\partial x}\frac{\partial N_j}{\partial z} \\ \\ \frac{3-2\nu}{1-\nu}\frac{\partial N_i}{\partial x}\frac{\partial N_j}{\partial y} \\ \times\frac{\partial N_i}{\partial y}\frac{\partial N_j}{\partial y}+\frac{1-2\nu}{2(1-\nu)}\left(\frac{\partial N_i}{\partial x}\frac{\partial N_j}{\partial x}+\frac{\partial N_i}{\partial z}\frac{\partial N_j}{\partial z}\right) \\ \times\frac{3-2\nu}{1-\nu}\frac{\partial N_i}{\partial z}\frac{\partial N_j}{\partial y} \\ \\ \frac{3-2\nu}{1-\nu}\frac{\partial N_i}{\partial x}\frac{\partial N_j}{\partial z} \\ \times\frac{3-2\nu}{1-\nu}\frac{\partial N_i}{\partial y}\frac{\partial N_j}{\partial z} \\ \times\frac{\partial N_i}{\partial z}\frac{\partial N_j}{\partial z}+\frac{1-2\nu}{2(1-\nu)}\left(\frac{\partial N_i}{\partial y}\frac{\partial N_j}{\partial y}+\frac{\partial N_i}{\partial x}\frac{\partial N_j}{\partial x}\right) \end{bmatrix}_{i,j=1,\ldots,8} dx\,dy\,dz\{u\}=\{f\}$$

(1.28)

where $\{u\}$ and $\{f\}$ are the nodal displacement and force components. See Smith et al. (2014) for details. The stiffness relationship for an element can be simply written as,

$$[k_m]\{u\}=\{f\} \tag{1.29}$$

where $[k_m]$ is the matrix multiplying $\{u\}$ in eq. (1.28).

Traditionally, for static equilibrium problems, computer programs assemble all the element $[k_m]$ matrices and $\{f\}$ vectors to form a global matrix of linear simultaneous equations having the form

$$[K_m]\{U\}=\{F\} \tag{1.30}$$

The global linear algebraeic system would then be solved by some form of Gaussian elimination. The solution of this matrix problem becomes numerically cumbersome as the domain size grows. For instance, for a 50 by 30 by 30 element mesh in three-dimensions, the global stiffness matrix requires about 2 GBytes of memory. Not only is this a concern for memory space, but the solution can take a long time and be vulnerable to significant round-off errors.

Alternatively, an element-by-element approach, such as the *Conjugate Gradient* iterative solver, can be employed to avoid the need to assemble the entire stiffness matrix in the finite element analysis and improve accuracy. This method proceeds by setting

$$\{P\}_0 = \{R\}_0 = \{F\} - [K_m]\{U\}_0 \tag{1.31}$$

where $\{R\}_0$ is the residual or error for a first trial displacement, $\{U\}_0$, followed by k steps of the process:

$$[Q]_k = [K_m]\{P\}_k$$
$$\alpha_k = \frac{\{R\}_k^T\{R\}_k}{\{P\}_k^T\{Q\}_k}$$
$$\{U\}_{k+1} = \{U\}_k + \alpha_k\{P\}_k$$
$$\{R\}_{k+1} = \{R\}_k - \alpha_k\{Q\}_k$$
$$\beta_k = \frac{\{R\}_{k+1}^T\{R\}_{k+1}}{\{R\}_k^T\{R\}_k}$$
$$\{P\}_{k+1} = \{R\}_{k+1} + \beta_k\{P\}_k \tag{1.32}$$

until the difference between $\{U\}_{k+1}$ and $\{U\}_k$ is small enough according to a convergence criterion. In eq. (1.32), α and β are scalars while $\{Q\}$, $\{P\}$, and $\{R\}$ are vectors of size n_{eq} (the number of equations to be solved). The vector $\{P\}$ is an approximation to the unknown $\{U\}$ in eq. (1.30). Making this replacement, eq. (1.30) now involves the product $[K_m]\{P\}$, with known vector $\{P\}$. The product $[K_m]\{P\}$ can be performed 'element-by'element' without assembly of $[K_m]$, that is

$$|Q| = \sum_{i=1}^{n_{els}} [k_m]_i\{p\}_i \tag{1.33}$$

where n_{els} is the number of elements, $[k_m]_i$ is the stiffness matrix of the ith element and $\{p\}_i$ is a displacement correction vector which is extracted on an element by element basis. For example, for $i = 1$ (element 1) in Figure 1.5, $\{p\}_i = [p_4\ p_1\ p_2\ p_5]^T$.

Using this element-by-element algorithm reduces the required storage by an order of magnitude, increasing linearly with increase in number of elements (or equations), rather than as the square. Element-by-element algorithms can be further improved using 'preconditioning' (Griffiths and Smith, 2006) techniques which accelerate the convergence in some cases.

In this thesis, the finite element model used to predict the settlement of a pile founded in a three-dimensional linearly elastic soil mass supporting a vertical load, F_T, employs a mesh of eight-node brick elements each having dimensions 0.3 m by 0.3 m in the $x - y$ plane and 0.5 m in the z-directions. A cross-section through the three-dimensional mesh is illustrated in Figures 1.1 and 1.2 for single and two pile cases, respectively. Within the mesh, the pile is modeled as a column of elements having depth H and elastic modulus E_p. Typically, E_p is several orders of magnitude higher than that of the surrounding soil. Due to the finite element modeling, the pile is assumed here to be of square cross-section with fixed cross-sectional dimension $d \times d$, where $d = 0.3$ m.

1.5 RANDOM FIELDS

"Random fields" provide realistic representations of the ground, allowing for more natural geotechnical failure mechanisms. A random field $X(\underset{\sim}{t})$ is a collection of random variables, $X_1 = X(\underset{\sim}{t}_1)$, $X_2 = X(\underset{\sim}{t}_2)$, ..., whose values are associated with each spatial location, $\underset{\sim}{t}$. Values in a random field are usually spatially correlated in one way or another and the interdependence between the points in a random field are characterized by an infinite-dimensional probability density function $f_{X_1 X_2 ..}(x_1, x_2, ...)$. Since infinite-dimensional probability density functions are difficult to estimate, the following simplifying assumptions are commonly made;

1) *Gaussian process*: The joint PDF is a multivariate normally distributed random field. Such a field is conveniently specified by only its mean, variance, and correlation structure.

2) *Stationary (statistical homogeneity)*; The joint PDF is independent of spatial position and only depends on relative positions between points and not on their spatial position. In other words, the mean, variance, and higher order moments are spatially constant.

3) *Isotropy*: The joint PDF is invariant under rotation, that is, the correlation between two points only depends on the distance between the two points and not on their orientation relative to one another.

A convenient measure of the correlation structure of a random field is *correlation length*, θ, which loosely speaking, is the distance beyond which points are negligibly correlated. Mathematically, θ is defined here as the area under the correlation function (Vanmarcke, 1984),

$$\theta = \int_{-\infty}^{\infty} \rho(\tau)\, dt \tag{1.34}$$

where the correlation function, $\rho(\tau)$, expresses the correlation coefficient between random field values at points seperated by the lag distance, τ. A common correlation function will be discussed shortly.

Figure 1.6 demonstrates how fields with small θ tend to be `rough'(left), while fields with larger θ are usually smoother (Fenton and Griffiths, 2008).
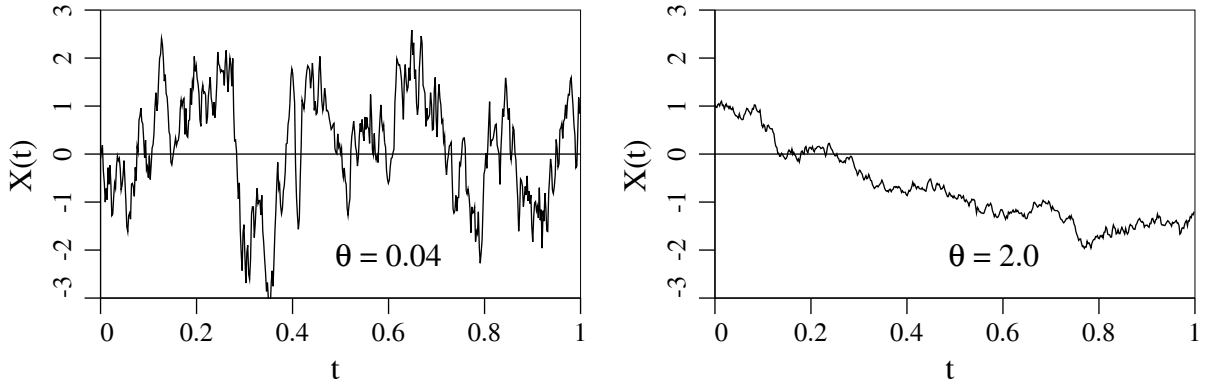
Figure 1.6   Sample realizations of $X(t)$ for two different correlation lengths

The spatial dependence in a random field is characterized by the field correlation structure, which is usually specified through a correlation function parameterized by a correlation length, θ. There are several commonly used correlation functions, among which the isotropic exponentially decaying Markov correlation function is used here due to its simplicity. The Markov correlation function is a memoryless process in one-dimension, which implies that for a stochastic process the future of the random process only directly depends on the present and not on the past. The Markov correlation function has the form

$$\rho(t) = \exp\left\{-\frac{2|\tau|}{\theta}\right\} \tag{1.35}$$

where τ is the distance between any two points in the field and θ is the correlation length (Fenton and Griffiths, 2008).

Almost all engineering properties are in fact local averages of some sort. A local average is defined as an arithmetic average of the random field, X(t), over a region of some size, T, as follows (in one-dimension)

$$X_T(t) = \frac{1}{T}\int_{t-\frac{T}{2}}^{t+\frac{T}{2}} X(\xi)d\xi \tag{1.36}$$

The main effect of local averaging is to reduce the variance, and the amount of variance reduction is directly related to the degree of dependence in the random field. For a stationary

random field, $X(t)$, the mean of a local average is

$$\mu_{X_T} = \mathrm{E}\left[X_T(t)\right] = \mathrm{E}\left[\frac{1}{T}\int_{t-\frac{T}{2}}^{t+\frac{T}{2}} X(\xi)d\xi\right] = \frac{1}{T}\int_{t-\frac{T}{2}}^{t+\frac{T}{2}} \mathrm{E}\left[X(\xi)\right]d\xi = \mathrm{E}\left[X\right] = \mu_X \quad (1.37)$$

which indicates that local averaging preserves the mean of the random field. The variance of the local average, on the other hand, is given by

$$\mathrm{Var}\left[X_T(t)\right] = \mathrm{E}\left[(X_T(t) - \mu_{X_T})^2\right] = \mathrm{E}\left[(\frac{1}{T}\int_{t-\frac{T}{2}}^{t+\frac{T}{2}} X(\xi)d\xi - \mu_{X_T})^2\right]$$

$$= \mathrm{E}\left[\left(\frac{1}{T}\int_{t-\frac{T}{2}}^{t+\frac{T}{2}} [X(\xi) - \mu_{X_T}]d\xi\right)^2\right]$$

$$= \mathrm{E}\left[\frac{1}{T}\int_{t-\frac{T}{2}}^{t+\frac{T}{2}} [X(\xi) - \mu_{X_T}]d\xi \cdot \frac{1}{T}\int_{t-\frac{T}{2}}^{t+\frac{T}{2}} [X(\eta) - \mu_{X_T}]d\eta\right]$$

$$= \frac{1}{T^2}\int_{t-\frac{T}{2}}^{t+\frac{T}{2}}\int_{t-\frac{T}{2}}^{t+\frac{T}{2}} \mathrm{E}\left[(X(\xi) - \mu_{X_T})(X(\eta) - \mu_{X_T})\right]d\xi d\eta$$

$$= \frac{1}{T^2}\int_{t-\frac{T}{2}}^{t+\frac{T}{2}}\int_{t-\frac{T}{2}}^{t+\frac{T}{2}} C_X(\xi - \eta)d\xi d\eta$$

$$= \frac{\sigma_X^2}{T^2}\int_{t-\frac{T}{2}}^{t+\frac{T}{2}}\int_{t-\frac{T}{2}}^{t+\frac{T}{2}} \rho_X(\xi - \eta)d\xi d\eta$$

$$= \sigma_X^2 \gamma(T) \quad (1.38)$$

where C_X and $\rho_X(\tau)$ are the covariance and correlation functions of $X(t)$ respectively, such that $C_X(\tau) = \sigma_X^2 \rho_X(\tau)$. In the final expression, $\gamma(T)$ is the variance reduction function corresponding to the spatial correlation function, $\rho_X(\tau)$, having the mathematical definition

$$\gamma(T) = \frac{1}{T^2}\int_{t-\frac{T}{2}}^{t+\frac{T}{2}}\int_{t-\frac{T}{2}}^{t+\frac{T}{2}} \rho_X(\xi - \eta)d\xi d\eta = \frac{1}{T^2}\int_{0}^{T}\int_{0}^{T} \rho_X(\xi - \eta)d\xi d\eta \quad (1.39)$$

which specifies how the variance is reduced upon local averaging over the length T. $\gamma(T) = 1$ when $T = 0$, which implies that $X_T(t) = X(t)$ when $T = 0$, hence no reduction in variance when no averaging is performed.

In a three-dimensional averaging of a volume of soil surrounding a pile, $\gamma(V)$ is the variance reduction function over some volume V. It will be assumed in this thesis that averaging of

the soil around a pile will take place within a box of dimension $V_p = B_p \times B_p \times C$, so that $\gamma(V_p)$ is given by

$$\gamma(V_p) = \frac{1}{V_p^2} \int_0^{V_p} \int_0^{V_p} \rho_X \left(\underset{\sim}{x}_1 - \underset{\sim}{x}_2 \right) \, d\underset{\sim}{x}_1 \, d\underset{\sim}{x}_2 \tag{1.40}$$

where $\underset{\sim}{x}_1$ and $\underset{\sim}{x}_2$ are spatial positions (x, y, z) within V_p. The pile is centered in the volume V_p in plan, although the depth C will extend below the pile, as will be shown later. Note that $\gamma(V_p)$ is essentially just the average correlation coefficient between all points within the volume V_p.

Although the normal distribution is known to be the single most important distribution since many natural "additive" type phenomena tend towards a normal distribution (according to the central limit theorem), it is not well suited to represent non-negative engineering properties. Conveniently, positive-definite non-Gaussian random fields, such as lognormal, can be produced from a Gaussian random field. For instance, if $X(t)$ is a Gaussian field, then the random field $Y(t)$ produced by the transformation

$$Y(t) = e^{X(t)} \tag{1.41}$$

has a lognormal distribution with correlation function (Fenton and Griffiths, 2008)

$$\rho_Y(\tau) = \frac{\exp\left\{\sigma_X^2 \rho_X(\tau)\right\} - 1}{\exp\left\{\sigma_X^2\right\} - 1} \tag{1.42}$$

As seen in Figure 1.7, the lognormal distribution is positive-definite and as such, is often used to represent quantities that cannot have negative values. Lognormal distibution is commonly used for modeling loads and material properties, such as a soil's elastic modulus, since these properties often cannot be negative.
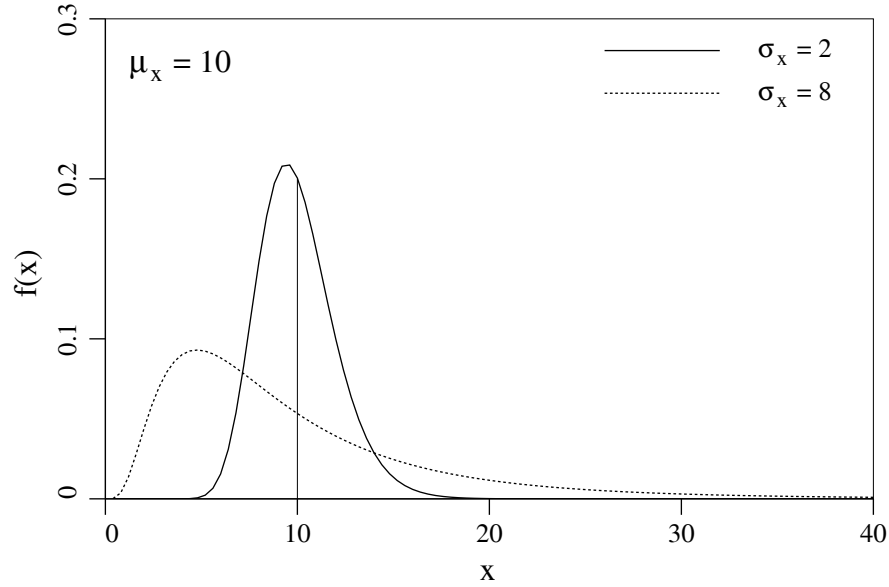
Figure 1.7 Two lognormal distributions with common mean, $\mu_X = 10$, and standard deviations $\sigma_X = 2$ and 8

In general, the random variable X is lognormally distributed if $\ln(X)$ is normally distributed. X will have probability density function (PDF)

$$f_X(x) = \begin{cases} \frac{1}{x\sigma_{\ln x}\sqrt{2\pi}} \exp\left\{-\frac{1}{2}\left(\frac{\ln x - \mu_{\ln x}}{\sigma_{\ln x}}\right)^2\right\} & \text{if } 0 < x < \infty \\ 0 & \text{otherwise} \end{cases} \tag{1.43}$$

and cumulative distribution function (CDF),

$$F_X(a) = P\left[X \leq a\right] = P\left[\ln X \leq \ln(a)\right] = P\left[Z \leq \frac{\ln(a) - \mu_{\ln X}}{\sigma_{\ln X}}\right] = \Phi\left(\frac{\ln(a) - \mu_{\ln X}}{\sigma_{\ln X}}\right)$$

where Φ is the standard normal cumulative distribution function. $\mu_{\ln X}$ and $\sigma_{\ln X}$ are the mean and standard deviation of $\ln(X)$ given by

$$\mu_{\ln X} = \ln(\mu_X) - \tfrac{1}{2}\sigma_{\ln X}^2 \tag{1.44a}$$

$$\sigma_{\ln X}^2 = \ln\left(1 + v_X^2\right) \tag{1.44b}$$

where $v_X = \sigma_X / \mu_X$ is the coefficient of variation of X. Conversely, if $\mu_{\ln X}$ and $\sigma_{\ln X}$ are known then

$$\mu_X = e^{\mu_{\ln x} + \frac{1}{2}\sigma^2_{\ln x}} \tag{1.45a}$$

$$\sigma^2_X = \mu^2_X (e^{\sigma^2_{\ln x}} - 1) \tag{1.45b}$$

In other words, the lognormal distribution is closely related to and can be easily converted to a normal distribution.

Multiplication and division preserve the lognormal distribution, that is, multiplying and/or dividing lognormal random variables also results in a lognormal random variable. For example, if X is

$$X = \frac{X_1 X_2}{X_3} \tag{1.46}$$

where X_1, X_2, and X_3 are lognormally distributed random variables, then X is also lognormal with

$$\mu_{\ln x} = \mu_{\ln x_1} + \mu_{\ln x_2} - \mu_{\ln x_3} \tag{1.47a}$$

$$\sigma^2_{\ln x} = \sigma^2_{\ln x_1} + \sigma^2_{\ln x_2} + \sigma^2_{\ln x_3} \tag{1.47b}$$

where X_1, X_2 and X_3 are assumed to be independent in eq. (1.47b).

1.6   RANDOM FIELD MODELING OF SOILS

As mentioned previously, the lognormal distribution is commonly used to represent non-negative soil properties. Since the elastic modulus, E, is non-negative with no arbitrary upper bound, it willl be assumed here that the elastic modulus is lognormally distributed. This means that $\ln E$ is normally distributed with parameters $\mu_{\ln E}$ and $\sigma_{\ln E}$, given by eq's. (1.44a) and (1.44b). Furthermore, the elastic modulu s is spatially varying random field with one additional parameter being its correlation length, $\theta_{\ln E}$.

The spatially varying elastic modulus field may be characterized by two numbers in a design; one is the effective soil elastic modulus, E_{eff}, a value which yields the same settlement in a uniform elastic modulus field as the pile experiences in the actual spatially varying soil (Fenton and Griffiths, 2007). The second is the characteristic soil elastic modulus, $\hat{E}$, which is an estimate of E_{eff} obtained from a soil sample. Investigations by Fenton and Griffiths (2002) suggest that the effective elastic modulus as seen by a shallow foundation is a geometric average of the soil's elastic modulus under the foundation. It will be similarly assumed here that both $\hat{E}$, and the effective elastic modulus, E_{eff}, as seen by a pile are defined here as geometric average of the soil's elastic modulus field, E, which is assumed to be lognormally distributed with mean μ_E, standard deviation σ_E and spatial correlation length, $\theta_{\ln E}$. The effective elastic modulus as seen by a pile of length, H, could be written as the following mathematical definition in a one-dimensional analysis (only variation along the pile)

$$E_{eff} = \exp \left\{ \frac{1}{H} \int_0^H \ln E(z) \, dz \right\} \tag{1.48}$$

where $E(z)$ is the elastic modulus of the soil at depth z adjacent to the pile.

Note that, unlike friction and/or adhesion along a pile, which only disturbs the soil at the surface of the pile, any displacement of a pile in general leads to deformation of a soil volume surrounding the pile, and as such, the effective elastic modulus seen by the pile, E_{eff}, should be calculated as the average of the elastic modulus over some volume V, and not simply as the average along the pile. In three-dimensional analysis, thus, the effective elastic modulus is a geometric average of the soil's elastic modulus over a volume surrounding the pile,

$$E_{eff} = \exp \left\{ \frac{1}{V_p} \int_{V_p} \ln E(\underline{x}) \, d\underline{x} \right\} = \exp \left\{ \frac{1}{B_p^2 C} \int_0^{B_p} \int_0^{B_p} \int_0^C \ln E(x, y, z) \, dz \, dy \, dx \right\} \tag{1.49}$$

where $E(x, y, z)$ is the elastic modulus of the soil at spatial position (x, y, z). As mentioned previously in Section 1.5, the pile is centered on the volume $B_p \times B_p \times C$.

If the soil's elastic modulus, E, is lognormally distributed, as assumed, then E_{eff} is also lognormally distributed with parameters

$$\mu_{\ln E_{eff}} = \ln(\mu_{E_{eff}}) - \tfrac{1}{2}\sigma^2_{\ln E_{eff}} \qquad (1.50a)$$

$$\sigma^2_{\ln E_{eff}} = \ln\left(1 + \frac{\sigma^2_{E_{eff}}}{\mu^2_{E_{eff}}}\right) \qquad (1.50b)$$

1.7   SIMULATION OF SOIL PROPERTIES

Many different random field generator algorithms exist of which the Local Averaging Subdivision, or LAS, method is employed in this research to provide realizations of the random elastic modulus field. LAS is an efficient and reasonably accurate method of producing realizations of a disrete "local average" random process. Amongst the available approximation methods, the LAS is considered the most difficult to implement, yet the easiest to use.

LAS is commonly used because

1) most engineering measurements are actually local averages of the property of interest. For example, CPT measurements only record the effects of deforming a bulb of soil around the cone.

2) The LAS is well suited to stochastic finite element modeling. Each discrete local average given by realization becomes the property assigned to each discrete finite element. The statistics of the random property mapped to the element changes with a change in the element size, providing finite element modelers with great flexibility to change mesh resolution without losing stochastic accuracy.

The LAS method is discussed in detail in Fenton and Griffiths (2008), and Fenton and Vanmarcke (1990), and is summarized in this section.

Consider a standard Gaussian random field, $G(\underset{\sim}{x})$, having some correlation structure, in this case as given by eq. (1.35), which is the exponentially decaying Markovian function. Now define $G_e(\underset{\sim}{x}_i)$ to be the local average of $G(\underset{\sim}{x})$ over some volume (or area), e, where $\underset{\sim}{x}_i$ is the spatial location of the centroid of the ith element,

$$G_e(\underset{\sim}{x}_i) = \frac{1}{e} \int_e G(\underset{\sim}{x})d\underset{\sim}{x} \tag{1.51}$$

Assuming that the elastic modulus field, E, is lognormal, the local averages obtained by eq. (1.51) are mapped to finite element elastic modulus properties according to

$$E(\underset{\sim}{x}_i) = \exp\left\{\mu_{\ln E} + \sigma_{\ln E}G(\underset{\sim}{x}_i)\right\} \tag{1.52}$$

The construction of the local average process via LAS proceeds in a top-down recursive algorithm depicted in Figure 1.8. It begins initially by generating a global average for the process at Stage 0, and subsequent stages are obtained by subdividing each parent cell and generating values for the resulting two regions while maintaining upwards averaging. In this way, the global average remains constant throughout the subdivision. The algorithm is as follows:

Stage 0					Z_1^0				

Figure 1.8 shows the LAS construction with stages:
- Stage 0: Z_1^0
- Stage 1: Z_1^1, Z_2^1
- Stage 2: Z_1^2, Z_2^2, Z_3^2, Z_4^2
- Stage 3: Z_1^3, Z_2^3, Z_3^3, Z_4^3, Z_5^3, Z_6^3, Z_7^3, Z_8^3
- Stage 4
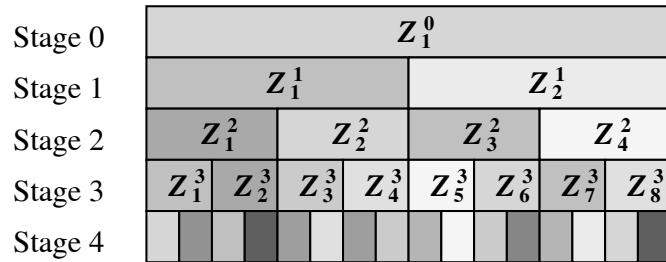
Figure 1.8   One-dimensional LAS construction of local average random process

1) generate a normally distributed global average (Z_1^0 in Figure 1.8) with mean zero and variance obtained from local averaging theory (stage 0),

2) subdivide the field into two equal parts,

3) generate two normally distributed values, Z_1^1 and Z_2^1 (stage 1), which satisfy three criteria;

    a) show the correct variance according to local averaging theory,

    b) they are properly correlated with one another,

    c) they average to the parent value, i.e. $\frac{1}{2}(Z_1^1 + Z_2^1) = Z_1^0$.

In other words, the distributions of Z_1^1 and Z_2^1 are conditioned on the value of Z_1^0.

4) subdivide each cell in stage 1 into two equal parts,

5) for each part, generate two normally distributed values, e.g. Z_1^2 and Z_2^2 (stage 2), which satisfy four criteria;

    a) show the correct variance according to local averaging theory,

    b) they are properly correlated with one another,

    c) they average to the parent value, i.e. $\frac{1}{2}(Z_1^2 + Z_2^2) = Z_1^1$ (The distributions of Z_1^2 and Z_2^2 are conditioned on the value of Z_1^1),

    d) they are properly correlated with their neighboring cells Z_3^2 and Z_4^2.

6) subdivide each cell in stage 2 into two equal parts (stage 3), and repeat steps 5 and 6.

Figure 1.9 shows a 2-D LAS, in which each cell is divided into 4 equal sized cells.

$$
\begin{array}{|c|c|c|}
\hline
Z^i_1 & Z^i_2 & Z^i_3 \\
\hline
Z^i_4 \quad \begin{array}{c|c} Z^{i+1}_1 & Z^{i+1}_2 \\ \hline Z^i_5 & \\ \hline Z^{i+1}_3 & Z^{i+1}_4 \end{array} & Z^i_6 \\
\hline
Z^i_7 & Z^i_8 & Z^i_9 \\
\hline
\end{array}
$$
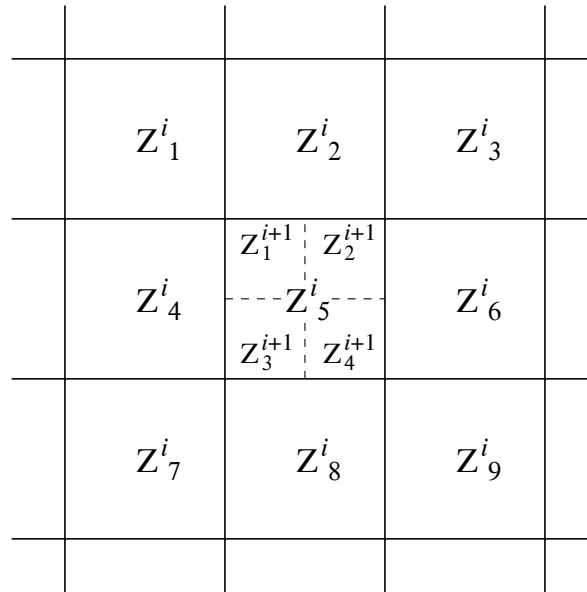
Figure 1.9 Two-dimensional LAS

Fenton(1994) compared LAS to other random field generating methods, such as FFT (Fast Fourier Transform) and TBM (Turning Bands Method), with respect to efficiency and accuracy, and the results are summerized in Tables 1.1 and 1.2, respectively. In Table 1.1, the times have been normalized with respect to the FFT, so a value of 0.5 means that the method took half as long as did the FFT. It is evident that LAS outperforms other methods in terms of efficiency. In terms of accuracy, the results outlined in Table 1.2 (upper and lower 90% percentiles) indicate that all three methods lead to good results with respect to the mean and variance of quantiles. The TBM perhaps is the most accurate on the basis of accuracy in the mean and covariance structures, however, it is not a stand alone random field generator as it depends on an accurate 1-D generator, such as LAS or FFT. The FFT method suffers from symmetry in the covariance structure of the realizations, which can be overcome by generating fields twice as large as required in each coordinate direction, and that in turn lowers the efficiency of this method. The LAS method has a slight grid-like pattern in the variance field, but it is easiest to use since it requires no decisions regarding its parameters, and is the most efficient.

Table 1.1 Comparison of Run Times of FFT, TBM, and LAS algorithms in One and Two Dimensions (Fenton and Griffiths, 2008)

			TBM	
Dimension	**FFT**	**LAS**	**16 Lines**	**64 Lines**
One	1.0	0.70	-	-
Two	1.0	0.55	0.64	2.6

Table 1.2 Upper and Lower 90 Percentiles of Estimated Mean and Variance Fields for FFT, TBM, and LAS Methods (200 realizations) (Fenton and Griffiths, 2008)

Algorithm	**Mean**	**Variance**
FFT	$(-0.06, 0.12)$	$(0.87, 1.19)$
TBM	$(-0.11, 0.06)$	$(0.83, 1.14)$
LAS	$(-0.12, 0.09)$	$(0.82, 1.13)$
Theory	$(-0.12, 0.12)$	$(0.84, 1.17)$

1.8 THE RANDOM LOAD MODEL

In this research only live and dead loads are considered, which is a typical assumption in code development. The load employed in reliability-based design of a pile has two important values.

One is the `true', and random, total load applied to the pile, F_T. The total load is equal to the sum of the maximum lifetime live load, F_L, and the relatively static dead load, F_D, i.e,

$$F_T = F_L + F_D \tag{1.53}$$

Both F_L and F_D are assumed here to be lognormally distributed. The mean and variance of the total load, F_T, assuming live and dead loads are independent, are given by,

$$\mu_T = \mu_L + \mu_D \tag{1.54a}$$

$$\sigma_T^2 = \sigma_L^2 + \sigma_D^2 \tag{1.54b}$$

Although the sum of two lognormally distributed random variables is not lognormally distributed, Fenton et al. (2008) found that F is nevertheless approximately lognormally distributed. Assuming this to be true, the distribution parameters of the total load, F_T, are

$$\sigma^2_{\ln F_T} = \ln\left(1 + v_T^2\right) \tag{1.55a}$$

$$\mu_{\ln F_T} = \ln(\mu_T) - \tfrac{1}{2}\sigma^2_{\ln F_T} \tag{1.55b}$$

where $v_T = \sigma_T/\mu_T$ is the coefficient of variation of the total load.

The other important value is the characteristic total load used in the pile design, which comes from current code provisions and is assumed to be deterministic,

$$\hat{F}_T = \alpha_L \hat{F}_L + \alpha_D \hat{F}_D \tag{1.56}$$

where $\hat{F}_L$ is the characteristic live load, $\hat{F}_D$ is the characteristic dead load, and α_L and α_D are the live and dead load factors, respectively. The load factors used here are as given by the National Building Code of Canada: at ULS, these are $\alpha_L = 1.5$ and $\alpha_D = 1.25$ (NRC, 2005). At SLS, the load factors are $\alpha_L = \alpha_D = 1.0$.

Characteristic load values can be defined as

$$\hat{F}_L = \frac{\mu_L}{k_L} \tag{1.57a}$$

$$\hat{F}_D = \frac{\mu_D}{k_D} \tag{1.57b}$$

where μ_L and μ_D are the means of the live and dead loads, and k_L and k_D are live and dead load bias factors, respectively (Fenton et al., 2012). In general, the bias factors capture the difference between the characteristic design values and their means, and are usually defined as the ratio of the mean to characteristic value. The values of k_L and k_D are suggested by Bartlett et al. (2003) and Ellingwood et al. (1980) to be $k_L = 0.9$ and $k_D = 1.05$, respectively. Assuming these to be correct, the characteristic loads are thus calculated to be $\hat{F}_L = \mu_L/0.9$ and $\hat{F}_D = \mu_D/1.05$.

Using these results, and assuming that the ratio of mean dead to mean live load is $R_{D/L} = \mu_D/\mu_L = 3.0$, for example at SLS where $\alpha_L = \alpha_D = 1.0$, the characteristic total design load, $\hat{F}$, is approximately equal to the mean total load, μ_T,

$$\hat{F}_T = \hat{F}_L + \hat{F}_D = \frac{\mu_L}{k_L} + \frac{\mu_D}{k_D} = \frac{\mu_T}{4k_L} + \frac{3\mu_T}{4k_D} = \frac{\mu_T}{4(0.9)} + \frac{3\mu_T}{4(1.05)} = 0.99\mu_T \simeq \mu_T \qquad (1.58)$$

The theoretical results given in Chapter 3 are valid for any $R_{D/L}$, although they are only confirmed by simulation for $R_{D/L} = 3.0$.

1.9   ORGANIZATION OF THESIS

This thesis concentrates on the determination of resistance and consequence factors required in the design of deep foundations against excessive settlement, obtained using reliability-based design methodology.

Chapter 2 presents a simple non-random regression to predict settlement of a single floating pile supported by a homogeneous elastic soil and subjected to a vertical load. The regression, which is calibrated by a finite element model, allows the direct computation of the pile geometry required for serviceability limit state design of deep foundations.

Chapter 3 studies the probabilistic behaviour of the settlement of a pile subjected to a random vertical load and supported by a spatially random soil. This understanding is used to determine the resistance factors required to achieve a target reliability index against excessive settlement. The regression model developed in Chapter 2 to predict pile settlement is utilized here.

Chapter 4 investigates how the consequence factor should be specified in order to adjust the reliability of a deep foundation to target values, which are dependant on the severity of failure consequences.

In Chapter 5, the effect of pile redundancy on reliability of pile systems is investigated, from which, the reliability index required for an individual pile to achieve a target system reliability is estimated.

In Chapter 6, a three-dimensional probabilistic model for differential settlement is presented and is validated via Monte Carlo simulation. The result are used to propose design provisions for piles to avoid excessive differential settlement.

Conclusions and suggested future work are presented in Chapter 7.

CHAPTER 2

PREDICTION OF PILE SETTLEMENT IN AN ELASTIC SOIL

2.1 GENERAL

The main objective of this chapter is to present a simple formula to predict the settlement of a single floating pile within an elastic soil. To accomplish this, a regression model is developed based on finite element results. One of the primary benefits of the model is that it is easily inverted to allow a direct computation of the pile length, H, required for the serviceability limit state design of floating piles.

In the next section, an analytical result is presented for the settlement of a pile under a given load, and a regression is developed and calibrated using a linear elastic finite element model, which can be used to easily compute pile length required for serviceability limit state design.

2.2 METHODOLOGY

Prediction of elastic pile settlement has been studied previously by various authors (Poulos and Davis 1980, Randolph and Wroth 1978, Das 2000, and Coduto 2001). The settlement prediction used in this research has the same form as suggested by Poulos (Poulos and Davis 1980) and Randolph (Randolph and Wroth 1978), for a single cylindrical pile embedded in a homogeneous elastic soil,

$$\delta = \frac{\hat{F}_T}{E_s d} I_p \qquad (2.1)$$

where δ is the settlement at the top of the pile, $\hat{F}_T$ is the applied load, E_s is the elastic modulus of the soil (assumed to be spatially constant), d is the diameter of the pile shaft, and I_p is a settlement influence factor which depends on a number of parameters such as Poisson's ratio of the soil, ν, the pile slenderness ratio, H/d, where H is the pile length, and the pile to soil stiffness ratio, $k = E_p/E_s$, E_p being the pile elastic modulus.

The following expression derived from closed-form solutions obtained by Randolph (Randolph and Wroth 1978), can be used to calculate I_p for a constant diameter cylindrical floating pile:

$$I_p = 4(1 + \nu) \left[1 + \frac{1}{\pi \lambda} \frac{8}{(1 - \nu)} \frac{\tanh(\mu H)}{\mu H} \frac{H}{d} \right] \bigg/ \left[\frac{4}{(1 - \nu)} + \frac{4\pi}{\zeta} \frac{\tanh(\mu H)}{\mu H} \frac{H}{d} \right] \qquad (2.2)$$

with

$$\zeta = \ln \left[5(1 - \nu)H/d \right]$$

$$\mu H = 2H/d\sqrt{2/\zeta\lambda}$$

$$\lambda = 2(1 + \nu)E_p/E_s$$

For piles shorter than $0.25d\sqrt{2(1 + \nu)E_p/E_s}$, Fleming et al. (2009) suggest that the settlement coefficient, I_p, should become

$$I_p = \frac{(1 + \nu)}{\frac{1}{(1-\nu)} + \frac{\pi}{\zeta}\frac{H}{d}} \qquad (2.3)$$

Alternatively, for piles longer than $1.5d\sqrt{2(1 + \nu)E_p/E_s}$, Fleming et al. (2009) suggest that the value of $\tanh(\mu H)$ approaches unity and hence eq. (2.2) reduces to

$$I_p = \frac{2(1 + \nu)\sqrt{2\zeta/\lambda}}{\pi} \qquad (2.4)$$

Furthermore, Fleming et al. (2009) state that, for long piles, the pile response should become independent of pile length, since very little load reaches the base of the pile, which is reasonable. However, both eq's. (2.2) and (2.4) show a slow increase in settlement

with pile length when the pile length exceeds $1.5d\sqrt{2(1+\nu)E_p/E_s}$, which is unexpected. It is believed that this slow increase is merely an artifact of approximations made in the settlement predictions and should be ignored.

Eq. (2.2) is not easily inverted to solve for the pile length, H. In this work a simpler power function of the form

$$I_p = a_0 + \frac{1}{(H/d + a_1)^{a_2}} \tag{2.5}$$

has been found to fit the I_p values estimated using 3-D finite element analysis for various values of k and H/d. The determination of the unknown coefficients, a_0, a_1, and a_2 will be discused shortly.

Substituting eq. (2.5) into eq. (2.1) results in the following settlement prediction

$$\delta = \frac{\hat{F}_T}{E_s d} \left(a_0 + \frac{1}{(H/d + a_1)^{a_2}} \right) \tag{2.6}$$

The primary motivation of the functional form assumed in eq. (2.5) is that it is easily inverted and solved for H. For a given I_p value, inverting eq. (2.5) and solving for H gives,

$$H = d \left[\left(\frac{1}{I_p - a_0} \right)^{1/a_2} - a_1 \right] = d \left[\left(\frac{1}{(\delta E_s d/\hat{F}_T) - a_0} \right)^{1/a_2} - a_1 \right] \tag{2.7}$$

where eq. (2.1) was used to substitute for I_p in the last step.

The calibration of the settlement influence factor, I_p, given by eq. (2.5) can be achieved either by fitting eq. (2.5) to eq. (2.2), or by fitting eq. (2.5) to elastic FE results. The latter was selected in this study because eq. (2.2) is not asymptotic to a minimum value and begins to erroneously increase for piles longer than $1.5d\sqrt{2(1+\nu)E_p/E_s}$. The FE results, on the other hand, do tend to a minimum value as the pile length increases.

This work looks specifically at the cases where the pile to soil stiffness ratio $k = E_p/E_s$ ranges between 200 and 1000. The calibration of I_p is done here by calculating the settlement of a pile of length H surrounded by a soil with uniform elastic modulus $E_s = 30$

MPa, Poisson's ratio $\nu = 0.3$, and supporting vertical load $\hat{F}_T = 1.6$ MN using the finite element method (Smith and Griffiths, 2004, Fenton and Griffiths, 2005 and 2007) with mesh size 50 elements by 30 elements in plan by 30 elements in depth, as shown in Figure 2.1. The pile settlement is obtained from a single finite element analysis of the problem. Note that the settlement coefficient, I_p, depends on $k = E_p/E_s$ and not on E_s directly nor does it depend on $\hat{F}_T$. The dependence on ν is only slight, showing changes of no more than about 5% for ν ranging from 0.1 to 0.4, with higher values showing slightly less settlement. The pile considered has elastic modulus ranging from 6 GPa to 30 GPa (which are several orders of magnitude higher than that of the surrounding soil) and pile depth ranging from 1 to 10 m (a maximum pile length of 10 m was selected to avoid boundary effects with the base). The pile is placed in the middle of the mesh where the pile settlement is computed more accurately due to the minimized influence of boundary conditions on pile settlement (to be discussed later in this chapter).
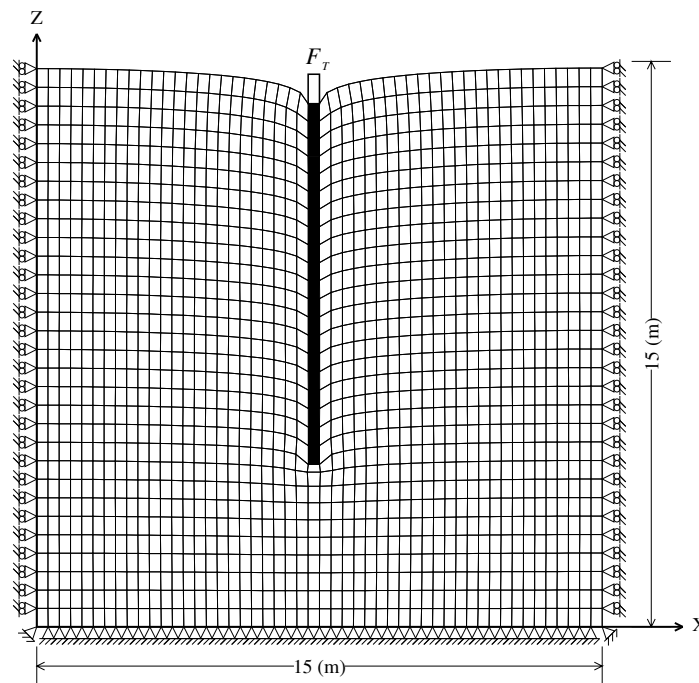
Figure 2.1   Typical FE mesh of 8-node square element (50 by 30 by 30 elements)

The proposed methodology to calibrate eq. (2.5) and thus predict elastic pile settlement proceeds as follows:

1) A finite element prediction of pile settlement is performed for each of a range of pile lengths $H = 1, ..., 10$ m, for given $\hat{F}_T = 1.6$ MN, $k = E_p/E_s$, $d = 0.3$, and $\nu = 0.3$, resulting in a set of settlement values, δ. Figure 2.1 illustrates one such analysis, which is basically identical to Figure 1.1, except with uniform soil elastic modulus.

2) I_p is computed for each H/d value by inverting eq. (2.1). A function of the form given by eq. (2.5) is then fit by regression to the finite element results, leading to a set of a_i values, $i = 0, 1, 2$.

3) Steps 1 through 2 are repeated for various values of $k = 200, ..., 1000$, producing a set of a_i values for each k.

4) Once the a_i values are obtained for each k, the following power functions are fit by a subsequent regression to predit a_i as a function of k,

$$a_0 = 2069.4633 \, (k + 350)^{-1.6054}$$

$$a_1 = 0.07 + (0.2934 \, k^{0.3108})$$

$$a_2 = 0.6903 + (8.2464 \, k^{-0.5268}) \tag{2.8}$$

5) Substituting eq's. (2.8) into eq. (2.6) results in a determ inistic elastic prediction of pile settlement as a function of the pile slenderness ratio, H/d, and the pile stiffness ratio, $k = E_p/E_s$.

Figure 2.2 shows the plot of I_p for $k = 200$, and 1000 obtained from finite element analysis along with their corresponding regressions. The agreement deemed to be is excellent. Figure 2.3 demonstrates the plot of pile settlements, δ, for $k = 200, 300, 500$, and 1000, along with their excellent matches produced by substituting eq's. (2.8) into eq. (2.6).
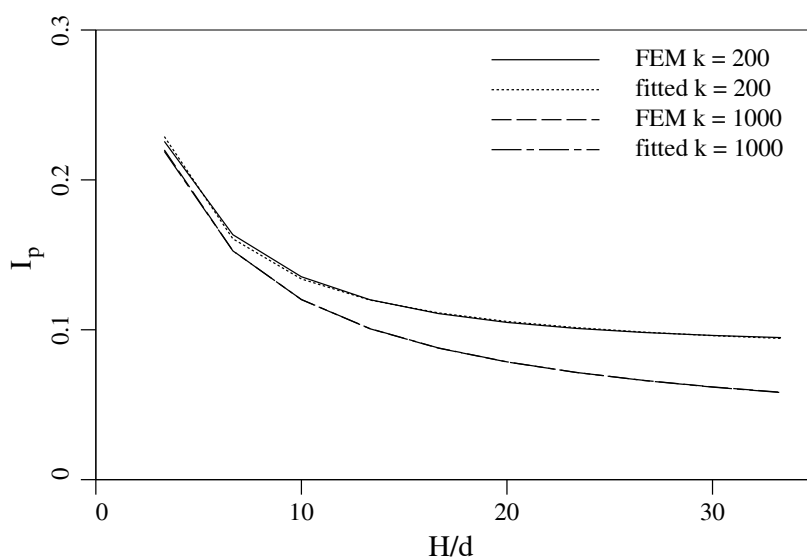
Figure 2.2   Calibration of I_p using FE model for $k = 200$, and 1000
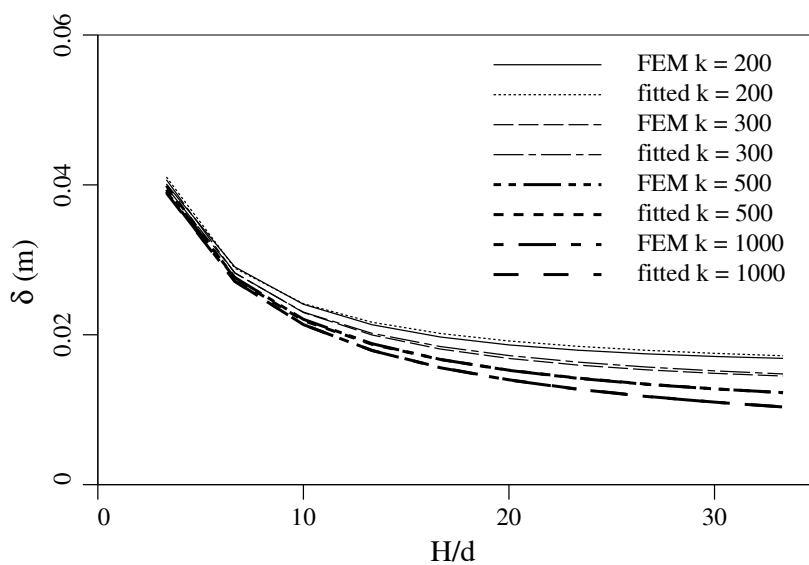
Figure 2.3   Calibration of δ using FE model for $k = 200, 300, 500,$ and $1000,$
produced by substituting eq's. (2.8) into eq. (2.6)

In order to make a direct comparison between the FE model and Randolph's analytical solution (Randolph and Wroth 1978), eq. (2.2) is substituted into eq. (2.1), which is then used to estimate elastic pile settlement. As mentioned earlier, Randolph's solution is developed for cylindrical piles, but it can be extended to non-cylindrical piles (e.g. square or H piles) by choosing a reasonable value of d (Randolph and Wroth, 1978). The pile considered in the FE model is of square cross-section with dimension 0.3 m, thus $d = 0.3(4/\pi)$ is used (adjusted by the ratio of square to circle perimeters) in eq's. (2.1) and (2.2) resulting in δ values illustrated in Figure 2.4, which compares Randolph's prediction to FE results. As shown in Figure 2.4, the agreement between the two methods is considered good for $H/d > 10$, however, an error of up to about 10% is evident for $H/d < 10$. This level of accuracy is considered reasonable since Randolph's solution shows errors of $20 - 30\%$ compared to numerical analysis for H/d values of about 2 (Randolph 1994b).
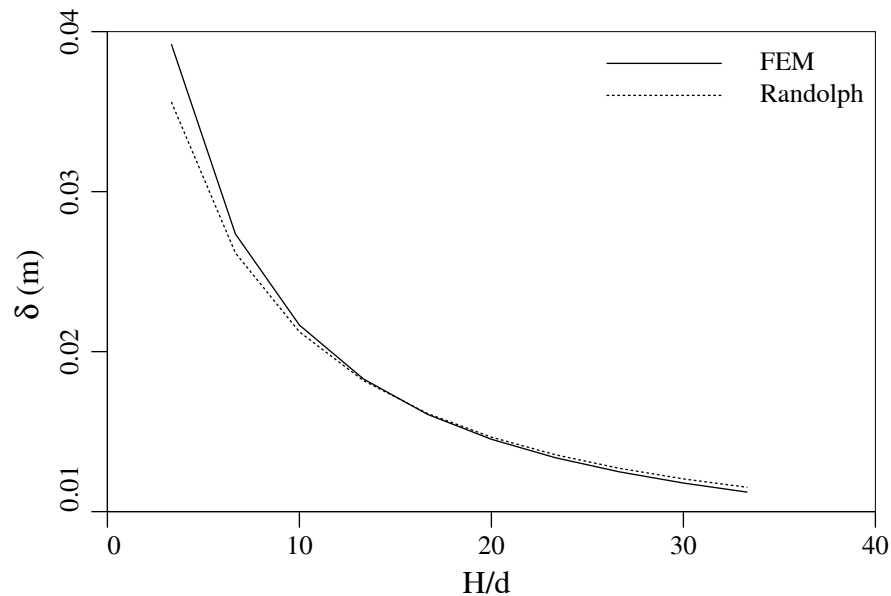
Figure 2.4 Comparison of pile settlement, δ, obtained by FE model and Randolph's analytical solution (Randolph and Wroth 1978) for $k = 700$

A study was performed to assess the influence of side distance on pile settlement. Figure 2.5 gives a plot of pile settlement versus l_x where l_x is pile location measured from the left edge of the soil mass ($l_x = 0$) in units of number of elements. The results indicate a steep reduction in settlement in the range $1 < l_x < 10$ elements (corresponding to relative error > 10%) and reasonably constant settlement values for $11 < l_x < 25$ (corresponding to relative error < 10%), where $l_x = 25$ denotes the center along the x-direction . For this study, thus, the pile is fixed at the center of the mesh to minimize the edge effects on pile settlement.
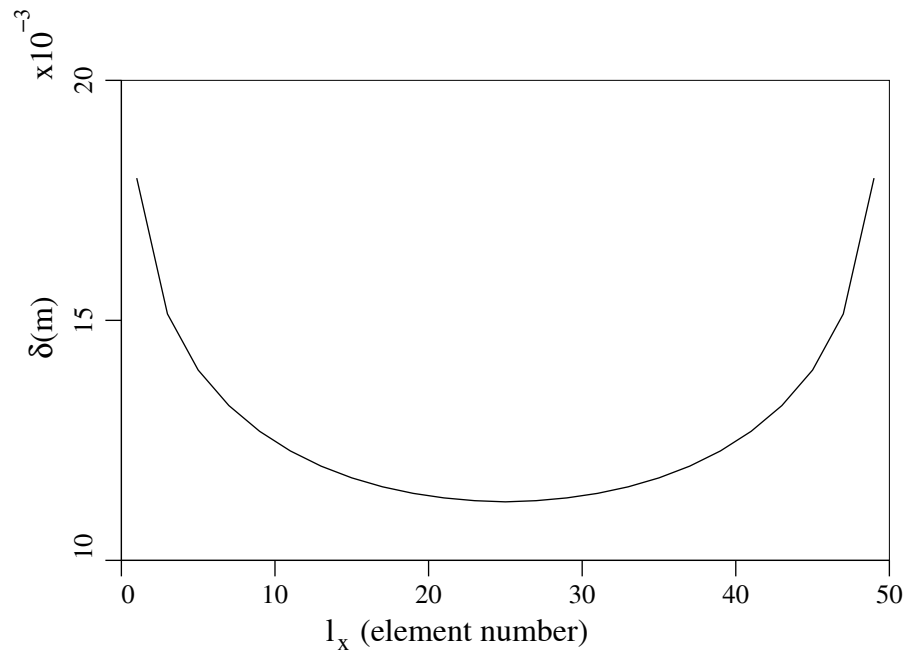
Figure 2.5 Influence of side distance on pile settlement, using FE model for $k = 700$

CHAPTER 3

RESISTANCE FACTOR CALIBRATION FOR DEEP FOUNDATIONS

3.1   GENERAL

To design a pile against exceeding the serviceability limit state, i.e., against entering a state where the pile's actual settlement exceeds a maximum tolerable settlement, a settlement prediction model is required. If the model is good, then it will provide a good estimate of the mean pile settlement and the actual in-situ pile settlement will be due to natural `residual' soil variability around the predicted mean. The settlement prediction model is used to determine the pile design such that the predicted mean settlement is some fixed fraction (specified by the load and resistance factors) of the maximum tolerable settlement. If the settlement prediction model is poor, then it also contributes to the variability in the prediction of the actual settlement. This source of variability will be referred to herein collectively as the "degree of site and prediction model understanding", which includes a) the degree of understanding of the ground properties and geotechnical properties throughout the site, and b) the accuracy and degree of confidence about the numerical performance prediction model used to estimate the serviceability geotechnical resistances.

It is assumed in this research that a sufficiently accurate settlement prediction model is used for the pile design, so that model error itself is due only to errors in the soil parameters used in the model, i.e. to the degree of site understanding. This is probably a reasonable assumption, since if the (possibly non-linear) properties of the soil through which the pile passes, along with the nature of the interface between the pile and the soil, are all

46

well known, then models exist which can provide very good estimates of the mean pile settlement.

This research is not attempting to provide an improved settlement prediction model. In fact a decision about the degree of site and prediction model understanding used in the pile design process is left to the designer. This chapter concentrates on the residual settlement variability (around the mean) after the design has been performed. It is assumed that this variability arises from the spatial variability of the soil itself, along with uncertainty in the soil property estimates used in the prediction model.

The main goal of this chapter is to investigate the probabilistic behaviour of the settlement of a pile subjected to a random vertical load and supported by a spatially random soil and use this understanding to allow the determination of the resistance factors required in the design process. It is assumed here that the term "resistance" refers to the force which must be applied to the pile in order to displace it into the soil by the maximum tolerable settlement for serviceability. This is the maximum resistance that the pile can provide at the serviceability limit state. The load and resistance factor design (LRFD) approach is then applied for the serviceability limit state (SLS) by specifying that the factored pile resistance be at least equal to the factored applied loads or actions. As discussed above, the settlement prediction model itself only changes the pile design, not its probability of failure, thus any reasonable settlement prediction model can be employed so long as it gives reasonable response results in the vicinity of the mean settlement point and reflects uncertainties in its input parameters in a reasonable fashion (e.g., if the soil parameters are incorrectly estimated to be less stiff than they actually are, a longer pile than necessary will be designed). The choice in the mean settlement prediction model, so long as it gives an accurate estimate of the mean settlement given perfect information about a particular site, will have no affect on the required resistance factors. Since the stress-strain curves typical of pile settlement are usually relatively smoothly varying, a linearization in the vicinity of

the mean will be employed in this chapter. That is, the soil will be assumed to be linearly elastic around the mean settlement point, and a linear elastic model will also be used as the settlement prediction model.

A reliability-based design approach, specifically the Load and Resistance Factor Design (LRFD), is implemented within the Random Finite Element Method (RFEM) to perform this investigation, as described in Chapter 1.

At the Serviceability Limit State (SLS), the LRFD design requirement is

$$\varphi_{gs}\hat{R}_s \geq \hat{F}_L + \hat{F}_D \tag{3.1}$$

where $\hat{F}_L$ is the characteristic live load, $\hat{F}_D$ is the characteristic dead load.

In order to determine the resistance factor required in eq. (3.1) to achieve a target reliability, the target reliability must be established. The Eurocode design basis, BS EN1990:2002 (British Standards Institute, 2002), suggests a one-year target reliability index of 2.9 for SLS which corresponds to an annual failure probability 2×10^{-3}. Phoon et al. (1995) suggests an annual target reliability index of 2.6 with corresponding failure probability 5×10^{-3} for foundations at SLS, while Zhang and Xu (2005) recommend a reliability index of 2.46 with annual failure probability 7×10^{-3}.

It probably makes more sense to consider lifetime failure probabilities, rather than annual, since the design lifetime is, or at least should be, targeted for all aspects of optimization of the overall system (e.g., to consider the time value of periodic maintenance required by the design over the design lifetime, incorporating climate change effects into load and resistance models, including the effect of degradation of resistance with time, and so on). The difference between annual and lifetime target failure probabilities can be quite substantial. For example, if it is assumed that annual extremes in loads and resistances from year to year are independent, then an annual target reliability index of 2.9 ($p_{max} \simeq 2 \times 10^{-3}$) corresponds

to a 50-year lifetime target reliability index of 1.35 ($p_{max} \simeq 10^{-1}$). The exact relationship between annual and lifetime failure probabilities, under the assumption of independence between annual load and resistance extremes, is given by $p_{max} = 1 - (1 - p_{ann})^n$, where p_{ann} is the annual target maximum acceptable failure probability and n is the design lifetime in years.

The actual target lifetime failure probability will likely be somewhere between the value of p_{max} suggested above and the target annual failure probability because annual extremes in load and resistances are not likely to be truly independent. In addition, if a lifetime maximum failure probability is targeted, then the load and resistance distributions must also be targeted for that lifetime (and the same statement must be made about annual maximum failure probability).

The basic question is what lifetime failure probability is society willing to accept? Is society willing to accept that more than 1 in 10 ($p_{max} = 10^{-1}$) piles will experience excessive settlement over the design life of a geotechnical system on average? Probably not, given the huge expense of repairing a foundation. Alternatively, is society willing to spend the money required so that less than 1 in 10,000 ($p_{max} = 10^{-4}$) piles will experience excessive settlement? Probably not, especially considering the fact that piles are usually redundant systems. Excessive settlement of one pile is often mitigated by adjacent piles.

Thus, typical maximum lifetime failure probability of excessive settlement of a single pile lying somewhere between 10^{-1} and 10^{-4} is deemed to be reasonable and this range has been considered in this research. The resistance factors required to achieve these target probabilities will be recommended in Section 3.4.

To estimate the probability of excessive pile settlement, a linear elastic model is employed, as discussed in Chapter 1, which assumes that the soil surrounding the pile is perfectly bonded to the pile shaft through friction and/or adhesion. Any displacement of the pile is

thus associated with an equivalent displacement of the adjacent soil. This displacement is assumed to be resisted by a force which is proportional to the soil's (residual around the mean) elastic modulus and the magnitude of the displacement. As stated by Vesic (1977), the fraction of pile settlement due to deformation of the soil is a constant (dependent on Poisson's ratio and pile geometry) times F_T/E_{eff}, where F_T is the applied load and E_{eff} is the effective soil elastic modulus. The effective soil elastic modulus, E_{eff}, is defined here as the uniform (spatially constant) value of the elastic modulus which would produce a settlement identical to the actual pile settlement in a spatially variable soil (Fenton and Griffiths, 2007).

The pile is assumed to be rigid and placed in a three-dimensional spatially random soil (see Figure 1.1). A random load is applied vertically to the pile and the settlement of the pile is calculated using a linear elastic finite element model (Smith and Griffiths, 2004, and Fenton and Griffiths, 2005). The pile length, H, is determined as follows; i) the random soil is sampled (see Figure 3.1) at some location over a depth D (for example, as would occur if a CPT sounding was taken) to obtain a series of observations of the soil's residual elastic modulus (in the vicinity of the mean soil strain), ii) the characteristic elastic modulus used in design, $\hat{E}$, is determined from the soil sample, and iii) the required pile length H is obtained via the LRFD requirement of eq. (3.1). The details are discussed in the following sections. Once the pile length has been determined, the `failure' probability that the pile settlement exceeds the maximum tolerable settlement can be determined from the theory developed in this chapter (as validated by simulation). Plots of failure probability can then be developed as a function of the statistics of the soil's residual random elastic modulus field (mean, variance, and correlation length) and the resistance factor used in the design process. These plots can then be used to select the required resistance factor for given p_{max}.

$F_T(kN)$

ground level

H

soil sample

D

pile

r
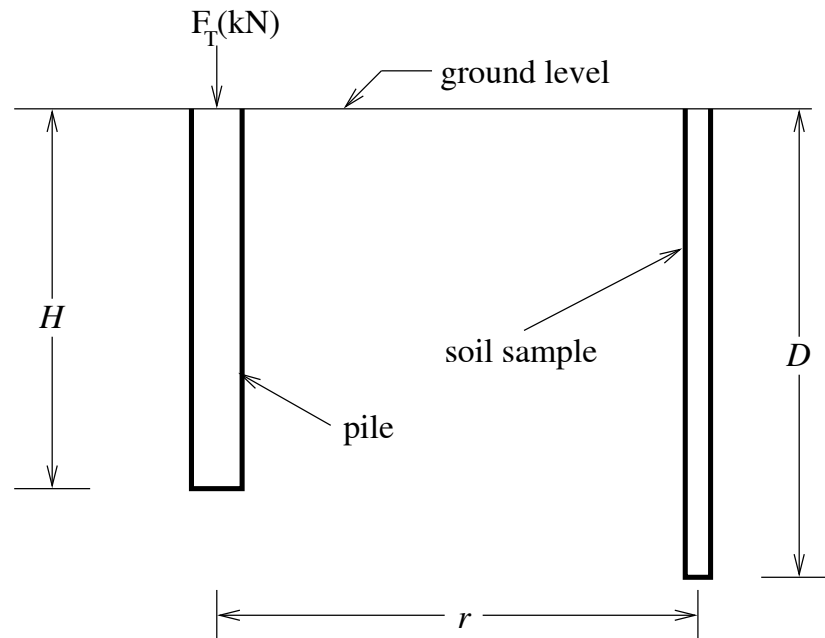
Figure 3.1   Relative location of pile and soil samples

In the following section, a theoretical approach to estimating the probability of excessive pile settlement is developed, which is then validated by simulation in Section 3.3. In Section 3.4, the resistance factors required to achieve a target reliability index against excessive settlement of deep foundations are recommended.

3.2   PROBABILITY OF EXCESSIVE PILE SETTLEMENT

In this section, a reliability-based design methodology is presented to determine the required pile length and a subsequent theory proposed to estimate the excessive settlement failure probability of an individual pile placed in a spatially varying soil. The theory is validated by simulation in the following section. If a mean settlement model is used which differs from the elastic model used here, as discussed in earlier in this chapter, then only the design changes. As long as the `residual' random behaviour of the in-situ pile remains

approximately linearly elastic around the mean, then the results of this section will also apply to other prediction models.

To assess the probabilistic behaviour of pile settlement, the first task is to determine the nature of the settlement distribution. To accomplish this, a series of simulations, each with 2000 realizations, were performed using RFEM to estimate the pile settlement distribution. Figure 3.2 shows one of the best (a) and one of the worst (b) fits of the lognormal distribution to the pile settlement histogram, having chi-square goodness-of-fit p-values of 0.2371 and 0.0037, respectively. The null hypothesis for this goodness-of-fit test is that the settlement displacement follows a lognormal distribution. Figure 3.2(b) rejects the null hypothesis for any significance level exceeding 0.37%. The visual inspection of the plots, however, suggests that the lognormal distribution is a reasonable distribution type for pile settlement even in case(b), as suggested also by Fenton and Griffiths (2007).
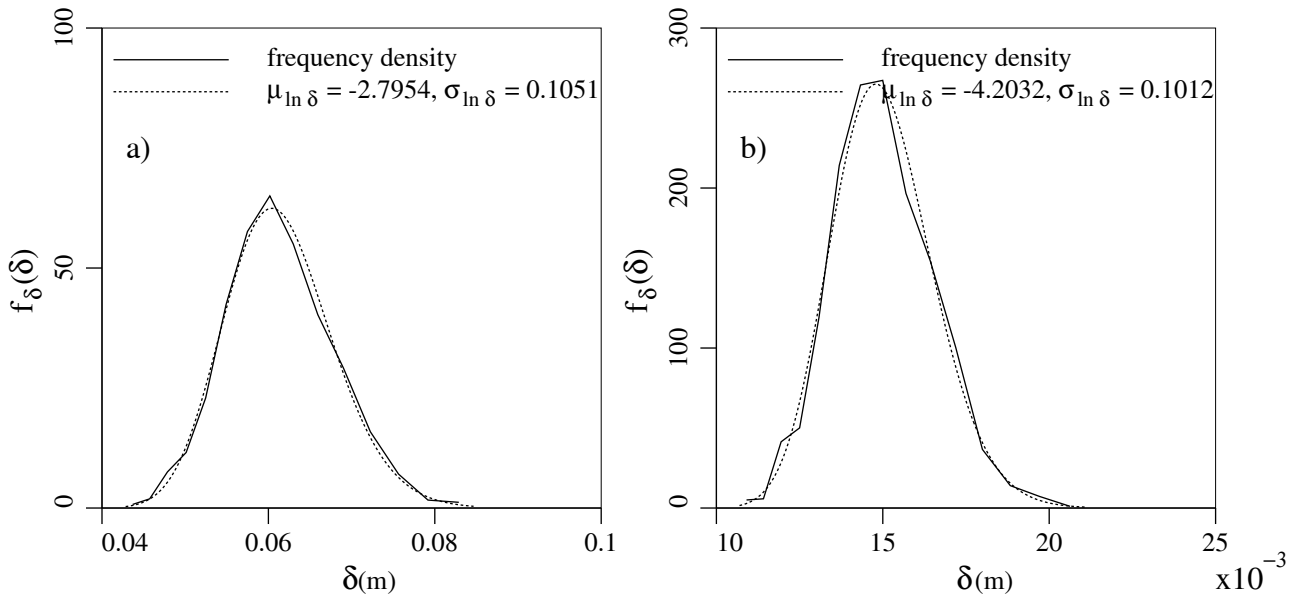
Figure 3.2 Estimated and fitted lognormal distributions of settlement for a) $H = 1$ m, and $d = 0.3$ m (p-value=0.2371) and b) $H = 14$ m, and $d = 0.3$ m (p-value = 0.0037)

The reliability-based design goal is to determine the required pile length, H, and diameter, d, such that the probability, p_f, of exceeding a specified maximum tolerable settlement,

δ_{max}, is acceptably small, i.e. to find H and d such that

$$P\left[\delta > \delta_{max}\right] = p_f \leq p_{max} \tag{3.2}$$

in which δ is the actual (random) pile settlement, p_f is the probability of design failure, and p_{max} is the maximum acceptable probability of design failure. It is assumed here that the pile type, and thus its cross-section, has already been decided on, so that its length is the only design parameter of concern. Design failure is assumed to occur if the actual pile settlement, δ, exceeds the maximum tolerable settlement, δ_{max}.

Various methods are available to calculate the mean settlement of a pile, as discussed above; the basis of design used in this research has the same form as suggested by Poulos (Poulos and Davis 1980) and Randolph (Randolph and Wroth 1978),

$$\hat{\delta} = \frac{\hat{F}_T}{\hat{E}d}I_p \tag{3.3}$$

where $\hat{\delta}$ is the predicted pile settlement, $\hat{F}_T$ is the characteristic load (see eq. 1.58), d is the pile width, $\hat{E}$ is the estimated characteristic soil elastic modulus, and I_p is a settlement influence factor which depends on a number of parameters such as Poisson's ratio, ratio of pile length, H, to pile width, d, and the pile to soil stiffness ratio, $k = E_p/\hat{E}$, E_p being the pile elastic modulus. A function of form

$$I_p = a_0 + \frac{1}{(H/d + a_1)^{a_2}} \tag{3.4}$$

has been found here which well fits the I_p values obtained using 3-D finite element analysis. The calibration of I_p was discussed in detail in Chapter 2.

As discussed earlier in this chapter, the simple elastic prediction of $\hat{\delta}$ can be replaced by a more sophisticated non-linear prediction.

The predicted settlement, $\hat{\delta}$, given by eq. (3.3) can be used to calculate the characteristic serviceability geotechnical resistance, $\hat{R}_s$, introduced in eq. (3.1). Replacing the predicted

settlement, $\hat{\delta}$, with the maximum tolerable settlement, δ_{max}, and solving for corresponding

value of $\hat{F}_T$ gives the characteristic serviceability geotechnical resistance, $\hat{R}_s$, as

$$\hat{R}_s = \frac{\delta_{max}\hat{E}d}{I_p} \tag{3.5}$$

If $\hat{E}$ is an estimate of the mean effective elastic modulus, then $\hat{R}_s$ is an estimate of the mean

geotechnical resistance corresponding to δ_{max}. Note that if an alternative settlement pre-

diction model is used to determine $\hat{\delta}$, then eq. (3.3) can be used to solve for the `equivalent'

value of $\hat{E}$ to use in eq. (3.5).

Replacing $\hat{R}_s$ in the LRFD design requirement of eq. (3.2) leads to

$$\varphi_{gs}(\frac{\delta_{max}\hat{E}d}{I_p}) \geq \hat{F}_L + \hat{F}_D \tag{3.6}$$

The design pile length can now be determined by taking eq. (3.6) at the equality, replacing

I_p with eq. (3.4), and solving for H, given an initial estimate for d,

$$H = d\left[\left(\frac{1}{(\delta_{max}\varphi_{gs}\hat{E}d/\hat{F}_T) - a_0}\right)^{1/a_2} - a_1\right] \tag{3.7}$$

Note that eq. (3.7) could be solved for d (given H), or for H/d, using a root finding

algorithm, such as 1-pt iteration.

Turning attention now to the actual (random) pile settlement, δ, it is hypothesized that δ can

be determined using eq. (3.3) by replacing the characteristic load $\hat{F}_T$ with the true (random)

load F_T and the characteristic elastic modulus $\hat{E}$ with the actual (random) effective elastic

modulus E_{eff},

$$\delta = \frac{F_T}{E_{eff}d}I_p \tag{3.8}$$

As mentioned previously in Chapter 1, the effective elastic modulus, E_{eff}, as seen by

a pile is assumed to be a geometric average of the soil's elastic modulus over a volume

surrounding the pile, and is given by eq. (1.49).

The characteristic elastic modulus, $\hat{E}$, is estimated using observed values of the soil's elastic modulus obtained by sampling somewhere in the vicinity of the pile, which yields a sequence of m observed elastic modulus values, $E_1^o, E_2^o, ..., E_m^o$. If $\hat{E}$ is to be a good estimate of E_{eff}, then it should be similarly determined as a geometric average of the observed sample $E_1^o, E_2^o, ..., E_m^o$

$$\hat{E} = \left(\prod_{j=1}^{m} E_j^o \right)^{1/m} = \exp\left\{ \frac{1}{m} \sum_{j=1}^{m} \ln E_j^o \right\} \simeq \exp\left\{ \frac{1}{V_s} \int_{V_s} \ln E(\underset{\sim}{x})\, d\underset{\sim}{x} \right\} \tag{3.9}$$

The probability that the design fails (see eq. 3.2), i.e. that the actual pile settlement δ exceeds the design maximum tolerable settlement δ_{max}, can now be estimated. Using eq. (3.4) in eq. (3.8), and replacing H with eq. (3.7), the actual (random) pile settlement can be expressed as

$$\delta = \frac{\delta_{max} \varphi_{gs} \hat{E}}{E_{eff}} \left(\frac{F_T}{\hat{F}_T} \right) \tag{3.10}$$

which means that the design requirement of eq. (3.2) now becomes to find φ_{gs} such that

$$P\left[\delta > \delta_{max} \right] = P\left[\frac{\varphi_{gs} \hat{E}}{E_{eff}} \left(\frac{F_T}{\hat{F}_T} \right) > 1 \right] = P\left[F_T \left(\frac{\hat{E}}{E_{eff}} \right) > \frac{\hat{F}_T}{\varphi_{gs}} \right] \leq p_{max} \tag{3.11}$$

If the soil's elastic modulus, E, is lognormally distributed, as assumed, then both $\hat{E}$ and E_{eff} will also be lognormally distributed since geometric averages preserve the lognormal distribution. In addition, if F_T is at least approximately lognormally distributed, as assumed here (Fenton et al., 2008), the quantity W,

$$W = F_T \frac{\hat{E}}{E_{eff}} \tag{3.12}$$

which combines all of the random quantities in eq. (3.11), will be (at least approximately) lognormally distributed and its parameters can be determined by considering the individual distributions of F_T, $\hat{E}$, and E_{eff} as follows. Since W is assumed lognormally distributed, then

$$\ln W = \ln F_T + \ln \hat{E} - \ln E_{eff} \tag{3.13}$$

is normally distributed and p_f can be found from

$$
\begin{aligned}
p_f &= \mathrm{P}\left[W > \hat{F}_T/\varphi_{gs}\right] = \mathrm{P}\left[\ln W > \ln\left(\hat{F}_T/\varphi_{gs}\right)\right] \\
&= 1 - \Phi\left(\frac{\ln\left(\hat{F}_T/\varphi_{gs}\right) - \mu_{\ln W}}{\sigma_{\ln W}}\right) \\
&= 1 - \Phi\left(\beta\right)
\end{aligned}
\tag{3.14}
$$

where Φ is the standard normal cumulative distribution function, and the argument to Φ, β, is the desired reliability index so that $p_f = p_{max}$. The required resistance factor can then be determined from eq. (3.14) as

$$
\varphi_{gs} = \frac{\hat{F}_T}{\exp\left(\mu_{\ln W} + \beta\sigma_{\ln W}\right)}
\tag{3.15}
$$

The mean and variance of $\ln W$ are

$$
\mu_{\ln W} = \mu_{\ln F} + \mu_{\ln \hat{E}} - \mu_{\ln E_{eff}}
\tag{3.16}
$$

$$
\sigma_{\ln W}^2 = \sigma_{\ln F}^2 + \sigma_{\ln \hat{E}}^2 + \sigma_{\ln E_{eff}}^2 - 2\mathrm{Cov}\left[\ln \hat{E}, \ln E_{eff}\right]
\tag{3.17}
$$

assuming that the total load and soil elastic modulus are independent and where $\mathrm{Cov}\left[X, Y\right]$ denotes the covariance between random variables X and Y. As discussed previously in Chapter 1, the total load, F_T, is equal to the sum of the live load, F_L, and the dead load, F_D, i.e. $F_T = F_L + F_D$, so that the mean and variance of $\ln F_T$ can be estimated using eq.'s (1.53), (1.54), and (1.55).

With reference to eq. (3.9), the mean and variance of $\ln \hat{E}$ are

$$
\mu_{\ln \hat{E}} = \mathrm{E}\left[\ln \hat{E}\right] = \mathrm{E}\left[\frac{1}{m}\sum_{j=1}^{m}\ln E_j{}^o\right] = \frac{1}{m}\sum_{j=1}^{m}\mu_{\ln E} = \mu_{\ln E}
\tag{3.18}
$$

where $\mathrm{E}\left[.\right]$ is the expectation operator, and

$$
\sigma_{\ln \hat{E}}^2 = \mathrm{E}\left[(\ln \hat{E} - \mu_{\ln \hat{E}})^2\right]
$$

$$= \mathrm{E}\left[\left(\left(\frac{1}{m}\sum_{j=1}^{m}\ln E_j^o\right) - \mu_{\ln \hat{E}}\right)^2\right]$$

$$= \mathrm{E}\left[\left(\frac{1}{m}\sum_{j=1}^{m}\left(\ln E_j^o - \mu_{\ln E}\right)\right)^2\right]$$

$$= \mathrm{E}\left[\frac{1}{m^2}\sum_{i=1}^{m}\sum_{j=1}^{m}(\ln E_i^o - \mu_{\ln E})(\ln E_j^o - \mu_{\ln E})\right]$$

$$= \frac{1}{m^2}\sum_{i=1}^{m}\sum_{j=1}^{m}\mathrm{E}\left[(\ln E_i^o - \mu_{\ln E})(\ln E_j^o - \mu_{\ln E})\right]$$

$$= \frac{1}{m^2}\sum_{i=1}^{m}\sum_{j=1}^{m}\mathrm{Cov}\left[\ln E_i^o, \ln E_j^o\right]$$

$$\simeq \frac{\sigma_{\ln E}^2}{m^2}\sum_{i=1}^{m}\sum_{j=1}^{m}\rho(\underset{\sim}{x}_i^o - \underset{\sim}{x}_j^o) \tag{3.19}$$

in which $\underset{\sim}{x}_i^o$ is the spatial location of the center of the ith soil sample, for $i = 1, ..., m$, and ρ is the correlation function defined by eq. (1.35). An approximation in the variance occurs due to the fact that correlation coefficients between the local averages associated with observations are approximated by correlation coefficients between the local average centers. Assuming that $\ln \hat{E}$ represents a local average of $\ln E$ over the sample domain of volume $V_s = B_s \times B_s \times D$, as also suggested by eq. (3.9), then $\sigma_{\ln E}^2$ may be better estimated as

$$\sigma_{\ln \hat{E}}^2 \simeq \sigma_{\ln E}^2 \gamma(V_s) \tag{3.20}$$

where $\gamma(V_s)$ is the variance reduction function that measures the reduction in variance due to local averaging over the sample domain V_s (see eq. 1.40 using V_s rather then V_p).

Similarly, and with reference to eq. (1.49), the mean and variance of $\ln E_{eff}$ are

$$\mu_{\ln E_{eff}} = \mathrm{E}\left[\ln E_{eff}\right] = \mathrm{E}\left[\frac{1}{V_p}\int_0^{V_p}\ln E(\underset{\sim}{x})\,d\underset{\sim}{x}\right] = \frac{1}{V_p}\int_0^{V_p}\mathrm{E}\left[\ln E(\underset{\sim}{x})\right]\,d\underset{\sim}{x} = \frac{1}{V_p}\int_0^{V_p}\mu_{\ln E}\,d\underset{\sim}{x} = \mu_{\ln E} \tag{3.21}$$

$$\sigma_{\ln E_{eff}}^2 = \mathrm{E}\left[(\ln E_{eff} - \mu_{\ln E_{eff}})^2\right]$$

$$= \mathrm{E}\left[\left(\left(\frac{1}{V_p}\int_0^{V_p}\ln E(\underset{\sim}{x})\,d\underset{\sim}{x}\right) - \mu_{\ln E_{eff}}\right)^2\right]$$

$$= \mathrm{E}\left[\left(\frac{1}{V_p}\int_0^{V_p}\left(\ln E(\underset{\sim}{x}) - \mu_{\ln E_{eff}}\right)d\underset{\sim}{x}\right)^2\right]$$

$$= \mathrm{E}\left[\frac{1}{V_p^2}\int_0^{V_p}\int_0^{V_p}(\ln E(\xi) - \mu_{\ln E_{eff}})(\ln E(\eta) - \mu_{\ln E_{eff}})d\xi d\eta\right]$$

$$= \frac{1}{V_p^2}\int_0^{V_p}\int_0^{V_p}\mathrm{E}\left[(\ln E(\xi) - \mu_{\ln E_{eff}})(\ln E(\eta) - \mu_{\ln E_{eff}})\right]d\xi d\eta$$

$$= \frac{1}{V_p^2}\int_0^{V_p}\int_0^{V_p}\mathrm{Cov}\left[\ln E(\xi), \ln E(\eta)\right]$$

$$= \frac{\sigma_{\ln E}^2}{V_p^2}\int_0^{V_p}\int_0^{V_p}\rho(\underset{\sim}{x}_1 - \underset{\sim}{x}_2)d\underset{\sim}{x}_1 d\underset{\sim}{x}_2$$

$$= \sigma_{\ln E}^2\gamma(V_p) \tag{3.22}$$

The covariance appearing in eq. (3.17) between the geometric average of the observed elastic modulus values over the sample volume, V_s, and the effective elastic modulus as seen by the pile length over the volume V_p is obtained as follows, using the rightmost approximate in eq. (3.9)

$$\mathrm{Cov}\left[\ln\hat{E}, \ln E_{eff}\right] = \mathrm{E}\left[\left(\ln\hat{E} - \mu_{\ln\hat{E}}\right)\left(\ln E_{eff} - \mu_{\ln E_{eff}}\right)\right]$$

$$= \mathrm{E}\left[\left(\left(\frac{1}{V_s}\int_0^{V_s}\ln E(\underset{\sim}{x}_1)d\underset{\sim}{x}_1\right) - \mu_{\ln\hat{E}}\right)\left(\left(\frac{1}{V_p}\int_0^{V_p}\ln E(\underset{\sim}{x}_2)d\underset{\sim}{x}_2\right) - \mu_{\ln E_{eff}}\right)\right]$$

$$\simeq \frac{1}{V_s V_p}\int_{V_s}\int_{V_p}\mathrm{Cov}\left[\ln E_j^o, \ln E_i\right]d\underset{\sim}{x}_1 d\underset{\sim}{x}_2$$

$$\simeq \frac{\sigma_{\ln E}^2}{V_s V_p}\int_{V_s}\int_{V_p}\rho\left(\sqrt{r^2 + (\underset{\sim}{x}_i - \underset{\sim}{x}_j^o)^2}\right)d\underset{\sim}{x}_1 d\underset{\sim}{x}_2$$

$$\simeq \sigma_{\ln E}^2\gamma_{V_s V_p} \tag{3.23}$$

where $\gamma_{V_s V_p}$ is the average correlation coefficient between the log-elastic modulus samples over the sample volume, V_s, and the log-elastic modulus over the pile volume, V_p, and ρ is the correlation function between $\ln E(\underset{\sim}{x}_1)$ and $\ln E(\underset{\sim}{x}_2)$ (see eq.1.35). In detail, $\gamma_{V_s V_p}$ is

defined by,

$$\gamma_{V_s V_p} \simeq \frac{1}{V_s V_p} \int_{V_s} \int_{V_p} \rho\left(\sqrt{r^2 + (\underset{\sim}{x}_1 - \underset{\sim}{x}_2)^2}\right) d\underset{\sim}{x}_2 \, d\underset{\sim}{x}_1$$

$$\simeq \frac{1}{V_s V_p} \int_0^{B_s} \int_0^{B_s} \int_0^{D} \int_0^{B_p} \int_0^{B_p} \int_0^{C}$$

$$\rho\left(\sqrt{(r_x + x_s - x_p)^2 + (r_y + y_s - y_p)^2 + (z_s - z_p)^2}\right) \, dz_p \, dy_p \, dx_p \, dz_s \, dy_s \, dx_s \quad (3.24)$$

where r is the horizontal distance between the pile centerline and the centerline of the soil sample column shown in Figure 3.1, $r_x = r + (B_p - B_s)/2$, and $r_y = (B_p - B_s)/2$.

Substituting eq's. (1.55), (3.18), (3.19), (3.21), (3.22), and (3.23) into eq's. (3.16) and (3.17), leads to

$$\mu_{\ln W} = \mu_{\ln F} \quad (3.25)$$

$$\sigma_{\ln W}^2 \simeq \sigma_{\ln F}^2 + \sigma_{\ln E}^2 \left[\gamma(V_s) + \gamma(V_p) - 2\gamma_{V_s V_p}\right] \quad (3.26)$$

If the reliability index is specified, perhaps by $\beta = -\Phi^{-1}(p_{max})$, then the geotechnical resistance factor may now be determined by eq. (3.15).

The theoretical solution developed above is valid under the assumption that a single pile is sufficient to support the applied design load without excessive settlement (according to design). In other words, the above solution only applies if a pile can be increased in length sufficiently that its settlement becomes less than δ_{max} with probability p_{max}. However, some load-elastic modulus combinations are such that even an infinite length pile (of diameter d and elastic modulus E_p) will have a predicted settlement exceeding δ_{max}. This will occur if the maximum value of I_p required to just satisfy eq. (3.5), $I_{p,max}$, where

$$I_{p,max} = \frac{\phi_{gs} \delta_{max} \hat{E} d}{\hat{F}_T} \quad (3.27)$$

is less than the minimum value available from eq. (3.4), which occurs when $H \to \infty$,

$$b_1 = a_0 + \frac{1}{\left(\infty/d + a_1\right)^{a_2}} = a_0 \quad (3.28)$$

At the other extreme, if $I_{p,max}$ is greater than that given by eq. (3.4) when $H \to 0$,

$$b_0 = a_0 + a_1^{-a_2} \qquad (3.29)$$

then no pile is required to provide adequate settlement resistance.

What this means is that if $b_1 < I_{p,max} < b_0$, then the failure probability given by eq. (3.14) is valid. If $I_{p,max} > b_0$, then no pile is required by design, and the probability of excessive settlement is obtained from eq. (3.14) using $H = 0$.

If $I_{p,max} < b_1$, then a single pile is insufficient to carry the load, within an acceptable settlement, and multiple piles must be provided. if the design load, $\hat{F}_T$, is assumed to be shared equally between the provided piles, and the piles are assumed to act independently, then the load applied to each pile is thus $\hat{F}_T/n_p$, where n_p is the number of piles required to reduce the settlement to less than δ_{max}. Due to the assumption of independence, the probability of excessive settlement for each pile becomes

$$p_f = 1 - \Phi \left(\frac{\ln \left(\hat{F}_T/(n_p \varphi_{gs}) \right) - \mu_{\ln W}}{\sigma_{\ln W}} \right) \qquad (3.30)$$

Dividing the design load by the number of piles preserves the variance of $\ln F$ (see eq. 1.55a), therefore eq. (3.26) can still be used to obtain the variance of $\ln W$. The mean of $\ln F_T$, hence the mean of $\ln W$, is reduced as follows,

$$\mu_{\ln W} = \mu_{\ln F} = \ln(\mu_{F_T}/n_p) - \tfrac{1}{2}\sigma_{\ln F}^2 \qquad (3.31)$$

It can be shown that the number of piles, n_p, required *by design* to support the load $\hat{F}_T$ is

$$n_p = \text{int} \left(1 + \frac{b_1}{I_{p,max}} \right) \qquad (3.32)$$

However, since the ground is random, the value of $\hat{E}$ is random, so that $I_{p,max}$ and thus n_p are also random.

The failure probability is thus computed using the total probability theorem as

$$p_f = \sum_{i=0}^{\infty} \mathrm{P}\left[F_T | n_p = i\right] \mathrm{P}\left[n_p = i\right] \tag{3.33}$$

where $\mathrm{P}\left[F_T | n_p = i\right]$ is obtained by eq. (3.30). To find $\mathrm{P}\left[n_p = i\right]$, it is convenient to define

$$f_0 = \frac{\ln(b_0 \hat{F}_T / \delta_{max} \varphi_{gs} d) - \mu_{\ln \hat{E}}}{\sigma_{\ln \hat{E}}}$$

$$f_i = \frac{\ln(b_1 \hat{F}_T / i \delta_{max} \varphi_{gs} d) - \mu_{\ln \hat{E}}}{\sigma_{\ln \hat{E}}}, \text{ for } i = 1, 2, 3, ... \tag{3.34}$$

then

$$\mathrm{P}\left[n_p = 0\right] = \mathrm{P}\left[I_{p,max} \geq b_0\right] = 1 - \Phi\left(f_0\right)$$

$$\mathrm{P}\left[n_p = 1\right] = \mathrm{P}\left[b_1 \leq I_{p,max} < b_0\right] = \Phi\left(f_0\right) - \Phi\left(f_1\right)$$

$$\mathrm{P}\left[n_p = i\right] = \mathrm{P}\left[b_1/i \leq I_{p,max} < b_1/(i-1)\right]$$

$$= \Phi\left(f_{i-1}\right) - \Phi\left(f_i\right), \text{ for } i = 2, 3, ... \tag{3.35}$$

The mean and variance of $\ln \hat{E}$ are defined in eq's. (3.18) and (3.20).

Unlike eq. (3.14), eq. (3.33) is not easily inverted to solve for the required resistance factor, φ_{gs}, i.e. finding φ_{gs} such that eq. (3.2) is satisfied. To obtain the required φ_{gs}, root-finding algorithms, such as bisection, can be utilized to determine the root of

$$p_f - p_{max} = 0 \tag{3.36}$$

The calibration of I_p is done here by performing the finite element predictions of pile settlement over a range of H/d values and solving for I_p using eq. (3.3). For $k = E_p/\hat{E} = 700$, and $\nu = 0.3$, the solid curve shown in Figure 3.3 results. The following function was fit (by regression) to the solid curve in Figure 3.3,

$$I_p = 0.029 + \frac{1}{(H/d + 2.44)^{0.939}} \tag{3.37}$$

which is also shown on Figure 3.3 but is indistinguishable from the finite element results. The predicted I_p value given by eq. (3.37) is used in the next section, but a more general regression fit was developed in Chapter 2.
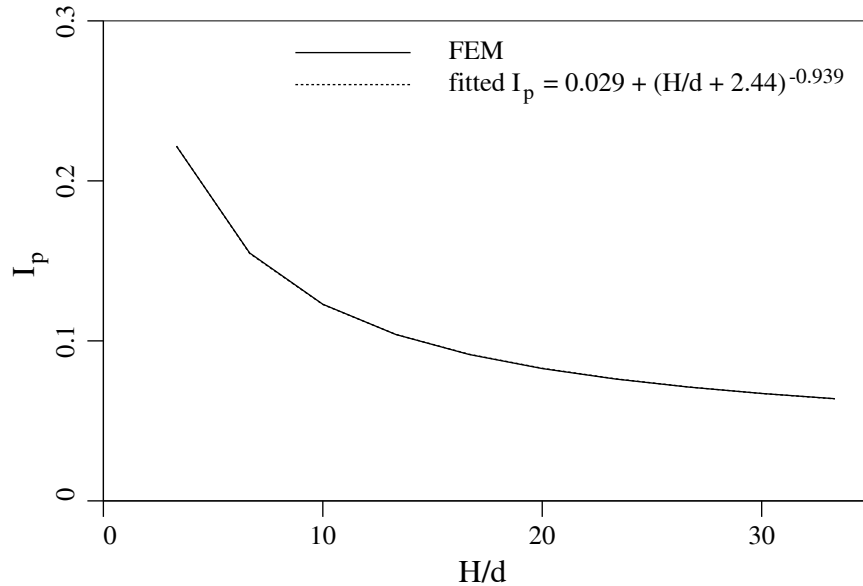
Figure 3.3 Calibration of I_p using FE model for $k = 700$

3.3 VALIDATION OF THEORY VIA MONTE CARLO SIMULA-TION

The objective of this section is to validate the theory developed in the previous section by comparing to the random finite element method (RFEM, Fenton and Griffiths, 2008). Only one specific pile diameter is considered in the simulation, $d = 0.3$ m, although several side studies were conducted to confirm that the agreement remains the same for differing pile diameters. The parameters used in the simulation are detailed in Table 3.1.

The simulation essentially proceeds by carrying out a series of hypothetical designs on simulated soil fields and checking to see what fraction of the designs fail (excessive settlement).

In practice, the accuracy of the Monte Carlo method depends on how well the assumed probability distribution fits the real stochastic process. If the fit is reasonable, the accuracy increases with the number of simulation runs, i.e. improved results will be obtained as the number of simulation realizations increases. In detail, the steps involved in the Monte Carlo simulation are;

Table 3.1   Input parameters used in the validation of theory

Parameters	Values Considered
μ_L	400 kN
$v_L = \sigma_L / \mu_L$	0.27
μ_D	1,200 kN
$v_D = \sigma_D / \mu_D$	0.1
Poisson's ratio, ν	0.3
μ_E	30 MPa
v_E	0.1, 0.2, 0.3, 0.4, 0.5
$\theta_{\ln E}$	0-30 m
φ_{gs}	0.6, 0.7, 0.8, 0.9
E_p	21 GPa
d	0.3 m
δ_{max}	0.025 m
B_s	0.3 m
B_p	2.0 m
D	10 m
C	$2H$

1) The elastic modulus, E, of a soil mass is simulated as a 3-D spatially variable random field using the Local Average Subdivision (LAS) method (Fenton and Vanmarcke, 1990). The numbers of soil cells are 54 by 30 in the X, Y (plan) and 30 in the Z (vertical) directions and each cell size is taken to be 0.3 m by 0.3 m by 0.5 m in the X, Y, and Z directions.

2) The simulated soil is sampled along a vertical line through the soil at some distance, r, from the pile, see Figure 3.1. The virtually sampled soil properties are used to estimate

the characteristic elastic modulus, $\hat{E}$, according to eq. (3.9). A sample of depth $D = 10$ m was selected arbitrarily and since the random field element sizes are 0.3 by 0.3 m in plan, the sampling volume is $V_s = B_s \times B_s \times D = 0.3 \times 0.3 \times 10$ m^3. Three sampling distances are considered: the first is at $r = 0$ m which means that the samples are taken at the pile location. In this case, uncertainty about the pile resistance only arises if the pile extends below the sampling depth or if the elastic modulus field near the piles differs significantly from the sample at the pile. Typically, probabilities of failure when $r = 0$ m are very small. The other two sample distances considered are $r = 5$ m and $r = 10$ m, corresponding to reducing understanding of the soil conditions at the pile location. Note that it is really the ratio, $r/\theta_{\ln E}$, which affects the failure probability and a wide range in the correlation length, $\theta_{\ln E}$, has been considered.

3) Once the characteristic elastic modulus has been established, the required design pile length, H, is calculated using eq. (3.7) for a specified value of φ_{gs} (Note, $k = E_p/\hat{E} = 700$ and eq. (3.37) were used in this step).

4) Dead and live loads, F_D and F_L, are simulated as independent lognormally distributed random variables and then added to produce the actual total load on the pile, $F_T = F_L + F_D$.

5) The `true' pile settlement, δ, is computed using the finite element method, the details of which can be found in Naghibi et al. (2014). If $\delta > \delta_{max}$ then the pile is assumed to have failed.

6) The entire process from step 1 to step 5 is repeated n_{sim} times (where $n_{sim} = 2,000$ in the present study). If n_f of these repetitions result in a pile failure, then an estimate of the probability of failure is $p_f = n_f/n_{sim}$.

7) Repeating steps 1 through 6 using various values of φ_{gs} in the design step allows plots of failure probability vs. geotechnical resistance factor to be produced for the various sampling distances, coefficients of variation of elastic modulus, and correlation lengths.

It is recognized that pile settlement becomes non-linear after about 2% of the pile diameter, and so the elastic modulus mean used in this simulation must be considered to be a secant modulus which approximates the curved nature of the actual pile load-settlement curve. However, as discussed earlier, the details of the mean settlement predictor used to design the pile are not important, and of course, the reader is encouraged to use the best settlement prediction available to them. The linear model used in this paper is, however, the best currently available to predict the effects of spatial variability of the soil on the required resistance factor.

The failure probabilities estimated by theory, via eq. (3.33), can be superimposed on the simulation-based failure probability plots, allowing a direct comparison of the methods. Figure 3.4 illustrates the agreement between theory and simulation for $v_E = 0.3$, and various resistance factors, φ_{gs}, when the soil is sampled at $r = 0$ m, $r = 5$ m, and $r = 10$ m from the pile location. The agreement is considered very good for $r = 5$ and $r = 10$, given all the approximations made in the theory, allowing the geotechnical resistance factors to be computed using the theory with some degree of confidence even at probability levels which the simulation cannot estimate. The simulation involved only $n_{sim} = 2,000$ realizations and so cannot accurately resolve probabilities less than about 1×10^{-3} – the standard deviation of the failure probability estimate is $\sqrt{p_f(1 - p_f)/n_{sim}} \simeq 0.02\sqrt{p_f}$ for small failure probability p_f. This means that if $p_f = 1 \times 10^{-3}$, then the standard deviation of its estimate is practically the same at 0.7×10^{-3}.

The very good agreement between simulation and theory seen in Figure 3.4 was obtained by adjusting by trial-and-error the soil volume surrounding the pile, $V_p = B_p \times B_p \times C$, for use in the geometric average of eq. (1.40). The (approximately) best averaging volume was found to occur when $B_p = 2$ m and $C = 2H$, as suggested in Table 3.1. The remaining small discrepancies are believed to arise due to the fact that the simulation assumes that the soil mass is underlain by firm bedrock at a depth of 15 m, while the theory assumes that

the pile is founded in an elastic half-space. The main implications of this is that the piles in the simulation cannot exceed a length of 15 m, and in fact boundary effects begin to show themselves well before this length. The solution was to limit the piles in the simulation to a maximum length of $H_{max} = 14$ m. If the design required a pile in excess of H_{max}, then multiple piles were provided. See the previous section for a discussion of multiple piles being used. In order to better compare with the simulation, the theory was adjusted temporarily by replacing eq. (3.28) with

$$b_1 = a_0 + \frac{1}{\left(H_{max}/d + a_1\right)^{a_2}} \tag{3.38}$$

In light of these uncertainties, the agreement between theory and simulation is deemed to be excellent so that the theory was felt to be accurate enough for the determination of resistance factors required for the design process, as discussed in the next section.
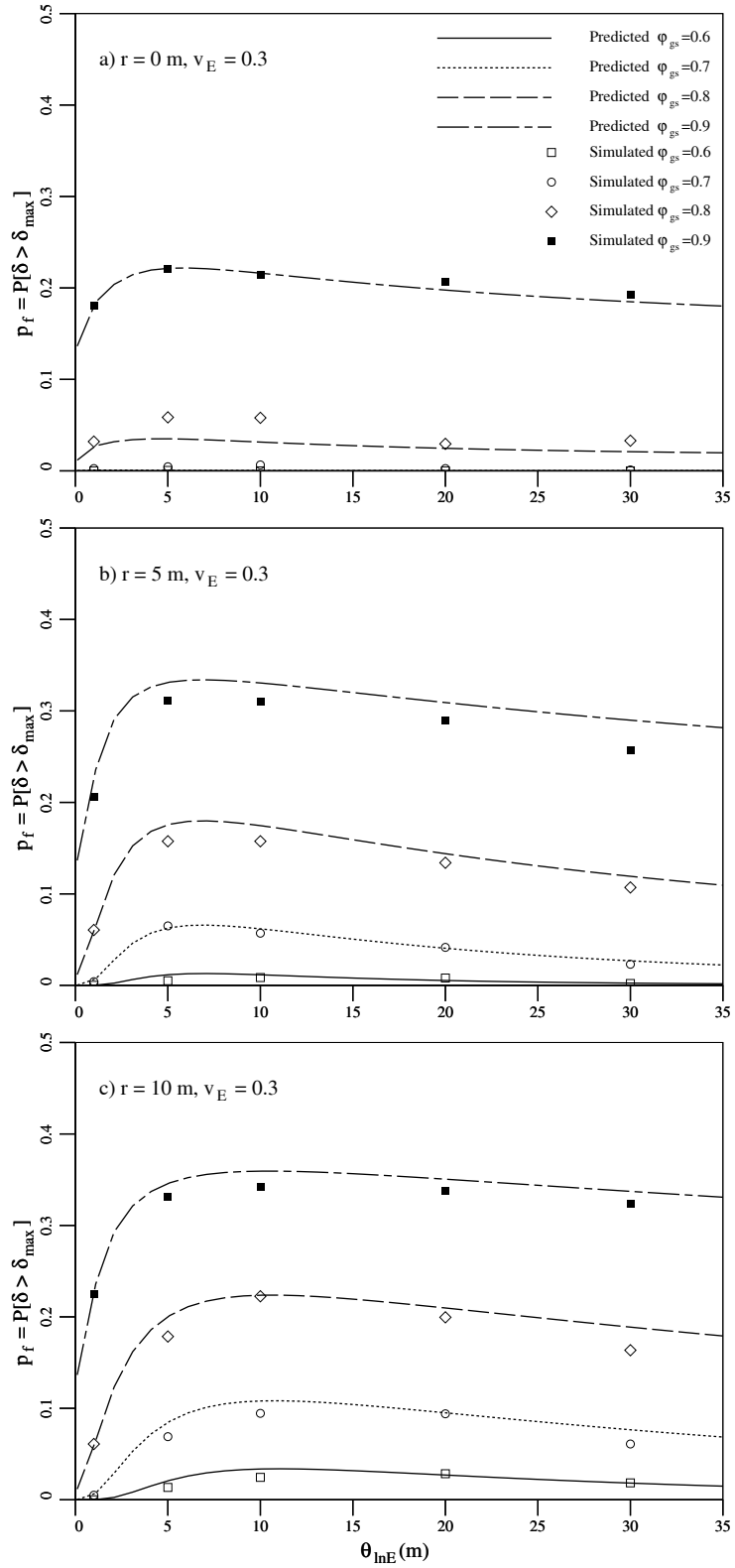
Figure 3.4 Effect of correlation length, $\theta_{\ln E}$, on probability of failure, p_f, for $v_E = 0.3$, and a) $r = 0$ m, b) $r = 5$ m, c) $r = 10$ m, generated by eq. (3.33)

It is evident from Figure 3.4 that the probability of failure reaches a maximum at an intermediate correlation length of around $\theta_{\ln E} = 3$ to 10 m for all three sampling schemes considered ($r = 0$, 5, and 10 m). This is as expected, since for small and large correlation lengths the values of $\hat{E}$ and E_{eff} become equal for stationary random fields and so the largest difference between $\hat{E}$ and E_{eff} will occur at intermediate correlation lengths. It is also observed from Figure 3.4 that the probability of failure, p_f, increases with resistance factor, φ_{gs}, as expected. Also, p_f is smaller when the soil is sampled directly at the pile location, which is also to be expected, and means that construction savings may be achieved by improving the sampling scheme. The worst case (lowest) resistance factor happens when the correlation length, $\theta_{\ln E}$ is approximately equal to the distance from the pile to the sampling location, a number between 1 and 10 m for the latter sampling schemes used in this study. This worst case is important, since the correlation length is very hard to estimate and will be unknown for most sites. In other words, in the absence of knowledge about the correlation length, the lowest resistance factor in these plots, at the worst case correlation length, can conservatively be used. Notice in Figure 3.4, that the worst case correlation length shows some increase as the distance to the sample location increases.

Figure 3.5 shows the effect of the resistance factor on the probability of failure, as estimated by eq. (3.33) for different values of v_E, and the corresponding worst case correlation $\theta_{\ln E} = 5$ m, when the soil is sampled at $r = 5$ m from the pile location. This figure can be used for design by drawing a horizontal line across at the target probability, p_{max}, and then reading off the required resistance factor for a given v_E. For example, if $p_{max} = 0.05$, it can be seen that φ_{gs} is almost 0.58 for the 'worst case' $v_E = 0.5$. For the other v_E's considered, the required resistance factor is between 0.62 and 0.81. For lower target probabilities, say $p_{max} = 0.01$, the resistance factor for the 'worst case' v_E decreases to 0.48, and ranges between 0.52 and 0.72, for all other considered v_E's. This means that construction savings may be achieved with lower target probabilities when residual soil variability is reduced by sufficient sampling.
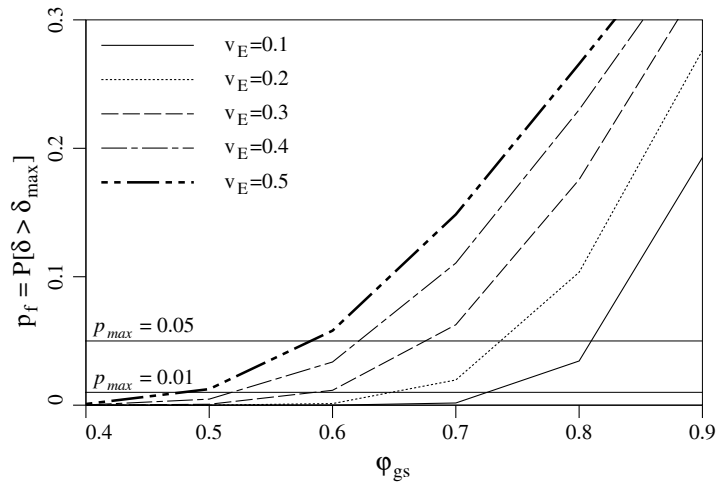
Figure 3.5 Effect of resistance factor, φ_{gs}, on probability of failure, p_f, for $r = 5$ m, and $\theta_{\ln E} = 5$ m, generated by eq. (3.33)

3.4 REQUIRED GEOTECHNICAL RESISTANCE FACTORS

In this section, the values of resistance factor, φ_{gs}, required to achieve maximum acceptable failure probability levels $10^{-1}, 10^{-2}, 10^{-3}$, and 10^{-4} will be investigated. The reliability indices, β, corresponding to these four target probabilities are $1.28, 2.3, 3.1$, and 3.7, respectively.

Figures 3.6, 3.7, and 3.8 demonstrate the resistance factors required for the three sampling schemes used in this study ($r = 0$ m, $r = 5$ m, and $r = 10$ m), to achieve the four maximum acceptable failure probabilities. In the case where the soil is sampled at the pile location, as depicted in Figure 3.6, the resistance factor exceeds 0.80 when $p_{max} \geq 10^{-1}$ and becomes as low as 0.61 for $p_{max} = 10^{-4}$.
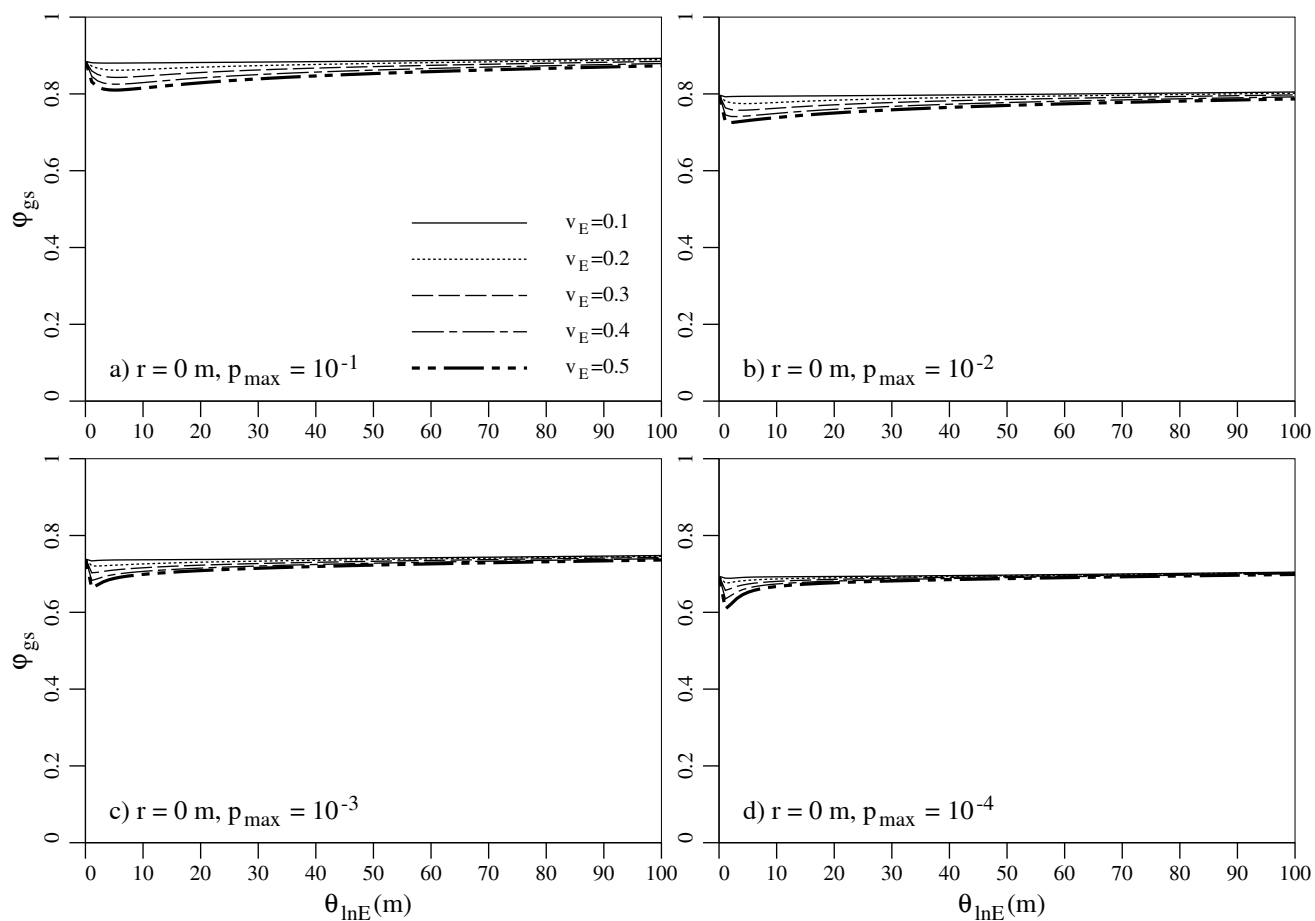
Figure 3.6 Geotechnical resistance factors for soil samples taken at the pile location ($r = 0$ m)
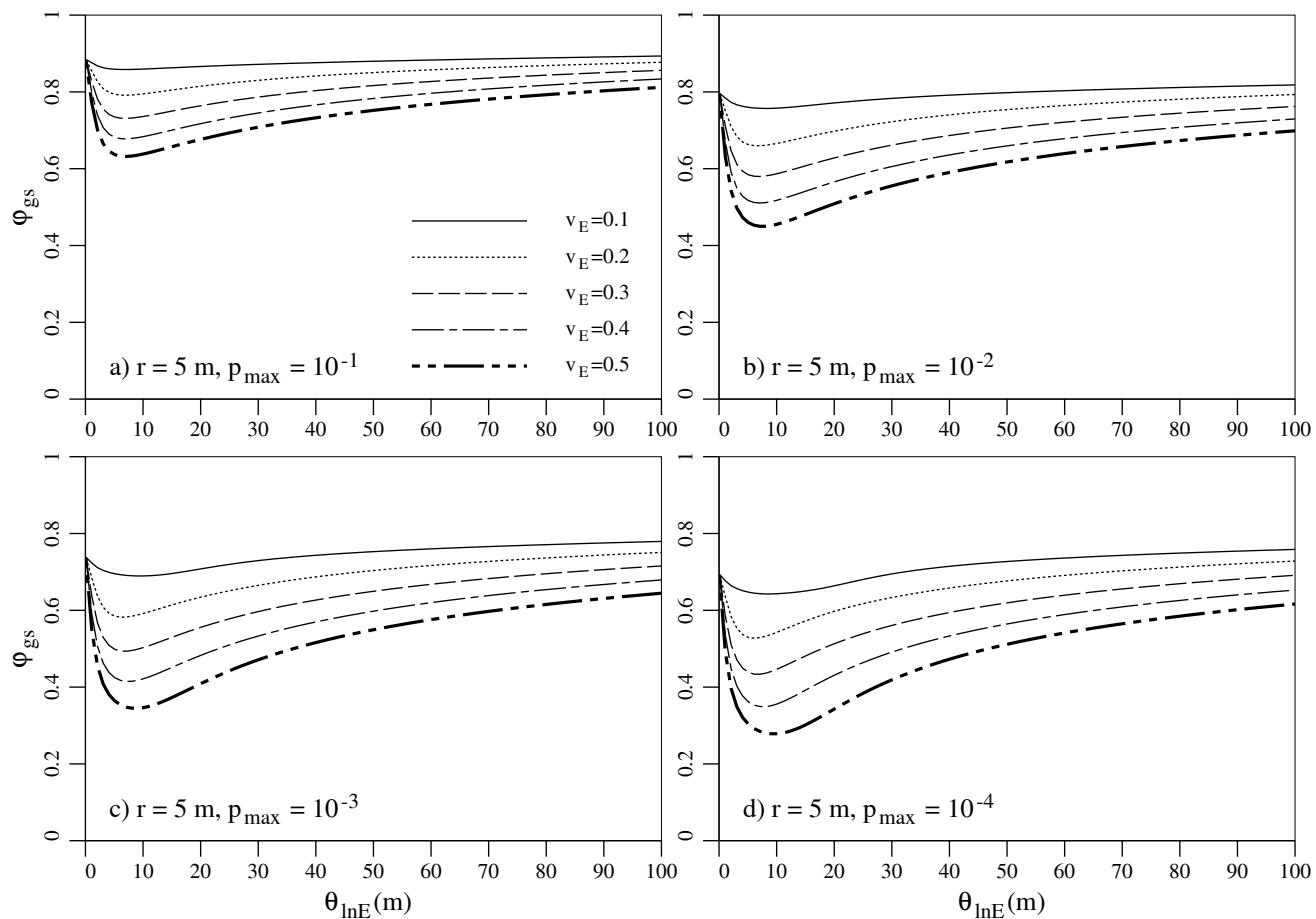
Figure 3.7 Geotechnical resistance factors for soil samples take at $r = 5$ m from the pile centerline
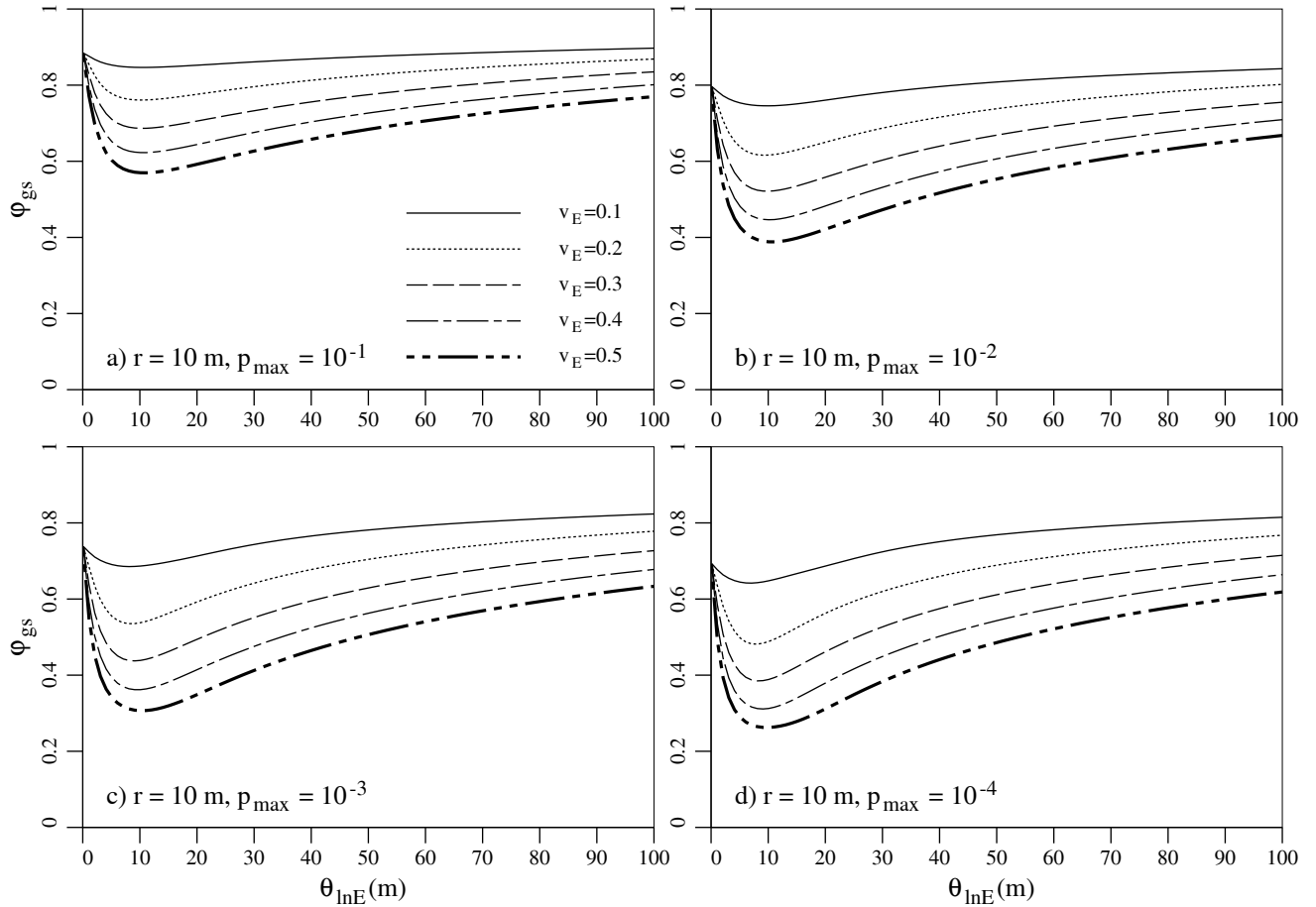
Figure 3.8 Geotechnical resistance factors for soil samples taken at $r = 10$ m from the pile centerline

The smallest resistance factors in Figure 3.8 correspond to the smallest acceptable failure probability, $p_{max} = 10^{-4}$, when the soil is sampled at $r = 10$ m away from the pile location. When the elastic modulus coefficient of variation is large ($v_E = 0.5$), the worst case values of φ_{gs} becomes as low as 0.26 in order to achieve $p_{max} = 10^{-4}$. This means that there will be a significant construction cost penalty if a highly reliable pile is to be designed using a site investigation which is insufficient to reduce the residual variability to less than $v_E = 0.5$. In the presense of sufficient site investigation, the upper bound in each plot (corresponding to $v_E = 0.1$) can probably be used, leading to a more economical design in terms of construction cost.

Table 3.2 summarizes the worst case resistance factors required to achieve the indicated

maximum acceptable failure prbabilities as seen in Figures 3.6, 3.7, and 3.8.

Table 3.2 Worst case geotechnical resistance factors for various coefficients of variation, v_E, distance to sampling location, r, and acceptable failure probabilities, p_{max}

r(m)	v_E	Geotechnical resistance factor			
		$p_{max} = 10^{-1}$	$p_{max} = 10^{-2}$	$p_{max} = 10^{-3}$	$p_{max} = 10^{-4}$
0	0.1	0.88	0.79	0.73	0.69
0	0.2	0.86	0.77	0.72	0.68
0	0.3	0.84	0.76	0.70	0.66
0	0.4	0.83	0.74	0.68	0.63
0	0.5	0.81	0.73	0.66	0.61
5	0.1	0.86	0.76	0.69	0.64
5	0.2	0.79	0.66	0.58	0.53
5	0.3	0.73	0.58	0.49	0.43
5	0.4	0.68	0.51	0.41	0.35
5	0.5	0.63	0.45	0.34	0.28
10	0.1	0.85	0.75	0.69	0.64
10	0.2	0.76	0.62	0.54	0.48
10	0.3	0.69	0.52	0.44	0.38
10	0.4	0.62	0.45	0.36	0.31
10	0.5	0.57	0.39	0.31	0.26

3.5   DISCUSSION

The recommended resistance factors listed in Table 3.2 have at least two significant advantages to their use in practice;

a) the resistance factor can be calibrated to account for the level of site and model understanding, represented approximately here by the sampling distance r, and

b) the target reliability can be explicitly adjusted for differing failure consequence and redundancy levels. For example, replacement or repair of a foundation due to excessive

settlement is often extremely expensive, and can be orders of magnitude higher than the original cost of the foundation. In this case, a higher reliability (lower p_{max}) may be warranted. Alternatively, if the foundation is part of a redundant system of multiple foundations (e.g., a series of piles) so that the excessive settlement of one foundation will not be noticed (the load is supported by adjacent stronger foundations), then a lower reliability (higher p_{max}) may be appropriate to use for the design of the individual foundation components.

The design approach adopted here takes advantage of the provision of reliability via a resistance factor and proceeds as follows;

1) Decide on a pile type, so that the pile elastic modulus, E_p, and diameter (or width), d, are known (alternatively d can also be obtained in the design process – see step 5);

2) Decide on a maximum acceptable failure probability, p_{max} for the pile. As discussed above, the choice of p_{max} depends on the severity of failure consequences and the level of pile redundancy;

3) Sample the soil. If a linear elastic design model is being used, estimate the characteristic soil elastic modulus using eq. (3.9). In this research, the estimate is a geometric average which is generally slightly lower than the arithmetic average (by 2 to 5% for most soils). For simplicity, an estimate of the mean elastic modulus (i.e. the arithmetic average) can also be used;

4) Select a geotechnical resistance factor for the maximum acceptable failure probability, p_{max}, and sampling distance from Table 3.2. The sampling distance has been used here as a proxy for level of site understanding. The actual geotechnical resistance factor used in design may also need to be reduced somewhat, depending on the magnitude of the model and measurement errors, as discussed below;

5) Compute the required pile length and/or diameter, using the selected geotechnical resistance factor, φ_{gs}, and the maximum tolerable settlement, δ_{max}, via eq. (3.7). or some other more accurate design process.

Three sampling schemes have been considered in this study. Better estimates of conditions at the pile are of course obtained when samples are taken at the pile location ($r = 0\,\text{m}$), which translates into lower probability of failure or, equivalently, larger geotechnical resistance factor values. The required geotechnical resistance factor also depends on the soil field uncertainty level (e.g. coefficient of variation, v_E), and correlation level (e.g. correlation length, $\theta_{\ln E}$). Since coefficient of variation, v_E and correlation length, $\theta_{\ln E}$, are usually unknown for a given site, various v_E values are considered in Table 3.2 using the worst case correlation length (highest failure probability). Assuming a coefficient of variation of around $v_E \simeq 0.3$ is probably reasonably conservative. Note that the use of the worst case correlation length can be quite conservative (see Figures 3.6 through 3.8).

The resistance factors recommended in this study for serviceability limit state design of deep foundations are upper bounds at the worst case correlation length, and therefore unconservative, because measurement and model errors are not explicitly considered in their determination. These additional error sources can be accommodated here by using a value of v_E greater than would actually be true at a site (e.g. if $v_E = 0.2$ at a site, the effects of measurement and model error might be accommodated by using $v_E = 0.3$ in the relationships presented here) or by assuming that the soil samples were taken further away from the pile centerline than they actually were, e.g., if low-quality soil samples are taken at the pile location ($r = 0$ m) the geotechnical resistance factor corresponding to a larger value of r (say $r = 5$ m) should be used. Note, however, that the actual correlation length at the site is unlikely to be equal to the worst case correlation length, so that to some extent the use of the conservative values in Table 3.2 may already be sufficient to account for measurement and model errors.

CHAPTER 4

CONSEQUENCE FACTOR CALIBRATION FOR DEEP FOUNDATIONS

4.1 GENERAL

This chapter presents the results of consequence factor calibrations for the design of deep foundations at SLS. The results are compared to the consequence factors obtained at ULS.

In order to compare the consequence factors, the estimation of the resistance factor at ULS is derived in the following section using the theoretical framework presented by Naghibi and Fenton (2011). Then the consequence factor, Ψ_u or Ψ_s, is studied in detail and how it varies with respect to target failure probability and site uncertainty for each limit state individually. A key question to address is: do we require two sets of consequence factors for ultimate and serviceability limit states since they have different maximum acceptable failure probabilities?

4.2 FAILURE PROBABILITY AT ULS

In order to determine the required resistance and consequence factors, the probability of a deep foundation reaching its bearing capacity ultimate limit state must be estimated. This probability will depend on the load distribution, the resistance distribution and the load and resistance factors selected. If an axially loaded pile founded within purely cohesive soils is considered, the characteristic ultimate bearing resistance, using the α method is given by Das(2000) to be,

$$\hat{R}_u = pH\alpha\hat{c} \tag{4.1}$$

for pile length H, in which p is the effective perimeter length of the pile section, α is an empirical adhesion factor, typically in the range from 0.5 to 1 (CGS, 2006), and $\hat{c}$ is the characteristic undrained shear strength (herein referred to as cohesion) which is commonly estimated from a set of m observations $\hat{c}_1, \hat{c}_2, ..., \hat{c}_m$ of soil cohesion taken at the site (each of which in turn may be estimated via some indirect measurement, such as CPT). In this research, an arithmetic average of the observations will be used to define the characteristic cohesion,

$$\hat{c} = \frac{1}{m} \sum_{j=1}^{m} \hat{c}_j \tag{4.2}$$

and measurement error is ignored (i.e. the obtained resistance factors are actually upper bounds).

The required minimum design pile length, H, is then obtained by substituting eq's. (1.56) and (4.1) into eq. (1.15a), giving for the ULS case,

$$H = \frac{\hat{F}_T}{\varphi_{gu} p \alpha \hat{c}} \tag{4.3}$$

The probability of failure involves determining the probability that the actual lifetime extreme load acting on the pile, F_T, exceeds the actual ultimate resistance, $R_u = pH\alpha\bar{c}$ (where $\bar{c}$ is the equivalent cohesion as 'seen' by the pile over its enti re length). In other words, the probability of failure is computed as

$$p_f = \mathrm{P}\left[F_T > R_u\right] = \mathrm{P}\left[\frac{F_T \hat{c}}{\bar{c}} > \frac{\hat{F}_T}{\varphi_{gu}}\right] \tag{4.4}$$

All three quantities on the left hand side of the inequality, i.e. F_T, $\hat{c}$ and $\bar{c}$, are random. See Naghibi and Fenton (2011) for the details of their joint distribution and how the probability in eq. (4.4) is computed.

Once the probability of failure is computed via eq. (4.4), it can be compared to the maximum acceptable failure probability, p_{max}. If p_f exceeds p_{max}, then the resistance factor and/or

the consequence factor need to be reduced (specifically, the product $\Psi_u \varphi_{gu}$ needs to be reduced). The determination of required consequence factors then proceeds in two steps;

1) Consider first the typical consequence level and set $\Psi_u = 1$. For a variety of different levels of variability in soil properties, degrees of spatial correlation between soil properties, and distance between pile and sample location (which is taken as a proxy for site understanding), estimate the probability of pile failure using eq. (4.4). For each case, adjust the resistance factor, φ_{gu}, until $p_f = p_{max}$. These then are the required resistance factors.

2) Using the required resistance factor(s) determined in step 1, repeat the procedure of step 1 except now at the high (reduced p_{max}) and low (increased p_{max}) consequence levels and adjust the consequence factor, Ψ_u, until $p_f = p_{max}$. This then yields the required consequence factors.

4.3   FAILURE PROBABILITY AT SLS

A complete discussion of the theory, along with the simulation-based validation, can be found in Chapter 3. Once the probability of failure is computed as described in Chapter 3, the 2-step approach mentioned in Section 4.2 can be followed to obtain the required resistance and consequence factors of piles at SLS.

4.4   THEORETICAL CONSEQUENCE FACTORS AT ULS

Consequence factors were determined for a particular example problem with parameters as follows;

1) The mean lifetime maximum live load acting on the pile is assumed to be $\mu_L = 20$ kN with coefficient of variation $v_L = 0.3$. The mean dead load is assumed to be $\mu_D = 60$

kN with coefficient of variation $v_D = 0.15$. The mean values assumed here are not particularly important, since the design (see eq. 4.3) takes the separation between the load and resistance distributions into account in the design process (e.g. the higher the load is *relative* to the resistance, the larger the required pile length). Both live and dead loads are assumed to be lognormally distributed.

2) The mean cohesion is assumed to be $\mu_c = 50$ kN/m^2 with coefficient of variation $v_c = 0.1, 0.2, 0.3, 0.4$ and 0.5. As mentioned above, the mean value is expected to have little influence on the results, but the coefficient of variation definitely affects the resistance factor and has a slight influence on the consequence factor, as will be shown. The cohesion is assumed to be lognormally distributed.

3) This research looks specifically at the case where the soil is frictionless ($\phi = 0$) and the cohesion, $c = s_u$, is the undrained shear strength.

4) The correlation length, $\theta_{\ln c}$, is varied from a low of 0.1 m to a high of 50 m. Low values of $\theta_{\ln c}$ lead to soil properties varying rapidly spatially, while high values mean that the soil properties vary only slowly with position. A large correlation length, of say $\theta_{\ln c} = 50$ m, means that soil samples taken well within 50 m from the pile location will (e.g. at $r = 10$ m) will be quite representative of the soil properties along the pile. Lower failure probabilities are expected when the soil is sampled well within the distance $\theta_{\ln c}$ from the pile. Interestingly, because the characteristic value derived from the soil sample is generally some form of average, when $\theta_{\ln c}$ is very small (say, 0.01 m) then the sample will again accurately reflect the average conditions along the pile regardless of the sampling location. The worst case correlation length occurs when $\theta_{\ln c}$ is approximately equal to the distance from the pile to the sampling location.

5) Three soil sampling locations are considered; directly along the pile location ($r = 0$), corresponding to good site understanding, $r = 4.5$ m, corresponding to moderate site

understanding, and $r = 9$ m, corresponding to lower site understanding. An upper limit of $r = 9$ m was selected here because the soil model happens to be 9 m wide.

6) Three consequence levels are considered; high failure consequence, typical failure consequence, and low failure consequence. Maximum acceptable failure probabilities have been assigned to these consequence levels; $p_{max} = 1/1,000, 1/5,000, 1/10,000$ and for low, typical, and high failure consequence levels, respectively. These failure probabilities correspond to reliability indices of 3.1, 3.5, and 3.7, respectively, which is in the range of foundation reliabilities suggested in the literature (see, e.g., Meyerhof, 1995, and Becker, 1996).

Figure 4.1 illustrates the variation of p_f with θ and the observation of the worst case correlation length for both theory and simulation. The figure presents failure probabilities for the case where the soil is sampled at $r = 4.5$ m from the pile. Clearly, the worst case failure probability (highest) occurs for values of correlation length near 4.5 m. The Figure is shown for the typical consequence case ($p_{max} = 1/5,000$), for which the consequence factor $\Psi_u = 1.0$ was selected. The theoretical results shown in Figure 4.1 have also been validated by simulation, as shown by the plotted circles and squares.
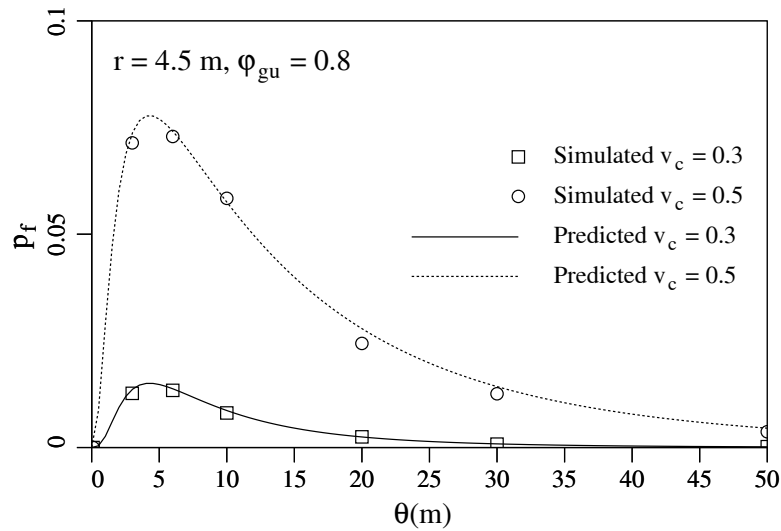
Figure 4.1 Failure probability versus correlation length for $\Psi_u = 1.0$ (typical consequence), $\varphi_{gu} = 0.8$, and $r = 4.5$ m at ULS computed via eq. (4.4)

As mentioned previously in Chapter 1, the consequence factor should ideally depend only on the target failure probability, p_{max}, and not on soil variability, correlation length, and sampling location. Variations in the latter three parameters should ideally be entirely handled by the resistance factor, φ_{gu}. Figures 4.2 and 4.3 illustrate the effect of correlation length and sampling location on the consequence factor for low consequence level (Figure 4.2) and for high consequence level (Figure 4.3). Both figures are shown for a moderate variability ($v_c = 0.3$).

The overall change in the consequence factor in Figure 4.2 with respect to correlation length and sampling location ranges from about 1.06 to 1.18, which is about a 10% relative change. Similarly, in Figure 4.3, the overall change in Ψ_u is from about 0.936 to 0.975, which is about a 4% relative change. These two plots demonstrate that the consequence factor is little affected by soil parameters, at least for $v_c \leq 0.3$, particularly when soil properties are well understood ($r = 0$ m), and is mostly dependent on the target acceptable failure probability alone.
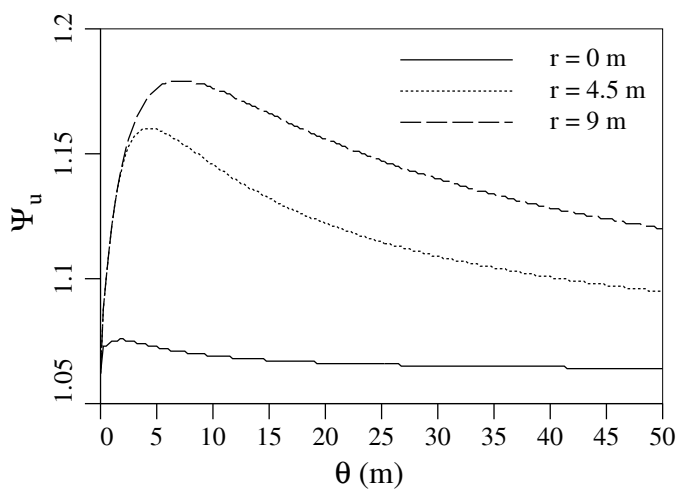
Figure 4.2   Consequence factor versus correlation length for various sampling locations at low consequence level ($p_{max} = 1/1,000$) for $v_c = 0.3$ at ULS
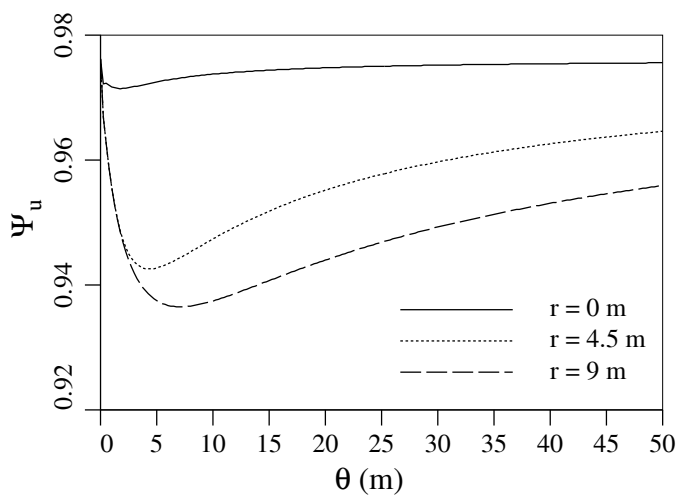
Figure 4.3   Consequence factor versus correlation length for various sampling locations at high consequence level ($p_{max} = 1/10,000$) for $v_c = 0.3$ at ULS

4.5 THEORETICAL CONSEQUENCE FACTORS AT SLS

Consequence factors for SLS design were determined for a particular example problem with parameters as follows;

1) The mean lifetime maximum live load acting on the pile is assumed to be $\mu_L = 400$ kN with coefficient of variation $v_L = 0.27$. The mean dead load is assumed to be $\mu_D = 1,600$ kN with coefficient of variation $v_D = 0.1$. Both live and dead loads are assumed to be lognormally distributed.

2) The mean soil elastic modulus is assumed to be $\mu_E = 30$ MPa with coefficient of variation $v_E = 0.1, 0.2, 0.3, 0.4$ and 0.5, also assumed to be lognormally distributed.

3) The correlation length, $\theta_{\ln E}$, is varied from a low of 0.1 m to a high of 100 m.

4) Three soil sampling locations are considered; directly along the pile ($r = 0$ m), corresponding to good site understanding, $r = 5$ m, corresponding to moderate site understanding, and $r = 10$ m, corresponding to lower site understanding.

Similar to ULS case, three consequence levels considered are high failure consequence, typical failure consequence, and low failure consequence. However, the maximum acceptable failure probabilities are much higher than for the ULS case, i.e. $p_{max} = 1/100, 1/300$, and $1/1,000$ for low, typical, and high failure consequence levels, respectively. These failure probabilities correspond to reliability indices of 2.3, 2.7, and 3.1, respectively, which is in the range of foundation reliabilities suggested in the literature at SLS (see, e.g., Phoon et al. 1995, and Eurocode, British Standard, 2002).

Figure 4.4 illustrates the effect of consequence factor on the probability of settlement failure. It can be seen that small changes in Ψ_s can make large differences in p_f, especially for larger v_E values.
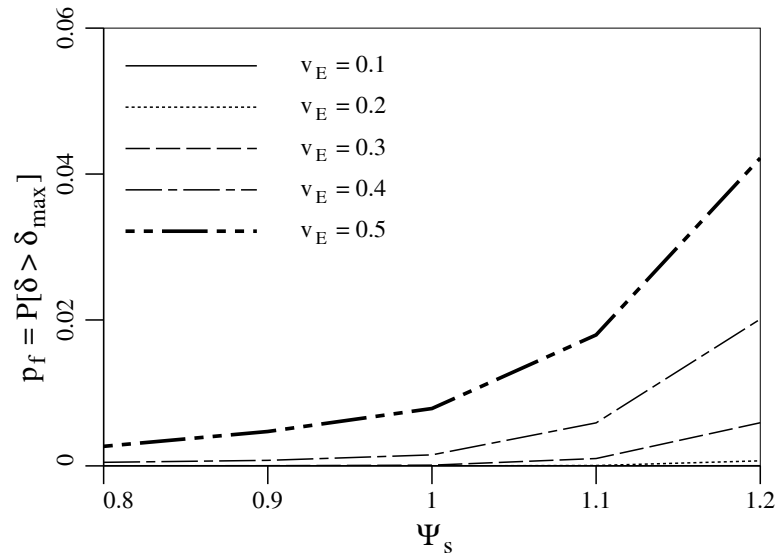
Figure 4.4   Failure probability versus consequence factor for $\theta_{\ln E} = 1$ m, $r = 5$ m, and $\varphi_{gs} = 0.5$ at SLS

Figure 4.5 presents failure probabilities estimated by theory, via eq. (3.33) and compared to simulation, for $v_E = 0.3$ and various resistance factors, φ_{gs}, when the soil is sampled at $r = 5$ m from the pile location. The agreement between simulation and theory is considered very good given all the approximations made in the theory. It is observed from Figure 4.5 that the probability of failure, p_f, increases with resistance factor, as expected.
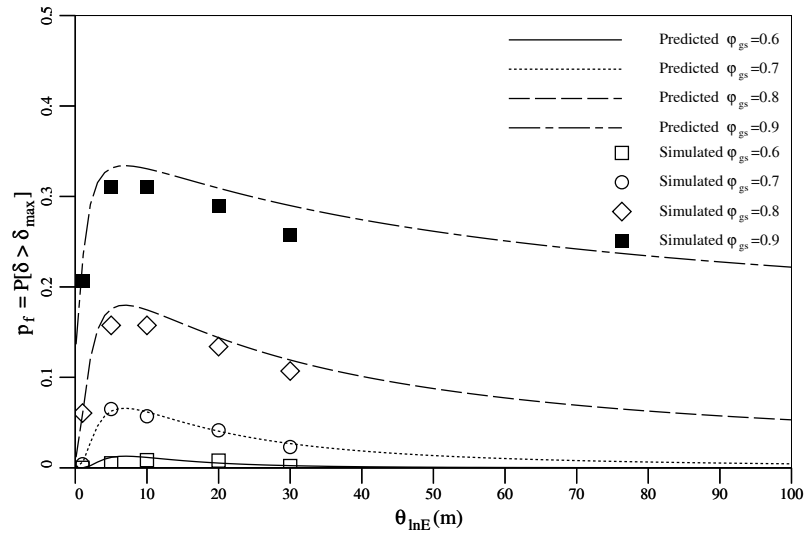
Figure 4.5   Failure probability versus correlation length for $\Psi_s = 1$ (typical consequence), $r = 5$ m, and $v_E = 0.3$ at SLS generated via eq. (3.33)

Figure 4.6 presents theoretical failure probabilities for the case where the soil is sampled $r = 5$ m away from the pile and for the low consequence case ($p_{max} = 1/100$), for which the consequence factor $\Psi_s = 1.1$ was selected. Similar to Figure 4.1, the presence of a worst case correlation length is evident in Figure 4.5. In addition, it is observed that the worst case probability of failure, p_f, is significantly less than the acceptable maximum probability when the coefficient of variation of the soil properties is at a moderate level ($v_E = 0.3$). However, the failure probability becomes unacceptable if the soil property variability exceeds $v_E = 0.3$. See, for example, the $v_E = 0.5$ curve, which slightly exceeds a failure probability of 0.03 at the worst case correlation length.
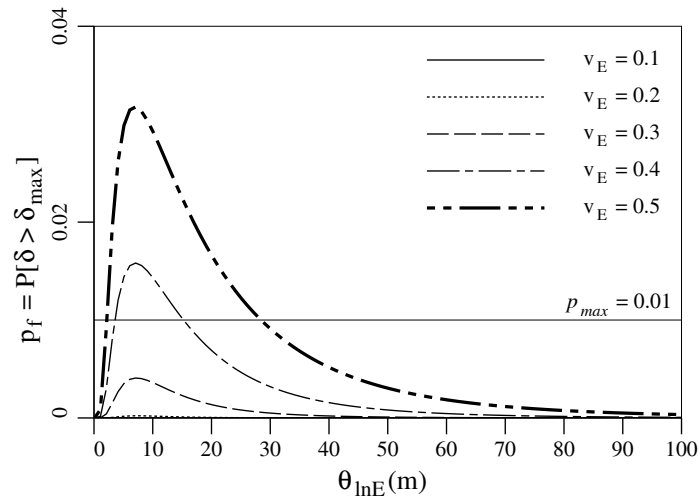
Figure 4.6   Failure probability versus correlation length for $\Psi_s = 1.1$ (low con-
sequence), $\varphi_{gs} = 0.5$, and $r = 5$ m at SLS generated via eq. (3.33)

The effect of correlation length and sampling location on the consequence factor is illustrated

in Figures 4.7 and 4.8 for low consequence level (Figure 4.7) and for high consequence

level (Figure 4.8). Both figures are shown for a moderate variability ($\upsilon_E = 0.3$).
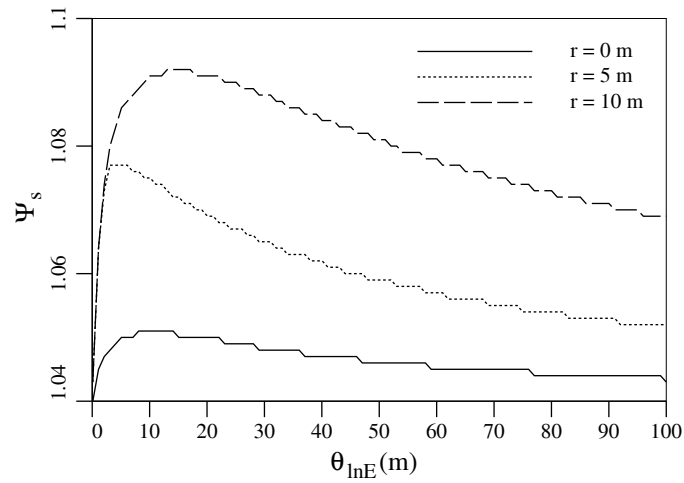
Figure 4.7   Consequence factor versus correlation length for various sampling locations at low consequence level ($p_{max} = 1/100$) for $v_E = 0.3$ at SLS
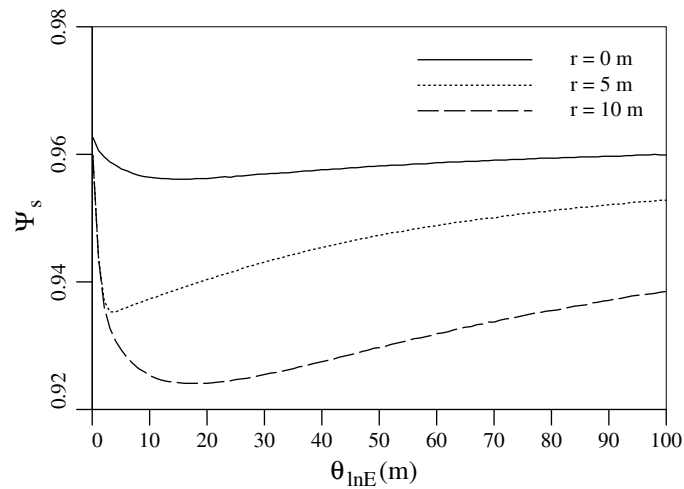
Figure 4.8   Consequence factor versus correlation length for various sampling locations at high consequence level ($p_{max} = 1/1,000$) for $v_E = 0.3$ at SLS

The overall change in the consequence factor in Figure 4.7 with respect to correlation length and sampling location ranges from about 1.05 to 1.09, which is about a 4% relative change. Similarly, in Figure 4.8, the overall change in consequence factor is from about 0.926 to 0.96, which is about a 3.5% relative change. Similar to the ULS case, these two plots demonstrate that the consequence factor is little affected by soil parameters, at least for $v_E \leq 0.3$, particularly when $r = 0$ m.

4.6   RECOMMENDED CONSEQUENCE FACTORS

Tables 4.1 and 4.2 present the recommended consequence values for design of deep foundations at ULS and SLS respectively, determined according to the methodology suggested in Sections 2 and 3 over the various parameter ranges considered in this work using the worst case correlation lengths and a moderate sampling distance.

For the low consequence level, it is evident that the consequence factors range from 1.06 to 1.18 at ULS and from 1.04 to 1.08 at SLS. Lower consequence factors lead to lower failure probabilities (see Figure 4.4, for example) and therefore are more conservative, hence a value of 1.1 would be reasonably conservative for ULS and possibly slightly unconservative for SLS. For the high consequence level, the consequence factor ranges from 0.94 to 0.98 at ULS and from 0.93 to 0.96 at SLS. A conservative consequence factor for the high consequence level would thus be about 0.9 for both ULS and SLS.

Table 4.1 Consequence factors at ULS at worst case correlation length and $r = 4.5$ m (moderate site understanding)

$\theta_{\ln E}$(m)	v_c	Consequence Factor Ψ_u	
		$p_f = 1/1,000$ (low)	$p_f = 1/10,000$ (high)
0	0.1	1.06	0.98
0	0.2	1.06	0.98
0	0.3	1.06	0.98
0	0.4	1.06	0.98
0	0.5	1.06	0.98
5	0.1	1.07	0.97
5	0.2	1.08	0.97
5	0.3	1.1	0.96
5	0.4	1.12	0.96
5	0.5	1.14	0.95
10	0.1	1.07	0.97
10	0.2	1.09	0.97
10	0.3	1.12	0.96
10	0.4	1.15	0.95
10	0.5	1.18	0.94

It is instructive to consider the values used by other codes to handle failure consequences. Most codes include an importance factor, I, which is (at least mathematically) the inverse of the consequence factor since it is applied to the load side of the LRFD equation (see eq. 1.13). Table 4.3 compares the consequence factors recommended above (0.9 for high consequence and 1.1 for low consequence levels) to the inverse of the importance factor from a variety of other codes. The low consequence level value of Ψ_s recommended in this study (1.1) is the most conservative, but is similar to the value appearing in the Eurocode. At the high consequence level, however, this study recommends a consequence factor of $\Psi = 0.9$ which is comparable to Eurocode and AASHTO but is less conservative than the values appearing in Australian and Canadian codes.

Table 4.2 Consequence factors at SLS at worst case correlation length and $r = 5$ m (moderate site understanding)

$\theta_{\ln E}$(m)	v_c	$p_f = 1/100$ (low)	$p_f = 1/1,000$ (high)
		Consequence Factor Ψ_s	
0	0.1	1.04	0.96
0	0.2	1.05	0.95
0	0.3	1.06	0.95
0	0.4	1.07	0.94
0	0.5	1.07	0.94
5	0.1	1.05	0.95
5	0.2	1.07	0.94
5	0.3	1.08	0.94
5	0.4	1.08	0.93
5	0.5	1.09	0.77
10	0.1	1.05	0.96
10	0.2	1.07	0.94
10	0.3	1.08	0.94
10	0.4	1.08	0.94
10	0.5	1.08	0.8

Table 4.3 Comparison of consequence factors recommended in this research to equivalent $(1/I)$ values recommended in other codes at ULS

Source	Low	Typical	High
	Consequence Level		
Recommended in this research	1.1	1.0	0.90
AASHTO (2007)	1.25	1.0	0.91
Australian Standard (AS5100, 2004)	–	1.0	0.83
Eurocode 1 (Gulvanessian 2002)	1.11	1.0	0.91
NBCC (NRC, 2005, snow and wind)	1.25	1.0	0.87
NBCC (NRC, 2005, earthquake)	1.25	1.0	0.77

4.7 DISCUSSION

The consequence factors recommended in this work, which are 0.9 for high failure consequence, 1.0 for typical failure consequences, and 1.1 for low failure consequence levels, are in basic agreement with the importance factors employed by other codes world-wide. These values appear reasonable and are generally conservative, except perhaps for SLS and high levels of soil variability. More detailed values can be obtained from Tables 4.1 and 4.2, which were developed assuming a moderate sampling distance and worst case correlation length.

Interestingly, the investigation shows that consequence factors are largely independent of limit states even though the target maximum failure probabilities for serviceability limit states are greater than those for ultimate limit states. For example, a typical geotechnical system might have a target maximum lifetime failure probability of $1/5,000$ for ultimate limit states, but only $1/300$ for serviceability limit states. If the geotechnical system has high failure consequences, the lifetime maximum acceptable failure probability might decrease by the same fraction, i.e. to $1/10,000$ for ULS and to $1/1,000$ for SLS. Therefore the same (or similar) consequence factor can be used to scale the target maximum acceptable failure probability for both ULS and SLS designs since the probabilities scale by the same amount.

CHAPTER 5

REDUNDANCY IN DEEP FOUNDATION DESIGN

5.1   GENERAL

System redundancy generally increases system reliability, which means that individual elements (e.g. piles) need not be designed to the same level of reliability if it is known that failure of individual piles will not result in system failure. In other words, if the load is distributed amongst a number of piles, redundancy should be accounted for to achieve construction savings while maintaining overall safety.

All systems are made up of one or more components, and the reliability of a system largely depends on the reliability of the individual components. Thus, it is necessary to first identify the components that make up a system, and how they individually contribute to system reliability. The next step is to establish the distribution of the individual component reliabilities from which reliability of the system is computed.

The main goal of this chapter is to investigate the relationship between number of piles and system reliability for various resistance statistics and various levels of dependency between piles.

5.2   METHODOLOGY

Piles are often used in groups and are connected at the top by a pile cap. A pile system consisting of n_p piles is considered here, which supports the total vertical load F_T. Practically speaking, the following three senarios can be considered when reliability of a pile system is of concern:

Approach 1) The supported structure is somewhat flexible, so that when a pile is displaced past its ultimate capacity, its load is distributed amongst the remaining piles (load sharing). System failure occurs when all piles are loaded beyond their ultimate capacities.

Approach 2) The supported structure is rigid, in which case the piles are all displaced equally by the applied total load. This implies that the foundation reaction is purely the sum of the individual pile resistances, where the resistance of each pile depends on its common imposed displacement.

Approach 3) Piles act independently and are loaded independently. It is assumed in this case that the supported structural performance is lost (system failure) if any of the piles fail. System failure thus occurs if one or more piles fail, i.e,

$$p_f = \mathrm{P}\left[F_T/n_p \geq \min_i R_i \right] \tag{5.1}$$

where R_i is the resistance provided by the ith pile. Since this approach does not involve any redundancy, it will not be considered further in this research. Therefore, only the first two approaches are investigated in detail here.

5.2.1   Approach 1

Assuming that F is the event corresponding to failure of the pile system, then

$$F = \{F_1 \cap F_2 \cap ... \cap F_{n_p}\} \tag{5.2}$$

That is, the failure of the pile system occurs only if all of its elements fail, where F_i denotes the failure of the ith pile, $i = 1, .., n_p$. Thus, the failure probability of the pile system can be computed using the multiplication rule as

$$p_f = P[F] = P\left[F_1 \cap F_2 \cap ... \cap F_{n_p}\right]$$
$$= P[F_1] \, P\left[F_2 \mid F_1\right] \, P\left[F_3 \mid F_1 \cap F_2\right] ...P\left[F_{n_p} \mid F_1 \cap F_2 \cap ... \cap F_{n_p-1}\right] \quad (5.3)$$

Assuming that R_i is the resistance provided by i^{th} pile, then

$$P[F_i] = P\left[R_i < F_T/n_p\right] \quad (5.4)$$

where all piles are assumed to have the same resistance distribution (with the same mean and variance).

The first probability in eq. (5.3) is calculated as follows. Assuming that the lognormal distribution is the appropriate distribution to represent both load and resistance, then the probability that the first pile fails under load F_T/n_p is

$$P[F_1] = P\left[R_1 < F_T/n_p\right] = P\left[n_p R_1/F_T < 1\right]$$
$$= P\left[\ln(n_p R_1/F_T) < 0\right] = P\left[\ln Z_1 < 0\right]$$
$$= \Phi\left(\frac{-\mu_{\ln Z_1}}{\sigma_{\ln Z_1}}\right) \quad (5.5)$$

where

$$Z_1 = n_p R_1/F_T \quad (5.6)$$

is lognormally distributed so that

$$\ln Z_1 = \ln(n_p) + \ln R_1 - \ln F_T \quad (5.7)$$

is normally distributed with mean and variance

$$\mu_{\ln Z_1} = \ln(n_p) + \mu_{\ln R} - \mu_{\ln F_T} \quad (5.8a)$$

$$\sigma_{\ln Z_1}^2 = \sigma_{\ln R}^2 + \sigma_{\ln F_T}^2 = \ln(1 + v_R^2) + \ln(1 + v_T^2) \tag{5.8b}$$

assuming independence between load and resistance. $v_R = \sigma_R/\mu_R$ and $v_T = \sigma_T/\mu_T$ are the coeficients of variation of R_1 and F_T respectively.

One simple way to introduce dependence between piles is to assume that they share the load F_T equally, but otherwise fail independently. This means that if one pile fails, the other $n_p - 1$ piles share the load $F_T/(n_p - 1)$. The second probability in eq. (5.3) corresponds to the case that a pile fails given that another pile has already failed. In this case, the total load F_T is assumed supported by, and distributed amongst the remaining $n_p - 1$ piles, so that

$$
\begin{aligned}
\mathrm{P}\left[F_2 \mid F_1\right] &= \mathrm{P}\left[R_2 < F_T/(n_p - 1)\right] = \mathrm{P}\left[(n_p - 1)R_2/F_T < 1\right] \\
&= \mathrm{P}\left[\ln((n_p - 1)R_2/F_T) < 0\right] = \mathrm{P}\left[\ln Z_2 < 0\right] \\
&= \Phi\left(\frac{-\mu_{\ln Z_2}}{\sigma_{\ln Z_2}}\right)
\end{aligned} \tag{5.9}
$$

where

$$Z_2 = (n_p - 1)R_2/F_T \tag{5.10}$$

is lognormally distributed so that

$$\ln Z_2 = \ln(n_p - 1) + \ln R_2 - \ln F_T \tag{5.11}$$

is normlly distributed with mean

$$\mu_{\ln Z_2} = \ln(n_p - 1) + \mu_{\ln R} - \mu_{\ln F_T} \tag{5.12}$$

and variance as given by eq. (5.8b). In general, the probability that a pile fails given that $i - 1$ piles have already failed is given by

$$
\begin{aligned}
\mathrm{P}\left[F_i \mid F_1 \cap ... \cap F_{i-1}\right] &= \mathrm{P}\left[R_i < F_T/(n_p - i + 1)\right] = \mathrm{P}\left[(n_p - i + 1)R_i/F_T < 1\right] \\
&= \mathrm{P}\left[\ln((n_p - i + 1)R_i/F_T) < 0\right] = \mathrm{P}\left[\ln Z_i < 0\right]
\end{aligned}
$$

$$= \Phi \left(\frac{-\mu_{\ln Z_i}}{\sigma_{\ln Z_i}} \right) \tag{5.13}$$

where

$$Z_i = (n_p - i + 1)R_i/F_T \tag{5.14}$$

is lognormal so that

$$\ln Z_i = \ln(n_p - i + 1) + \ln R_i - \ln F_T \tag{5.15}$$

is normal with mean

$$\mu_{\ln Z_i} = \ln(n_p - i + 1) + \mu_{\ln R} - \mu_{\ln F_T} \tag{5.16}$$

and variance as given by eq. (5.8b).

Substituting eq. (5.13) into eq. (5.3) results in

$$p_f = P[F] = \prod_{i=1}^{n_p} \Phi \left(\frac{-\mu_{\ln Z_i}}{\sigma_{\ln Z_i}} \right) \tag{5.17}$$

Once the probability of the system failure is determined, the number of piles, n_p, to achieve a certain target failure probability, p_{max}, can be found using root-finding algorithms, such as one-point iteration or bisection, to find the root of

$$p_{max} - \prod_{i=1}^{n_p} \Phi \left(\frac{-\mu_{\ln Z_i}}{\sigma_{\ln Z_i}} \right) = 0 \tag{5.18}$$

Similarly, for a given p_{max}, n_p, v_R, v_T, and μ_T, the required individual pile resistance, μ_R, can be found by using the bisection algorithm to solve for the required $\mu_{\ln R}$ in eq. (5.18) combined with eq. (5.16). Finally, required pile resistance, μ_R, can be found using the following transformation,

$$\mu_R = e^{\mu_{\ln R}} \sqrt{1 + v_R^2} \tag{5.19}$$

For a pile system consisting of n_p piles, the system reliability index, β_{sys} is defined as

$$\beta_{sys} = \Phi^{-1}(1 - p_{max}) = -\Phi^{-1}(p_{max}) \tag{5.20}$$

where p_{max} is the target failure probability. For a given β_{sys}, the reliability index for an indivicual pile, β_i can be obtained by first finding required n_p or $\mu_{\ln R}$ for given p_{max}, using the methods described above, then calculating individual pile failure using eq. (5.4), and finally

$$\beta_i = -\Phi^{-1}(\mathrm{P}\,[F_i]) \tag{5.21}$$

5.2.2 Approach 2

If the supported structure is rigid, then any displacement of the structure involves equal displacement of each pile. This means that the resistance provided by each pile is obtained from its load-displacement curve at a given common displacement. Each pile will have a different load-displacement curve due to variations in soil property, installation procedures, etc, so that the resistance provided by each pile will be a random variable. Let R_i be the resistance provided by the ith pile at the displacement imposed by the structure, so that the total resistance will be

$$R = \sum_{i=1}^{n_p} R_i \tag{5.22}$$

The problem now is to determine the distribution of R_i. General approaches are to statistically analyze individual pile tests and develop distribution fits. When pile groups are involved, correlation between piles can affect the overall pile system resistance. This phenomenon is typically handled by using the individual pile test results to develop the distributions and introducing a system efficiency factor, which adjusts the overall pile system resistance to account for this correlation. The total resistance thus becomes

$$R = \xi \sum_{i=1}^{n_p} R_i \tag{5.23}$$

where ξ is a system efficiency factor (typically ≤ 1), and is defined as the ratio of the ultimate resistance of a pile system to the sum of the resistances of the individual piles. The

failure probability of the pile system is calculated as

$$p_f = \mathrm{P}\left[F_T > \xi \sum_{i=1}^{n_p} R_i\right] = \mathrm{P}\left[F_T - \xi \sum_{i=1}^{n_p} R_i > 0\right] \tag{5.24}$$

Since sums of random variables tend to the normal distribution by the central limit theorem, the sum of individual resistance will be at least approximately normal. For simplicity, it will be assumed that the total load (also being a sum of individual structural loads) is also at least approximately normal. This means that the quantity $Y = F_T - \xi \sum_{i=1}^{n_p} R_i$ is normally distributed with mean and variance

$$\mu_Y = \mu_T - \xi n_p \mu_R \tag{5.25a}$$

$$\sigma_Y^2 = \sigma_T^2 + \xi^2 n_p \sigma_R^2 \tag{5.25b}$$

so that

$$p_f = \mathrm{P}\left[Y > 0\right] = 1 - \Phi\left(\frac{-\mu_Y}{\sigma_Y}\right) = \Phi\left(\frac{\mu_Y}{\sigma_Y}\right) \tag{5.26}$$

Eq. (5.25b) assumes that the individual pile resistances are uncorrelated. In general, this will not be true, and leads to a variance which is lower than if the pile resistances are positively correlated. The upper bound on σ_Y^2 is $\sigma_T^2 + \xi^2 n_p^2 \sigma_R^2$. The implication of correlation between piles has been discussed previously in this section and has been assumed to be handled by the system efficiency factor. Thus, it will be assumed here that the pile resistances are uncorrelated.

For a given target maximum failure probability, p_{max}, the required number of piles, n_p, can be found by solving

$$p_{max} - \Phi\left(\frac{\mu_T - \xi n_p \mu_R}{\sqrt{\sigma_T^2 + \xi^2 n_p \sigma_R^2}}\right) = 0 \tag{5.27}$$

for n_p. Alternatively, eq. (5.27) can be solved for μ_R, for a given p_{max} and n_p, to find the required individual pile resistance to achieve a given p_{max}. Once n_p or μ_R are obtained for a certain p_{max} associated with system reliability $\beta_{sys} = -\Phi^{-1}(p_{max})$, then the individual pile failure probability and in turn the individual pile reliability, β_i, can be found from

$$p_{f_i} = \mathrm{P}\left[F_T/n_p > R_i\right] = \mathrm{P}\left[F_T/n_p - R_i > 0\right] = \Phi\left(\frac{\mu_T/n_p - \mu_R}{\sqrt{\sigma_T^2/n_p^2 + \sigma_R^2}}\right) = \Phi(-\beta_i) \tag{5.28}$$

5.3 RESULTS

Figures 5.1 and 5.2 show the effect of target failure probability, p_{max} on the required number of piles, for μ_T = 50 kN, v_T = 0.1, v_R = 0.3 and for three different mean resistances, using both approaches. As expected, a higher number of piles is required to support the applied load as the mean resistance reduces.
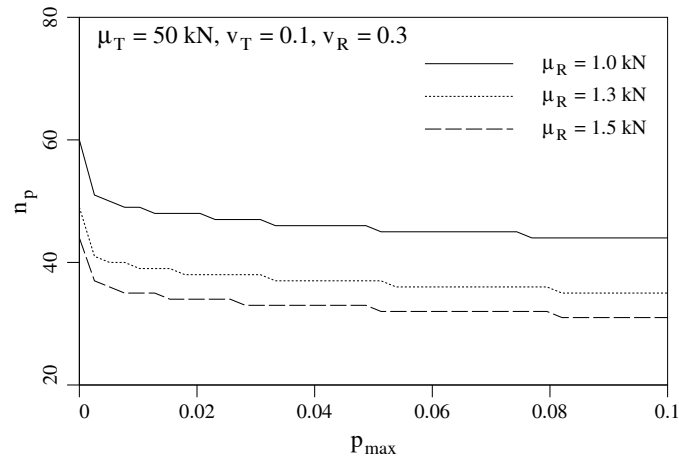
Figure 5.1   Plot of n_p versus p_{max} for $\mu_T = 50$ kN, $v_T = 0.1$, and $v_R = 0.3$, and various mean resistance values $\mu_R = 1.0$, 1.3, and 1.5 kN, generated by eq. (5.18) for approach 1
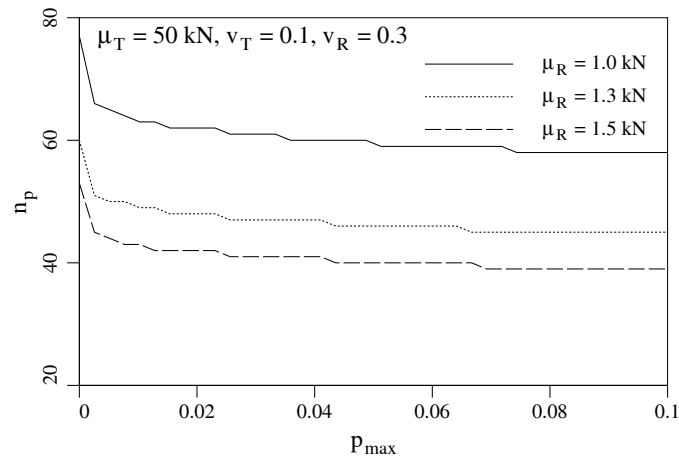
Figure 5.2   Plot of n_p versus p_{max} for $\mu_T = 50$ kN, $v_T = 0.1$, and $v_R = 0.3$, and various mean resistance values $\mu_R = 1.0$, 1.3, and 1.5 kN, generated by eq. (5.27) for approach 2 ($\xi = 1.0$)

Figure 5.2 indicates that using approach 2 with $\xi = 1$, a higher number of piles is required

to support the applied load on the system at a given reliability, and hence is a relatively conservative approach. Note that the discontinuities appearing in Figures 5.1 and 5.2 are due to the fact that n_p is a whole number.

The effect of number of piles on system failure probability is depicted in Figures 5.3 and 5.4 for $\mu_T = 50$ kN, $v_T = 0.1$, and $v_R = 0.3$, and various mean resistances, for the two approaches. When compared to Figure 5.3, Figure 5.4 demonstrates the need for a higher number of piles to support the applied (random) load, in agreement with Figures 5.1 and 5.2.

Figure 5.3 Plot of p_f versus n_p for $\mu_T = 50$ kN, $v_T = 0.1$, and $v_R = 0.3$, and various mean resistance values $\mu_R = 1.0$, 1.3, and 1.5 kN, generated by eq. (5.17) using approach 1
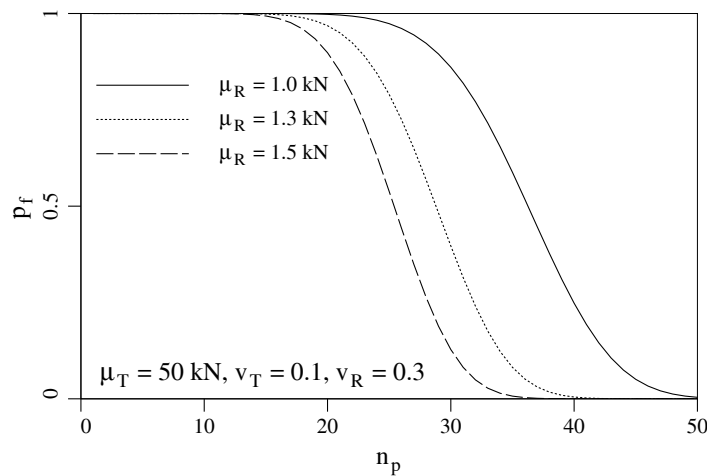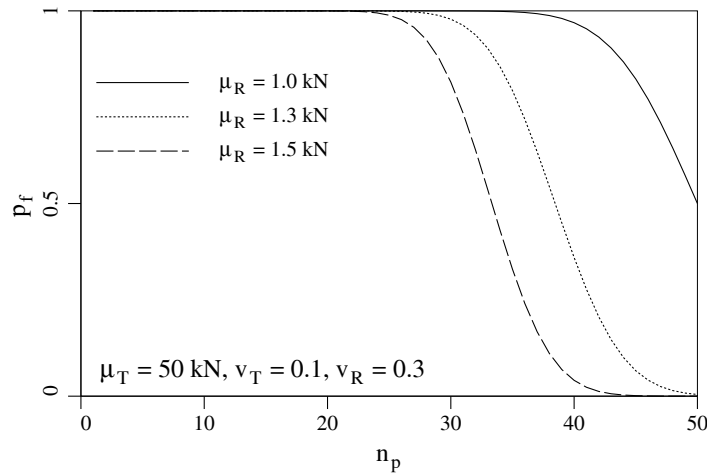
Figure 5.4   Plot of p_f versus n_p for $\mu_T = 50$ kN, $v_T = 0.1$, and $v_R = 0.3$, and various mean resistance values $\mu_R = 1.0$, 1.3, and 1.5 kN, generated by eq. (5.26) using approach 2 ($\xi = 1.0$)

As discussed previously, eq's. (5.18) and (5.19) in approach 1, and eq. (5.27) in approach 2, can be used to find the required mean resistance, μ_R, for a given number of piles, n_p, to achieve a target system reliability, p_{max}. Figures 5.5 and 5.6 show such calculations obtained for various target failure probabilities and number of piles for both approaches. The results indicate a steep reduction in required resistance, μ_R, in the range $1 < n_p < 5$ piles, and less steep reduction in μ_R for $n_p \geq 5$ piles. Figure 5.6 suggests higher resistance required for individual piles at a given number of piles in the system, relative to Figure 5.5.
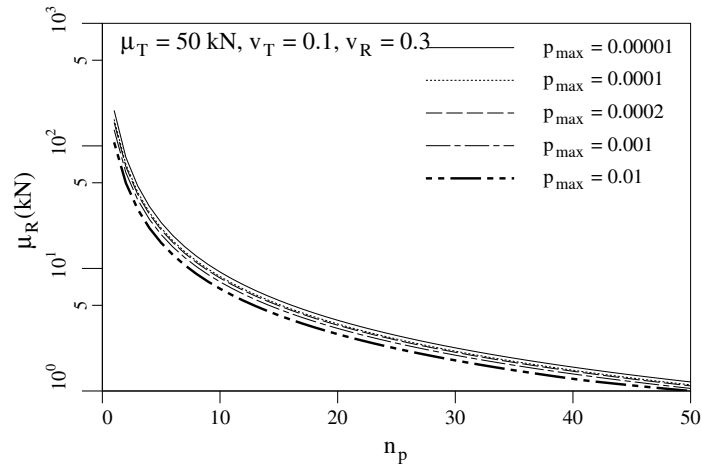
Figure 5.5 Plot of μ_R versus n_p for $\mu_T = 50$ kN, $v_T = 0.1$, and $v_R = 0.3$, and various target failure probabilities, p_{max}, generated by eq's. (5.18) and (5.19) using approach 1
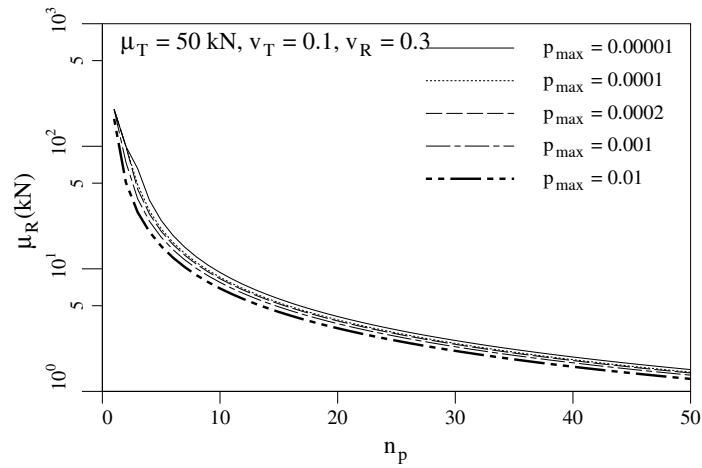
Figure 5.6 Plot of μ_R versus n_p for $\mu_T = 50$ kN, $v_T = 0.1$, and $v_R = 0.3$, and various target failure probabilities, p_{max}, generated by eq. (5.27) using approach 2 ($\xi = 1.0$)

Figures 5.7 and 5.8 illustrate how the reliability of individual piles, β_i, relates to the system

reliability, β_{sys}. For a given μ_T, v_T, v_R, and n_p, β_i is determined in Figure 5.7 by solving

eq. (5.18) for $\mu_{\ln R}$, finding μ_R via eq. (5.19), and finally calculating β_i using eq. (5.21).

Similarly, β_i values in Figure 5.8 are obtained by first solving eq. (5.27) for μ_R, for a given

μ_T, v_T, v_R, and n_p, and then calculating β_i via eq. (5.28). These figures can be used for design

by drawing a vertical line at the target system reliability index, β_{sys}, and then reading off

the required β_i for a given n_p. For example, for a moderate system reliability $\beta_{sys} = 3.5$

corresponding to $p_f = 1/5,000$ using approach 1, the required single pile reliability index

ranges from $\beta_i = 0.9$ for $n_p = 20$ to 2.15 for $n_p = 5$, which corresponds to individual pile

failure probabilities ranging from $p_f = 0.016$ to 0.18. Approach 2 recommends similar but

a narrower range for β_i (between 1.1 and 1.7) as shown in Figure 5.8.
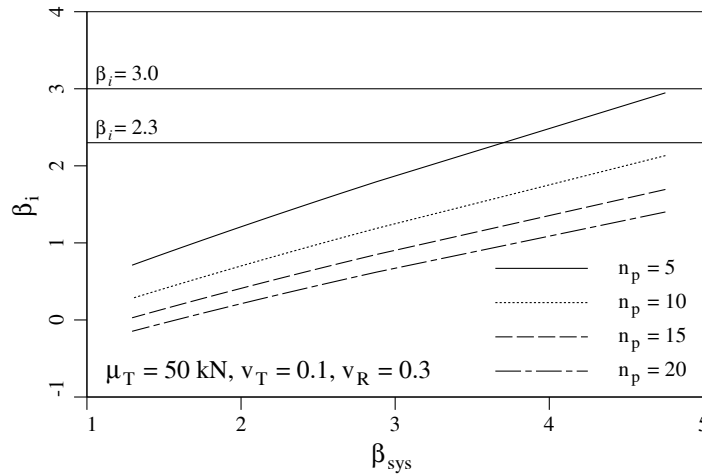
Figure 5.7   Plot of β_i versus β_{sys} for $\mu_T = 50$ kN, $v_T = 0.1$, and $v_R = 0.3$, and various number of piles, n_p, generated by eq's. (5.18), (5.19), and (5.21) using approach 1

Figure 5.9 compares the two approaches in terms of required individual reliability index,

β_i, recommended for a given target reliability index β_{sys}. It is observed that the values

generated by approach 2 with $\xi = 1$ fall inside the range generated by approach 1.
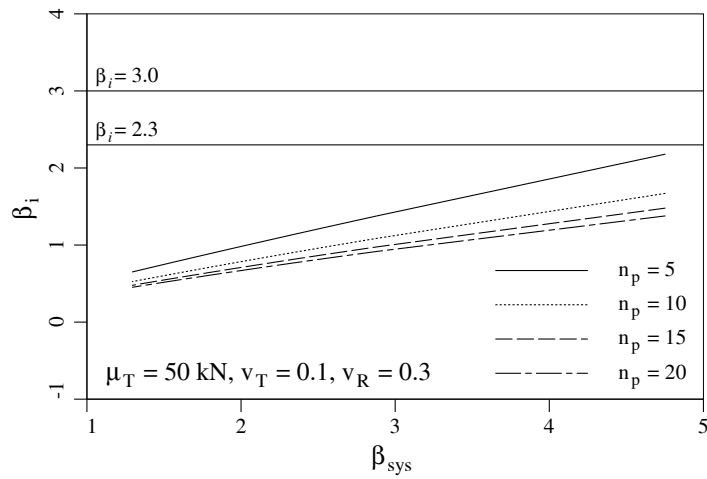
Figure 5.8 Plot of β_i versus β_{sys} for $\mu_T = 50$ kN, $v_T = 0.1$, and $v_R = 0.3$, and various number of piles, n_p, generated by eq's. (5.27) and (5.28) using approach 2 ($\xi = 1$)
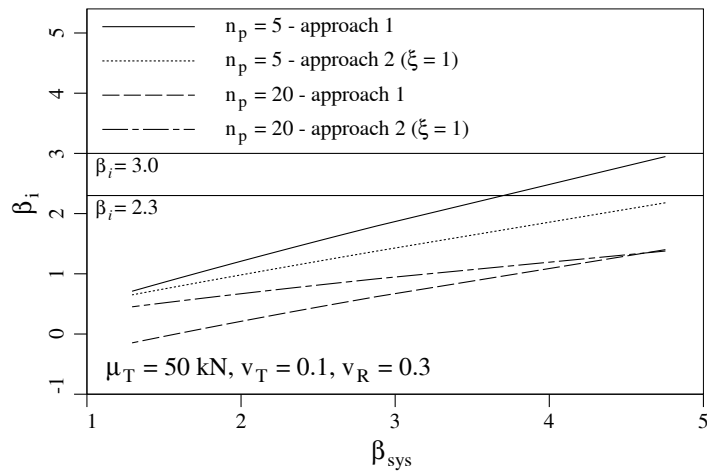
Figure 5.9 Comparison of two approaches in terms of β_i versus β_{sys} for $n_p = 5$ and 20 and $\xi = 1$

In general, a reliability index of $\beta_i = 3.0$ ($p_f = 1/1,000$) is prescribed in geotechnical design practice to target the design of an individual pile in non-redundant pile systems

($n_p \leq 4$), and $\beta_i = 2.3$ ($p_f = 1/100$) for redundant pile systems ($n_p \geq 5$) (Zhang et al. 2001, Paikowsky et al., NCHRP, 2004, Allen 2005, and Barker et al., NCHRP, 1991). According to Zhang et al. (2001), a β_{sys} value of 3.0 requires a $\beta_i = 2.0$ to 2.8. Figure 5.9 gives a $\beta_i = 0.7$ to 1.9 for $\beta_{sys} = 3.0$, when n_p ranges from 5 to 20 over both approaches. Evidently, Zhang et al. (2001) results are more conservative than suggested here. It is not possible to carefully investigate the cause of the discrepancy because Zhang et al. (2001) do not clearly describe their model. It is felt that perhaps some of the difference is due to natural tendencies towards conservatism in designing individual piles and to the fact that piles do not actually fail independently. More research is required to investigate the effects of correlation between pile resistances.

CHAPTER 6

DIFFERENTIAL SETTLEMENT OF DEEP FOUNDATIONS

6.1 GENERAL

Geotechnical foundations are typically governed by serviceability limit states (SLS), usually relating to settlement, rather than by ultimate limit states (ULS), which relate to safety. Most modern geotechnical design codes state that the serviceability limit state can be avoided by designing each foundation to settle by no more than a specified maximum tolerable settlement, δ_{max}. However, in the case of foundations, it is usually differential settlements which governs the serviceability of the supported structure. For example, if all of the foundations of a supported structure settle equally, but excessively, then the approaches to the structure will have to be modified, but the structure itself will not suffer from either a loss of serviceability nor from a loss of safety.

With probability 1, individual foundations will not settle equally and the differential settlement between foundations can lead to loss of serviceability and even catastrophic ultimate limit state failure in the supported structure. So the question is, how should differential settlement between foundations be properly accounted for in the foundation design process?

Design code provisions should be kept as simple as possible, while still achieving a target reliability with respect to both serviceability and ultimate limit states. This means that design codes should retain their requirements regarding the maximum settlement of individual foundations but that the specified maximum settlements should be reviewed to confirm

that the resulting differential settlements do not result in achieving either serviceability or ultimate limit states in the supported structure.

This chapter investigates in detail how the maximum settlement specified in a design code for an individual foundation relates to the distribution of the differential settlement between two foundations, as a function of the ground statistics and the distance between the two foundations. This chapter will suggest design code requirements on maximum settlements for individual foundations which aim to achieve target reliabilities against excessive differential settlements between foundations.

The remainder of this chapter is organized as follows: In Section 2, a theoretical approach to estimating the differential pile settlement is developed, and the parameters of differential settlement distribution are validated via simulation. Design code recommendations are then presented in Section 3.

6.2 METHODOLOGY

Settlement of a single pile, which has been studied in depth in Chapter 3, is highly dependent on elastic properties of the surrounding soil, as well as on pile geometry. However, when settlement of pile groups is of interest, mechanical interaction between piles plays an important role.

Two neighboring piles of identical geometry, supporting loads F_{T_1} and F_{T_2} and separated by distance s are considered, as depicted in Figure 6.1. If δ'_1 is the settlement of a vertically loaded individual pile, and δ_1 is the overall settlement of the pile due to its loading and also due to settlement of the neighboring pile, δ'_2, then

$$\delta_1 = \delta'_1 + \eta\delta'_2 \qquad (6.1)$$

where η is the mechanical interaction factor between the two piles, which is a function of pile spacing and pile length. Rearranging eq. (6.1) and solving for η gives

$$\eta = \frac{\delta_1 - \delta_1'}{\delta_2'} \qquad (6.2)$$
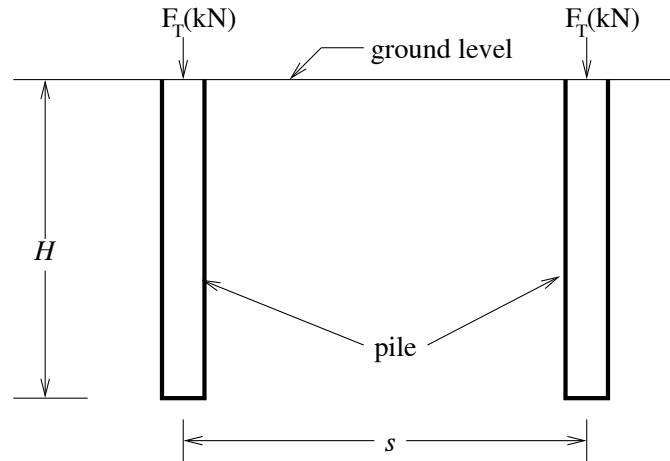
Figure 6.1   Relative location of two piles

Figure 6.2 demonstrates the finite element (Smith and Griffiths, 2004) prediction of η for various pile lengths, $H = 2, 4$, and 8 m and a wide range of s/d, between 2 and 30, where s is the center-to-center pile spacing and d is the pile diameter. It is evident that η increases with increasing pile length, H, and decreases with increasing s/d, as expected.

Assuming that the lognormal is a reasonable distribution type for pile settlement, as mentioned previously in Chapter 3, and that δ_1 and δ_2 are settlements of the two piles, then δ_1 and δ_2 are identically and lognormally distributed random variables. The differential settlement between two piles is defined here as $\Delta = \delta_1 - \delta_2$. If the elastic modulus field is statistically stationary, as assumed here, then the mean differential settlement, μ_Δ, is zero. The mean absolute differential settlement, can be approximated as
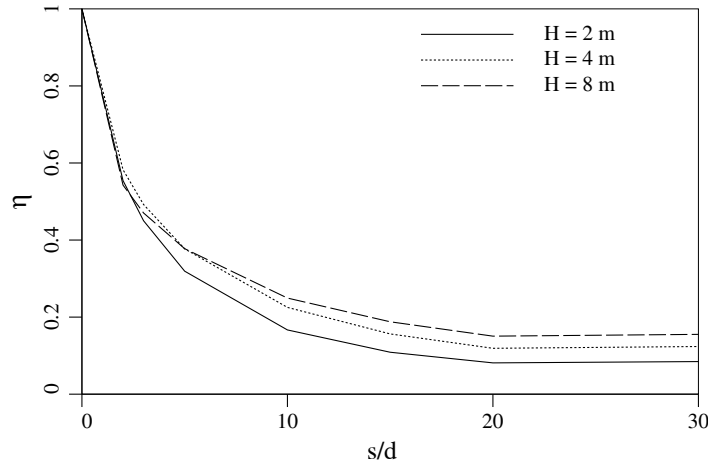
Figure 6.2 Plot of interaction factor, η, using FE model for $\hat{F}_T = 2.16$ MN, $k = 700$, $\nu = 0.3$, and $E_s = 30$ MPa

$$\mu_{|\Delta|} \simeq \sqrt{\frac{2}{\pi}}\,\sigma_\Delta \tag{6.3}$$

which indicates that the mean of the absolute differential settlement is directly related to the standard deviation of Δ, and hence related to the correlation between the elastic moduli surrounding the piles, and the variability of the elastic moduli. The approximation in eq. (6.3) is exact if Δ is normally distributed (Papoulis, 1991), and as will be shown shortly, this approximation is in reasonable agreement with simulation based results.

As mentioned previously in Chapter 1, the effective elastic modulus field seen by a pile of length H, E_g, is a geometric average of the soil surrounding the pile, and is given by eq. (1.49) in the three-dimentional case, from which the settlement of a single pile can be expressed as

$$\delta_i' = \delta_{det}\left(\frac{\mu_E}{E_g}\right)\left(\frac{F_{T_i}}{\mu_T}\right) \tag{6.4}$$

where δ_{det} is the deterministic settlement obtained from a single finite element analysis of the problem using $F_T = \mu_F$ and $E = \mu_E$ everywhere.

Substituting eq. (6.4) into eq. (6.1) leads to pile settlements δ_1 and δ_2 for the two piles as follows

$$\delta_1 = \delta_{det}\left(\frac{\mu_E}{\mu_T}\right)\left(\frac{F_{T_1}}{E_{g_1}} + \frac{\eta F_{T_2}}{E_{g_2}}\right) \tag{6.5a}$$

$$\delta_2 = \delta_{det}\left(\frac{\mu_E}{\mu_T}\right)\left(\frac{F_{T_2}}{E_{g_2}} + \frac{\eta F_{T_1}}{E_{g_1}}\right) \tag{6.5b}$$

Therefore, the differential settlement, Δ, between two piles becomes

$$\Delta = \delta_{det}(1 - \eta)\left(\frac{\mu_E}{\mu_T}\right)\left(\frac{F_{T_1}}{E_{g_1}} - \frac{F_{T_2}}{E_{g_2}}\right) \tag{6.6}$$

The variance of Δ is therefore

$$\sigma_\Delta^2 = \delta_{det}^2(1 - \eta)^2\left(\frac{\mu_E}{\mu_T}\right)^2 \text{Var}\left[\frac{F_{T_1}}{E_{g_1}} - \frac{F_{T_2}}{E_{g_2}}\right] \tag{6.7}$$

where

$$\text{Var}\left[\frac{F_{T_1}}{E_{g_1}} - \frac{F_{T_2}}{E_{g_2}}\right] = \text{Var}\left[\frac{F_{T_1}}{E_{g_1}}\right] + \text{Var}\left[\frac{F_{T_2}}{E_{g_2}}\right] - 2\,\text{Cov}\left[\frac{F_{T_1}}{E_{g_1}}, \frac{F_{T_2}}{E_{g_2}}\right] \tag{6.8}$$

Now let $X_i = F_{T_i}/E_{g_i}$, $i = 1, 2$, where both F_{T_i} and E_{g_i} are independent and lognormally distributed then X_i is lognormally distributed, and thus $\ln X_i = \ln F_{T_i} - \ln E_{g_i}$ is normally distributed with parameters (see eq's. (1.55b) and (3.22))

$$\mu_{\ln X_i} = \mu_{\ln F_{T_i}} - \mu_{\ln E_g} = \mu_{\ln F_T} - \mu_{\ln E}$$
$$= \ln(\mu_T) - \frac{1}{2}\sigma_{\ln F_T}^2 - \ln(\mu_E) + \frac{1}{2}\sigma_{\ln E}^2 \tag{6.9a}$$

$$\sigma_{\ln X_i}^2 = \sigma_{\ln F_T}^2 + \sigma_{\ln E_g}^2 = \sigma_{\ln F_T}^2 + \sigma_{\ln E}^2\gamma(V_p) \tag{6.9b}$$

where $\gamma(V_p)$ is a three-dimensional variance reduction function over volume $V_p = B_p \times B_p \times C$ surrounding the piles, and given by eq. (1.40).

The distribution parameters of X_i now can be obtained from the mean and standard deviation of $\ln X_i$ using the following transformations

$$\mu_{X_i} = \exp\{\mu_{\ln X_i} + \frac{1}{2}\sigma_{\ln X_i}^2\} \tag{6.10a}$$

$$\sigma_{X_i}^2 = \mu_{X_i}^2 (e^{\sigma_{\ln X_i}^2} - 1) \qquad (6.10b)$$

Using eq.'s (6.9a) and (6.9b) in eq.'s (6.10a) and (6.10b) re sults in

$$\mu_{X_i} = E\left[\frac{F_{T_i}}{E_{g_i}}\right] = \exp\left\{\ln(\mu_T) - \frac{1}{2}\sigma_{\ln F_T}^2 - \ln(\mu_E) + \frac{1}{2}\sigma_{\ln E}^2 + \frac{1}{2}\sigma_{\ln E}^2 \gamma(V_p)\right\}$$

$$= \mu_T \sqrt{(1 + v_E^2)^{\gamma(V_p)+1}} / \mu_E \qquad (6.11a)$$

$$\sigma_{X_i}^2 = \text{Var}\left[\frac{F_{T_i}}{E_{g_i}}\right] = \left(\mu_T^2 (1 + v_E^2)^{\gamma(V_p)+1} / \mu_E^2\right) \left(\exp\{\sigma_{\ln F_T}^2 + \sigma_{\ln E}^2 \gamma(V_p)\} - 1\right)$$

$$= \mu_T^2 (1 + v_E^2)^{\gamma(V_p)+1} \left((1 + v_T^2)(1 + v_E^2)^{\gamma(V_p)} - 1\right) / \mu_E^2 \qquad (6.11b)$$

where $v_E = \sigma_E / \mu_E$ is the coefficient of variation of the elastic modulus field, E.

The covariance between two lognormal random variables $X_1 = F_{T_1}/E_{g_1}$ and $X_2 = F_{T_2}/E_{g_2}$ can be computed as

$$\text{Cov}\,[X_1, X_2] = \text{Cov}\left[\frac{F_{T_1}}{E_{g_1}}, \frac{F_{T_2}}{E_{g_2}}\right] = \sigma_{X_i}^2 \,\rho_X \qquad (6.12)$$

where $\sigma_{X_i}^2$ is given by eq. (6.11b), the correlation coefficient, ρ_X, comes from the transformation (Fenton and Griffiths, 2008)

$$\rho_X = \frac{\exp\{\text{Cov}\,[\ln X_1, \ln X_2]\} - 1}{\exp\{\sigma_{\ln X_i}^2\} - 1} \qquad (6.13)$$

and $\sigma_{\ln X_i}^2$ is defined by eq. (6.9b). In addition

$$\text{Cov}\,[\ln X_1, \ln X_2] = \text{Cov}\left[\ln F_{T_1} - \ln E_{g_1}, \ln F_{T_2} - \ln E_{g_2}\right]$$

$$= E\left[(\ln F_{T_1} - \ln E_{g_1})(\ln F_{T_2} - \ln E_{g_2})\right]$$

$$= E\left[\ln F_{T_1} \ln F_{T_2}\right] + E\left[\ln E_{g_1} \ln E_{g_2}\right]$$

$$= \text{Cov}\left[\ln F_{T_1}, \ln F_{T_2}\right] + \text{Cov}\left[\ln E_{g_1}, \ln E_{g_2}\right]$$

$$\simeq \sigma_{\ln F_T}^2 \rho_{\ln F_T} + \sigma_{\ln E}^2 \gamma_{V_p V_p} \qquad (6.14)$$

where $\rho_{\ln F_T}$ is given by

$$\rho_{\ln F_T} = \frac{\ln(1 + \rho_{F_T} v_T^2)}{\ln(1 + v_T^2)} = \frac{\ln(1 + \rho_{F_T} v_T^2)}{\sigma_{\ln F_T}^2} \qquad (6.15)$$

and $\gamma_{V_p V_p}$ is the average correlation coefficient between two log-elastic modulus fields of sizes $V_p = B_p \times B_p \times C$ surrounding the two piles, which are seperated by distance s. In detail, $\gamma_{V_p V_p}$ is given by

$$\gamma_{V_p V_p} = \frac{1}{V_p^2} \int_0^{V_p} \int_0^{V_p} \rho_{\ln E} \left(\sqrt{s^2 + (\underset{\sim}{x}_1 - \underset{\sim}{x}_2)^2} \right) d\underset{\sim}{x}_1 \, d\underset{\sim}{x}_2 \tag{6.16}$$

where $\rho_{\ln E}$ is the correlation function which is assumed here to be Markovian and given by eq. (1.35). The distance, s, between the two pile centerlines is shown in Figure 6.1. The piles are centered in the volume V_p in plan, but the depth C will extend below the pile (see Table 6.1). In eq. (6.15), ρ_{F_T} is the correlation coefficient between two loads applied to the piles, and is assumed here to be $\rho_{F_T} = 1$ indicating that the two loads are identical.

Employing eq's. (6.9b) and (6.14) in eq. (6.13) leads to

$$\rho_X = \frac{\exp\{\sigma_{\ln F_T}^2 \rho_{\ln F_T} + \sigma_{\ln E}^2 \gamma_{V_p V_p}\} - 1}{\exp\{\sigma_{\ln F_T}^2 + \sigma_{\ln E}^2 \gamma(V_p)\} - 1} = \frac{(1 + \rho_{F_T} v_T^2)(1 + v_E^2)^{\gamma_{V_p V_p}} - 1}{(1 + v_T^2)(1 + v_E^2)^{\gamma(V_p)} - 1} \tag{6.17}$$

and using eq's. (6.11b) and (6.17) in eq. (6.12) results in

$$\text{Cov}\,[X_1, X_2] = \mu_T^2 \,(1 + v_E^2)^{\gamma(V_p)+1} \left((1 + \rho_{F_T} v_T^2)(1 + v_E^2)^{\gamma_{V_p V_p}} - 1\right) / \mu_E^2 \tag{6.18}$$

Finally substituting eq's. (6.11b) and (6.18) into eq. (6.8) gives

$$\text{Var}\left[\frac{F_{T_1}}{E_{g_1}} - \frac{F_{T_2}}{E_{g_2}}\right] = 2\mu_T^2(1 + v_E^2)^{\gamma(V_p)+1} \left[(1 + v_T^2)(1 + v_E^2)^{\gamma(V_p)} - (1 + \rho_{F_T} v_T^2)(1 + v_E^2)^{\gamma_{V_p V_p}}\right] / \mu_E^2 \tag{6.19}$$

from which the variance of differential settlement, σ_Δ^2, becomes

$$\sigma_\Delta^2 = 2\,\delta_{det}^2\,(1 - \eta)^2(1 + v_E^2)^{\gamma(V_p)+1} \left[(1 + v_T^2)(1 + v_E^2)^{\gamma(V_p)} - (1 + \rho_{F_T} v_T^2)(1 + v_E^2)^{\gamma_{V_p V_p}}\right] \tag{6.20}$$

Assuming $\rho_{F_T} = 1$, the above equation simplifies to,

$$\sigma_\Delta^2 = 2\,\delta_{det}^2\,(1 - \eta)^2(1 + v_E^2)^{\gamma(V_p)+1}(1 + v_T^2) \left[(1 + v_E^2)^{\gamma(V_p)} - (1 + v_E^2)^{\gamma_{V_p V_p}}\right] \tag{6.21}$$

For $s \to \infty$, pile settlements δ_1 and δ_2 become independent, and hence both η and $\gamma_{V_p V_p}$ in eq. (6.21) become zero. This will reduce eq. (6.21) to

$$\sigma_\Delta^2 = 2\,\delta_{det}^2(1 + v_E^2)^{\gamma(V_p)+1}(1 + v_T^2) \left((1 + v_E^2)^{\gamma(V_p)} - 1\right) \tag{6.22}$$

6.3   VALIDATION OF THEORY VIA MONTE CARLO SIMULA-TION

In this section, the parameters of differential settlement, Δ, are compared to Monte Carlo simulation results in order to validate the theory developed in the previous section. The statistical parameters used in this validation study are detailed in Table 6.1.

Table 6.1   Input parameters used in the validation of theory

Parameters	Values Considered
d	0.3 m
E_p	21 GPa
F_T	1.46, 2.16, 3.16 MN
μ_E	30 MPa
v_E	0.1, 0.3, 0.5
Poisson's ratio, ν	0.3
$\theta_{\ln E}$	0.01, 0.1, 0.5, 1.0, 5.0, 10.0 m
s	$2d, 3d, 5d, 10d, 15d, 20d, 30d$
n_{sim}	2000
B_p	2 m
C	$2H$

The simulations reported in this work resulting in differential settlement of two piles is estimated using a random finite element analysis. The piles are founded in a three-dimensional linearly elastic soil mass and a 50 by 30 by 30 elements mesh is used, as demonstrated in Figure 1.2. Eight-node brick elements are used with dimensions: 0.3 m by 0.3 m in the X, Y (plan) and by 0.5 m in the Z (vertical) directions. Within this mesh, each pile is modeled as a column of elements having depth H, and hence has a square cross-section with dimention $d = 0.3$m.

Three load cases (F_T) are considered for this analysis, as listed in Table 6.1. For each load case, a design pile length is determined using eq. (2.7), to achieve a target maximum settlement, $\delta_{max} = 0.025$ m. The pile to soil stiffness ratio is $k = 700$, from which

$a_0 = 0.029$, $a_1 = 2.44$, and $a_2 = 0.939$ are obtained by eq. (2.8). The design pile lengths $H = 2, 4$, and 8 m result for three load cases $F_T = 1.46, 2.16$, and 3.16 MN respectively.

The mechanical interaction factor, η, is obtained for each pile length and load case combination using the FE model, (see Figure 6.2), over a wide range of pile spacing, s, as listed in Table 6.2.

Figures 6.3 and 6.4 illustrate the comparison between theory and simulation-based estimates of $\mu_{|\Delta|}$ and σ_Δ. The theoretical estimates were obtained by eq's. (6.3) and (6.20) for $\rho_{F_T} = 1$ (identical loads), and $v_T = 0$ (non-random load). It is evident that theory somewhat overestimates σ_Δ and $\mu_{|\Delta|}$ for larger values of $\mu_{|\Delta|}$, which indicates that the prediction is conservative for larger mean absolute differential settlement. Figure 6.3 also demonstrates that theory is underestimating $\mu_{|\Delta|}$ when $\mu_{|\Delta|}$ is small and particularly for $H = 8$, $v_E = 0.1$, and small values of $\theta_{\ln E}$. The discrepancies between simulation and theory seen in Figures 6.3 and 6.4 arise mainly due to approximations made in the theory, which are as follows;

1) the choice of $B = 2$ m, and hence, the volume of the soil surrounding the pile, $V_p = B_p \times B_p \times C$, in the computation of effective elastic modulus, E_{eff}, was selected for the settlement of a single pile based on trial-and-error (see Chapter 3). This choice may not be the best for differential settlement and needs further investigation.

2) the theory assumes that Δ is normally distributed. In some cases this is not a good assumption.
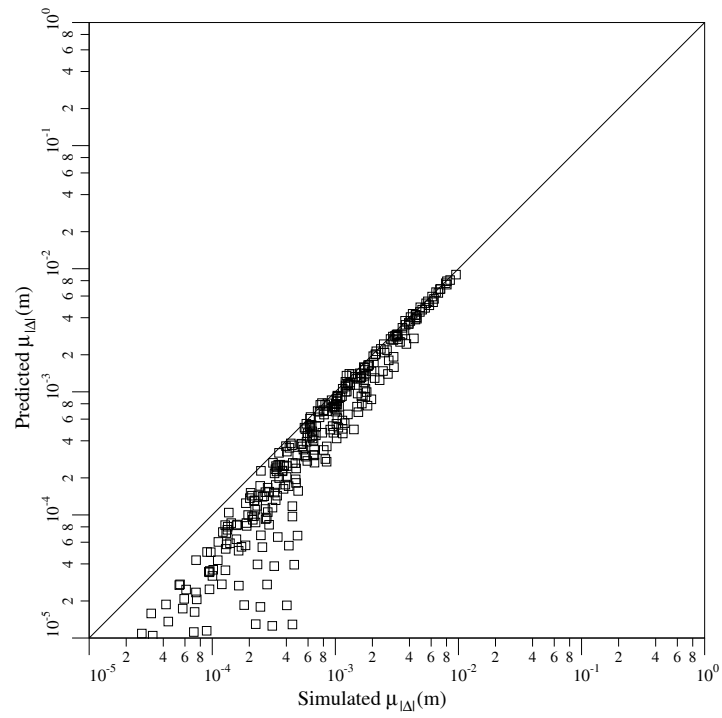
Figure 6.3 Predicted versus simulated mean absolute differential settlement, $\mu_{|\Delta|}$, obtained via eq. (6.3), for all cases listed in Table 6.1
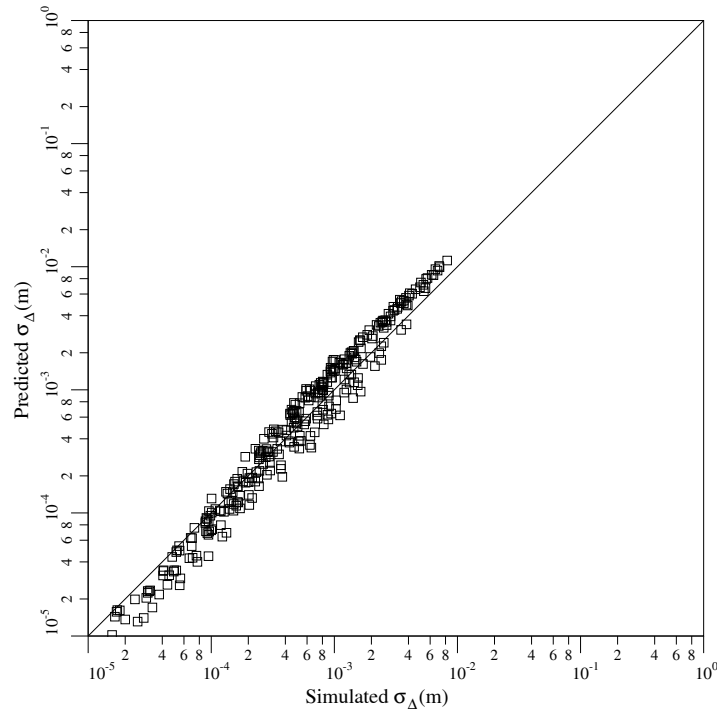
Figure 6.4 Predicted versus simulated standard deviation differential settlement, σ_Δ, obtained via eq. (6.20), for all cases listed in Table 6.1

The agreement between theory and simulation is nevertheless considered reasonably good given the approximations made in the theory especially at larger values of $\mu_{|\Delta|}$, which are also of more practical importance, and the theory is believed to be reliable enough to assist in design recommendations, as discussed shortly. Thus, the normal distribution can be used as a reasonable approximate distribution to model the differential settlement between two piles.

6.4   DESIGN RECOMMENDATIONS

The objective of this section is to study how the maximum tolerable settlement, δ_{max}, for an individual pile relates to the distribution of the differential settlement between two piles, and more specifically to the maximum tolerable differential settlement, Δ_{max}.

Table 6.2 Input parameters used in Figures 6.5, 6.6, and Table 6.4

Parameters	Values Considered
δ_{max}	6, 12, 25 mm
F_T	900 kN
d	0.3 m
E_p	21 GPa
μ_E	30 MPa
v_E	0.3
φ_{gs}	0.7, 1.0
$\theta_{\ln E} = s$	$2d, 3d, 5d, 10d, 15d, 20d, 30d$
B_p	2 m
C	$2H$

For a given δ_{max}, the required design pile length, H, is calculated using eq. (3.7) for various cases listed in Table 6.2 (note that, $k = E_p/\hat{E} = 700$ and eq. (3.37) were used here). The resulting values of H are given in Table 6.3. As seen in Table 6.3, higher values of δ_{max} lead to smaller designed pile lengths. This makes sense, since shorter piles are prone to higher deformations and thus larger mean differential settlement. Alternatively, there is a considerable increase in design pile length when the resistance factor, φ_{gs}, is reduced.

The H values in Table 6.3 are used along with B_p and C (see Table 6.2) to calculate $\gamma(V_p)$ and $\gamma_{V_p V_p}$, which are neccessary for predicting σ_Δ and hence $\mu_{|\Delta|}$, and ultimately to calculate the probability of differential settlement exceeding some maximum tolerable settlement.

Table 6.3 Required design pile length for various δ_{max}, and φ_{gs} obtained via eq. (3.7)

	H(m)	
δ_{max}(mm)	$\varphi_{gs} = 1$	$\varphi_{gs} = 0.7$
6	11.40	29.87
12	3.12	5.85
25	0.77	1.6

Figures 6.5 and 6.6 show the estimated $\mu_{|\Delta|}/s$ as a function of δ_{max}, for all cases listed in Table 6.2.
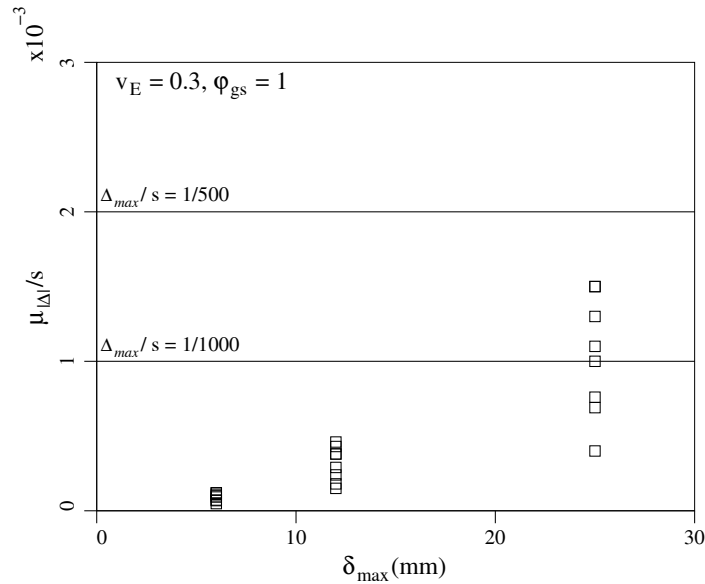
Figure 6.5   Predicted $\mu_{|\Delta|}/s$ versus δ_{max} predicted by eq. (6.3) for $\varphi_{gs} = 1.0$ shown with squares

Based on the discussion made previously in Chapter 3, the worst case correlation length, $\theta_{\ln E}$, is believed to be approximately equal to the distance between the two piles s, and hence $\theta_{\ln E}/s = 1$ is considered for the estimation of $\mu_{|\Delta|}$ in Figures 6.5 and 6.6, for s varying in the range $2d$ to $30d$. The horizontal lines in Figures 6.5 and 6.6 signify two possible maximum acceptable differential settlement to pile spacing ratio values, $\Delta_{max}/s = 1/500$ and $1/1000$ (taken from CHBDC, CSA, 2006).
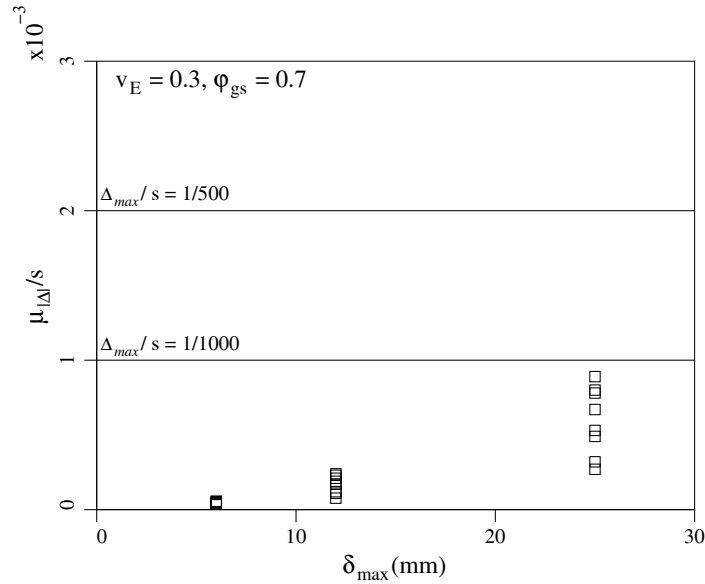
Figure 6.6   Predicted $\mu_{|\Delta|}/s$ versus δ_{max} predicted by eq. (6.3) for $\varphi_{gs} = 0.7$ shown with squares

Note the effect of using a resistance factor, $\varphi_{gs} < 1$ on lowering the mean absolute differential settlement, $\mu_{|\Delta|}$, which is observed in Figure 6.6. This is as expected, since lower values of φ_{gs} lead to larger design pile lengths, which justifiably provide higher resistance to settlement and hence smaller differential settlement. This information sheds light on the importance of resistance factor values such as the ones recommended previously in Chapter 3, and their contribution to safely designing piles against excessive total and differential settlements.

In order to further investigate the effect of resistance factor on differential selttlement, the probability that the mean absolute differential settlement, $\mu_{|\Delta|}$ exceeds some maximum tolerable differential settlement, Δ_{max} is compared for two cases $\varphi_{gs} = 0.7$ and 1.0. Assuming that normal distribution is a reasonable distribution to approximate the differential settlement of two piles, as discussed previously in this chapter, then

$$P\left[|\Delta| > \Delta_{max}\right] = P[\Delta < -\Delta_{max} \cup \Delta > \Delta_{max}]$$

$$= 2 \, \mathrm{P} \, [\Delta < -\Delta_{max}]$$

$$= 2 \, \Phi \left(\frac{-\Delta_{max} - \mu_{\Delta}}{\sigma_{\Delta}} \right)$$

$$= 2 \, \Phi \left(\frac{-\Delta_{max}}{\sigma_{\Delta}} \right) \tag{6.23}$$

since $\mu_{\Delta} = 0$, and where σ_{Δ} is calculated via eq. (6.20). Tables 6.4 and 6.5 show the results for Δ_{max}/s values $1/500$ and $1/1000$. The following observations can be made about the probabilities shown in these Tables;

1) The mean absolute differential settlement, $\mu_{|\Delta|}$, and hence, the probability of failure, $\mathrm{P}\left[|\Delta| > \Delta_{max}\right]$, is small for smaller values of pile spacing, s, due to the high mechanical interaction factor reducing the differential settlement between two piles.

2) As s increases, the mean absolute differential settlement, $\mu_{|\Delta|}$, and hence, the probability of failure, $\mathrm{P}\left[|\Delta| > \Delta_{max}\right]$, increases.

3) For fixed Δ_{max}/s, Δ_{max} increases as s increases, so that $\mathrm{P}\left[|\Delta|/s > \Delta_{max}/s\right] = \mathrm{P}\left[|\Delta| > \Delta_{max}\right]$ becomes smaller.

4) Maximum probability of excessive angular distortion occurs at an intermediate pile spacing.

5) Utilizing lower values of φ_{gs} significantly decreases both $\mu_{|\Delta|}$ and $\mathrm{P}\left[|\Delta| > \Delta_{max}\right]$.

Table 6.4 $P\left[|\Delta|/s > \Delta_{max}/s\right]$ for various δ_{max}, s, Δ_{max} and $\varphi_{gs} = 1.0$, computed via eq. (6.23)

δ_{max}(mm)	s(m)	$\mu_{|\Delta|}/s$	$P\left[|\Delta|/s > \Delta_{max}/s\right]$ for Δ_{max}/s	
			1/500	1/1000
6	0.6	0.48E-04	0.00E+00	0.70E-62
6	0.9	0.72E-04	0.23E-107	0.20E-27
6	1.5	0.10E-03	0.10E-51	0.22E-13
6	3.0	0.12E-03	0.12E-36	0.14E-09
6	4.5	0.12E-03	0.66E-40	0.21E-10
6	6.0	0.11E-03	0.92E-46	0.70E-12
6	9.0	0.92E-04	0.51E-67	0.29E-17
6	20.0	0.68E-04	0.51-120	0.13E-30
12	0.6	0.15E-03	0.27E-26	0.62E-07
12	0.9	0.24E-03	0.50E-10	0.10E-02
12	1.5	0.38E-03	0.23E-04	0.34E-01
12	3.0	0.46E-03	0.53E-03	0.83E-01
12	4.5	0.43E-03	0.20E-03	0.63E-01
12	6.0	0.38E-03	0.32E-04	0.38E-01
12	9.0	0.29E-03	0.62E-07	0.68E-02
12	20.0	0.18E-03	0.14E-18	0.60E-05
25	0.6	0.69E-03	0.20E-01	0.24E+00
25	0.9	0.11E-02	0.14E+00	0.46E+00
25	1.5	0.15E-02	0.29E+00	0.60E+00
25	3.0	0.15E-02	0.29E+00	0.60E+00
25	4.5	0.13E-02	0.20E+00	0.53E+00
25	6.0	0.10E-02	0.13E+00	0.45E+00
25	9.0	0.76E-03	0.36E-01	0.29E+00
25	20.0	0.40E-03	0.55E-04	0.44E-01

Table 6.5 $\mathrm{P}\left[|\Delta|/s > \Delta_{max}/s\right]$ for various δ_{max}, s, Δ_{max} and $\varphi_{gs} = 0.7$, computed via eq. (6.23)

δ_{max}(mm)	s(m)	$\mu_{|\Delta|}/s$	$\mathrm{P}\left[|\Delta|/s > \Delta_{max}/s\right]$ for Δ_{max}/s	
			1/500	1/1000
6	0.6	0.33E-04	0.00E+00	0.76-129
6	0.9	0.44E-04	0.00E+00	0.20E-73
6	1.5	0.55E-04	0.00E+00	0.11E-46
6	3.0	0.56E-04	0.00E+00	0.24E-44
6	4.5	0.51E-04	0.00E+00	0.34E-54
6	6.0	0.47E-04	0.00E+00	0.34E-64
6	9.0	0.39E-04	0.00E+00	0.24E-90
6	20.0	0.33E-04	0.00E+00	0.16-126
12	0.6	0.77E-04	0.82E-94	0.52E-24
12	0.9	0.12E-03	0.98E-37	0.14E-09
12	1.5	0.19E-03	0.45E-16	0.27E-04
12	3.0	0.24E-03	0.13E-10	0.72E-03
12	4.5	0.23E-03	0.21E-11	0.44E-03
12	6.0	0.21E-03	0.28E-13	0.14E-03
12	9.0	0.17E-03	0.17E-20	0.19E-05
12	20.0	0.11E-03	0.13E-44	0.14E-11
25	0.6	0.32E-03	0.84E-06	0.14E-01
25	0.9	0.53E-03	0.25E-02	0.13E+00
25	1.5	0.80E-03	0.45E-01	0.32E+00
25	3.0	0.89E-03	0.73E-01	0.37E+00
25	4.5	0.78E-03	0.40E-01	0.30E+00
25	6.0	0.67E-03	0.17E-01	0.23E+00
25	9.0	0.49E-03	0.12E-02	0.11E+00
25	20.0	0.27E-03	0.37E-08	0.32E-02

CHAPTER 7

CONCLUSIONS AND SUGGESTED FUTURE WORK

In this work, settlement of vertically loaded individual and pairs of piles is investigated using a random finite element model representing a three-dimensional soil. Total and differential settlement models are developed probabilistically, and are validated by simulation. Resistance and consequence factors are obtained using reliability-based approach for piles at serviceability limit state, provisions regarding differential settlement are suggested, and the effect of pile redundancy on the design of pile system is studied in detail.

In Chapter 2, an elastic prediction of pile settlement was developed employing a linear finite element program to derive the settlement prediction of a vertically loaded single floating pile founded in a homogeneous soil. A regression model is developed and a simple mathematical expression is found for pile settlement, δ, that fits the FE results well, and shows reasonably good agreement with the analytical solution derived by Randolph (Randolph and Wroth, 1978). The advantage of the simplified expression developed in this study is that it is easily inverted and solved for pile length, H, given δ and d, which can be used in the design of piles for serviceability limit states.

The deterministic elastic model developed in Chapter 2 is then used in Chapter 3 to establish a theoretical probabilistic model which assists in estimating the probability of excessive settlement of a pile founded in a random soil. The resulting model allows the determination of resistance factors required so that the probability of the actual pile settlement exceeding the maximum tolerable settlement is acceptably small. The model assumes that the pile has been designed using a reasonable mean settlement prediction, which in this thesis is a

linearly elastic prediction, but which can be generalized to more sophisticated non-linear predictors. The theoretical model was validated by the random finite element method, and used to estimate the geotechnical resistance factors required to achieve four maximum acceptable failure probabilities, $10^{-1}, 10^{-2}, 10^{-3}$ and 10^{-4}. The main assumptions made in this chapter are a) the total load is assumed to be approximately lognormally distributed, and b) the local averaging used to calculate the effective elastic modulus is calculated over a block of soil surrounding the pile. The best dimensions of the block were determined by trial and error. Thus, some discrepancies between this block average and the actual "deformation" average were expected and observed.

In Chapter 4, the consequence factors for the design of deep foundations at SLS were investigated for low, typical, and high consequence levels resulting in the following recommendations; 0.9 for high failure consequence, 1.0 for typical failure consequences, and 1.1 for low failure consequence levels. These factors are in basic agreement with the importance factors employed by other codes world-wide. It is observed in Chapter 4 that consequence factors are largely independent of limit states even though the target maximum failure probabilities for serviceability limit states are greater than those for ultimate limit states, for example. Therefore the same (or similar) consequence factors can be used to scale the target maximum acceptable failure probability for both ULS and SLS designs since the probabilities scale by the same relative amount.

Piles are usually used in groups, and Chapter 5 studies the reliability of a pile system for various levels of pile redundancy and resistance statistics, and establishes a relationship between reliability of a pile system and its individual components. Thus, for a given pile system reliability, the reliability of an individual pile can be determined analytically. The individual piles can then be designed to achieve the required individual pile reliability. The redundancy reliability model is simple and easy to implement. At the moment, it assumes that the individual pile resistances are independent, which is probably not generally true.

An improved model would include the correlation between pile resistances (through the soil) and its impact on reliability of a pile system.

Finally, the differential settlement between two piles is studied in Chapter 6, and a theoretical model is developed which can be used to calculate the probability of excessive differential settlement and hence influence design recommendations. The differential settlement model presented in Chapter 6 assumes that the loads applied to the piles are identical, i.e. completely correlated ($\rho_{F_T} = 1$), and also non-random ($v_T = 0$). The effect of load variablility as well as the correlation between the two loads should be taken into account to improve the differential settlement model. However, the current assumptions are quite reasonable given the difficulty of estimating joint load distributions.

In terms of future work, the following areas could be considered for further research;

a) Improved non-linear settlement prediction model in Chapter 2

b) Improved local average of elastic modulus field in Chapter 3 and 6

c) Considering correlation between pile resistances in Chapter 5

d) Including load variability and correlation between the two loads in Chapter 6

e) Further study of the effects of a bounded soil regime (i.e. edge effects) in the simulation model.

BIBLIOGRAPHY

AASHTO (2007). LRFD Bridge Design Specifications, American Association of State Highway and Transportation Officials, Washington, DC.

Allen, T.M. (2005). "Development of geotechnical resistance factors and downdrag load factors for LRFD foundation strength limit state design" , U.S. Department of Transportation, Federal Highway Administration, FHWA-NHI-05-052, Washington, D.C..

Australian Standard (2004). Bridge Design, Part 3: Foundations and Soil-Supporting Structures, AS 5100.3–2004, Sydney, Australia.

Banerjee, P. K. and Davis, T.G. (1977). "Displacement Field due to a Point Load at the Center of a Two-Layered Elastic Half-Space," *Geotechnique*, **28**(1), 43 – 56.

NCHRP (1991). *Manuals for the Design of Bridge Foundations*, Report 343, National Cooperative Highway Research Program, Transportation Research Board, NRC, Washington, DC.

Bartlett, F.M., Hong, H.P. and Zhou, W. (2003). "Load factor calibration for the proposed 2005 edition of the National Building Code of Canada: Statistics of loads and load effects," *Can. J. Civ. Engrg.*, **30**(2), doi: 10.1139/L02-087, 429–439.

Becker, D.E. (1996). "Eighteenth Canadian Geotechnical Colloquium: Limit states design for foundations. Part 1. An overview of the foundation design process," *Can. Geotech. J.*, **33**(6), 956–983.

British Standard BS EN 1990:2002 (2002). *Eurocode – Basis of Structural Design*, CEN (European Committee for Standardization), Brussels.

Butterfield, R. and Banerjee, P.K. (1971). "The elastic analysis of compressible piles and pile groups," *Geotechnique*, **21**(1), 43–60.

Canadian Geotechnical Society (2006). *Canadian Foundation Engineering Manual*, 4th Ed., Montreal, Quebec.

Canadian Standards Association (2006). *Canadian Highway Bridge Design Code*, CAN/CSA-S6-06, Mississauga, Ontario.

Coduto, Donald P. (2001). *Foundation Design: Principles and Practices*, (2nd Edition), Prentice Hall, New Jersey.

Coyle, H. M. and Reese, L. C. (1966). "Load transfer for axially loaded piles in clay," *ASCE Journal of the Soil Mechanics and Foundations Division*, **92**(2), 1 − 26.

Das, B.M. (2000). *Fundamentals of Geotechnical Engineering*, Brooks/Cole, Pacific Grove, California.

Ellingwood, B.R., Galambos, T.V., MacGregor, J.G. and Cornell, C.A. (1980). "Development of a Probability Based Load Criterion for American National Standard A58: Building Code Requirements for Minimum Design Loads in Buildings and Other Structures" , National Bureau of Standards, U.S. Dept. of Commerce, NSC Special Publication 577, Washington, D.C..

Fenton, G.A. and Vanmarcke, E.H. (1990). "Simulation of random fields via Local Average Subdivision," *ASCE J. Engrg. Mech.*, **116**(8), 1733–1749.

Fenton, G.A. (1994). "Error evaluation of three random field generators," *ASCE J. Engrg. Mech.*, **120**(12), 2478–2497.

Fenton, G.A. and Griffiths, D.V. (2007). "Reliability-based deep foundation design," *Probabilistic Applications in Geotechnical Engineering, GSP No. 170*, *ASCE*, Proc. Geo-Denver 2007 Symposium, Denver, Colorado, 1–12.

Fenton, G.A. and Griffiths, D.V. (2002). "Probabilistic foundation settlement on spatially random soil," *ASCE J. Geotech. Geoenv. Engrg.*, **128**(5), 381–390.

Fenton, G.A. and Griffiths, D.V. (2005). "Three-dimensional probabilistic foundation settlement," *ASCE J. Geotech. Geoenv. Engrg.*, **131**(2), 232–239.

Fenton, G.A., Naghibi, F. and Bathurst, R.J. (2012). "Comparison of geotechnical LRFD implementations," *Proceedings of the 65th Canadian Geotechnical Conference – GeoManitoba 2012*, Sept. 30 – Oct 3, Winnipeg, Manitoba, Canada, Paper No. 163 (CD–ROM), Bannister, Kent, ed., *Pub. Canadian Geotechnical Society, Richmond, BC, Canada*.

Fenton, G.A. and Griffiths, D.V. (2008). *Risk Assessment in Geotechnical Engineering*, John Wiley & Sons, New York.

Fenton, G.A., Griffiths, D.V. and Zhang, X.Y. (2008). "Load and resistance factor design of shallow foundations against bearing failure," *Can. Geotech. J.*, **45**(11), 1556-1571.

Fleming, W. G. K., Weltman, A. J., Randolph , M. F. and Elson, W. K. (2009). *Piling Engineering*, (3rd Edition), Taylor & Francis, New York.

Griffiths, D.V. and Smith, I.M. (2006). *Numerical Methods for Engineers*, (2nd Ed.), Chapman & Hall/CRC Press Inc., Boca Raton.

Jardine, R. J., Potts, D. M., Fourie, A. B. and Burland, J. B. (1986). "Studies of the influence of nonlinear stress strain characteristics in soil structure interaction," *Geotechnique*, **36**(3), 377 – 396.

Kraft, L. M., Ray , R. P. and Kagawa, T. J. (1981). "Theoretical T-Z curves," *ASCE*, **107**(NGT11), 1543 – 1561.

Gulvanessian, H., Calgaro, J. and Holicky, M. (2002). *Designer's Guide to EN 1990 Eurocode: Basis of Structural Design*, Thomas Telford Ltd., London, UK.

Meyerhof, G.G. (1995). "Development of geotechnical limit state design,' *Can. Geotech. J.*, **32**(1), 128–136.

Mindlin, R. D. (1936). "Force at a point in the interior of semi-finite solid," *Physics*, 195–202.

Naghibi, F., Fenton, G.A. and Griffiths, D.V. (2014). "Prediction of pile settlement in an elastic soil," *Computers and Geotechnics*, **60**(2), 29–32.

Naghibi, M. and Fenton, G.A. (2011). "Geotechnical resistance factors for ultimate limit state design of deep foundations in cohesive soils," *Can. Geotech. J.*, **48**(11), 1729–1741.

National Research Council (2005). *National Building Code of Canada*, 12th Ed., National Research Council of Canada, Ottawa.

NCHRP (2004). *Load and Resistance Factor Design (LRFD) for Deep Foundations*, Report 507, National Cooperative Highway Research Program, Transportation Research Board, NRC, Washington, DC.

Papoulis, A. (1991). *Probability, Random Variables, and Stochastic Processes*, (3rd Ed.), McGraw-Hill, Inc., New York, New York.

Phoon, K.K., Kulhawy, F.H. and Grigoriu, M.D. (1995). "Reliability-Based Design of Foundations for Transmission Line Structures" , Electric Power Research Institute, Report TR-105000, 380 p., Palo Alto, CA.

Poulos, H.G. and Davis, E.H. (1980). *Pile Foundation Analysis and Design*, John Wiley & Sons, New York.

Randolph, M.F. and Wroth, C. P. (1978). "Analysis of Deformation of Vertically Loaded Piles," *ASCE J. Geotech. Geoenv. Engrg.*, **104**(GT12), 1465–1488.

Randolph, M.F. (1994b). "Design Methods for Pile Groups and Pile Rafts," *Proceedings, Thirteenth International Conference on Soil Mechanics and Foundation Engineering*, New Delhi, 61–82.

Randolph, M.F. (1994a). "RATZ. Load Transfer analysis of axially loaded piles" , University of Western Australia.

Smith, I.M., Griffiths, D.V. and Margetts, L. (2014). *Programming the Finite Element Method*, (5th Ed.), John Wiley & Sons, New York, NY.

Smith, I.M. and Griffiths, D.V. (2004). *Programming the Finite Element Method*, (4th Ed.), John Wiley & Sons, New York, NY.

Szabo , Barna A. and Lee, George C. (1969). "Derivation of stiffness matrices for problems in plane elasticity by Galerkin's method," *International Journal for Numerical Methods in Engineering*, **1**(3), 301 – 310.

Timoshenko , S. P. and Goodier, J. N. (1982). *Theory of Elasticity*, (3rd Edition), McGraw-Hill, Singapore.

Vanmarcke, E.H. (1984). *Random Fields: Analysis and Synthesis*, The MIT Press, Cambridge, Massachusetts.

Vesic, A.S. (1977). *Design of Pile Foundations*, in *National Cooperative Highway Research Program Synthesis of Practice No. 42*, Transportation Research Board, Washington, D.C..

Zhang, L., Tang, W.H. and Ng, C.W.W. (2001). "Reliability of axially loaded driven pile groups," *ASCE Journal of Geotechnical and Geoenvironmental Engineering*, **127**(12), 1051–1060.

Zhang, L. M. and Xu, Y. (2005). "Settlement of building foundations based on field pile load based on pile load tests," *Proceedings of the 16th International Conference on Soil Mechanics and Geotechnical Engineering*, Osaka, Japan, Sept. 12–16, (CD–ROM), 16th ICMGE Committee, ed., *IOS press, Amsterdam, The Netherlands*.